Volume 8 Issue 3 July-September

ISSN (Online): 2521-0130
ISSN (Print): 2519-9404

LGU Journal of Life Sciences

LGU JOURNAL OF LIFE SCIENCES
Volume 8(3) JULY-SEP (2024)

CONTENTS

LGU Journal of
LIFE SCIENCES

LGU Society of Life Sciences

DOI: https://doi.org/10.54692/lgujls.2024.0803347

Paper Submission: 20th May 2024; Paper Acceptance: 7th Sep 2024; Paper Publication: 10th Sep 2024

Research Article | LGU J. Life. Sci
Vol 8 Issue 3 July- Sep 2024 | ISSN 2519-9404
eISSN 2521-0130

Records of some Oxyinae (Acrididae: Orthoptera) from Sindh, Pakistan

Sadaf Soomro*[1], Riffat Sultana[1]

1. Department of Zoology, University of Sindh Jamshoro, Sindh, Pakistan

Corresponding Author's Email: Sadafsoomro137@gmail.com

ABSTRACT: *Sindh is in the Oriental region and makes a significant contribution to the agricultural sector, partly due to its widespread moderate climatic conditions. Oxyinae can easily survive in this region and various species of Oxyinae cause harm to crops, specifically paddy crops. An extensive survey of different cultivated and uncultivated areas of Sindh was planned to assess the identification and zoogeographical affinities of Oxyinae. A random survey of selected areas was conducted from 2021 to 2023. A total of 917 specimens were collected and sorted into four species of Oxyinae: Oxya hyla (Serville, 1831), Oxya. velox (Fabricius, 1787), Oxya. fuscovittata (Marschall, 1836), of the genus Oxya, and Oxyina bidentata (Willemse, 1925), of the genus Oxyina. Specimens were collected from various habitats, including rice fields, short, long, and thick grasses, semi-desert areas, vegetation, herbs, shrubs, and along roadsides. According to geological history, the eco-fauna of Oxyinae hoppers depends on their taxonomic composition.*

Keywords: Harm, Crops, Taxonomy, Zoogeographical affinities, Sindh

INTRODUCTION

Oxyinae grasshoppers, belonging to the order Orthoptera (Acrididae), are zoogeographically distributed around the world, including Australia, Southeastern Russia, China, and Pakistan (Hollis, 1971). In Africa and Asia, they are abundant. Oxyinae is considered a major pest of various cultivated and valuable crops, damaging maize, sugar cane, wheat, fodder crops, and rice (Sultana et al., 2021). Due to their small size, capturing Oxyinae during data collection is very challenging. These grasshoppers are polyphagous, attacking and damaging a variety of valuable crops (Sultana et al., 2013). They are considered major pests of rice (*Oryza sativa*) fields (Karim and Riazuddin, 1999). Adult Oxyinae grasshoppers chew holes in leaves using their mandibles (Sultana et al., 2013). They also do so during their developmental stages (Uvarov, 1926). There are numerous publications on food preference, taxonomy, pest status, plant control, and distribution. The genus *Oxya* was established by Audinet-Serville in 1831 and revised multiple times by (Hollis 1971, 1975), and (Willemse 1925). Particularly important are Hollis's revision identifying 18 species based on quantitative analysis. Some cytological and morphological characteristics have helped establish the taxonomic position of Oxyinae grasshoppers (Ma et al., 1994) and (Xu et al., 1997). (Mohan and Manoharan 1987), (Yusuf 1996), (Usmani and Nayeem 2012), and (Samejo and Sultana 2019), provided detailed descriptions of the taxonomic status of *Oxya* grasshoppers. (Dirsh 1956), introduced a comprehensive value of Acridoidea genera from Africa. (Hollis 1971, 1975), carried out significant work on revising many sub-families of Acrididae, including Oxyina, noting many revolutionary changes in this group. European fauna was discovered by (Harz, 1975). However, none of these studies fully covered the taxonomy of Oxyinae from Sindh. Although, a detailed account of the systematics of Oxyinae was given by Sultana et al. (2020a, 2020b, 2021), Kumar et al. (2013) and Soomro et al. (2015, 2016, 2017, 2018) no study had been carried out on the zoogeographical affinities of this group. Therefore, the present study was designed to assess the presence of Oxyinae hoppers and their geographical position. In the present study, we provide the taxonomy of four species from two genera (i.e., *Oxya* and *Oxyina*) of Oxyinae based on their variation and covariance with other variables. Beside this, zoogeographical distribution of Oxyinae was also discussed.

Oxyinae are phytophagus insects damaging a variety of valuable crops e.g., sugarcane (*Saccharum*

officinarum), wheat (*Triticum aestivum*), rice (*Oryza sativa*) and other economically important crops. Additionally, these hoppers also attack and damage trees, herbs and shrubs (Sultana et al. 2012). Owing to their great reproductive potential and power of dispersal, these insects are considered major pests of valuable plants and crops. Their destructive impact on the leaves is evident at all developmental stages of the plants. According to the geographic distribution, Sindh has great important with its relevance to Indomalayan, Ethiopian and Palearctic elements. The distribution of eco-fauna in each continent or area reflects a connecting link between the existing life forms and the types and patterns of herbiage in the area. Analogous fauna of different continents differs in their taxonomic composition, owing to the geological history of the general fauna. According to the zoogeographic position, Pakistan is unique in covering three major zoogeographic regions, i.e., Palaearctic, Ethiopian and Indomalayan, among the world's six major zoogeographic regions. The Indomalayan region is bounded with the Indus River at the west, the Himalayas in the north, China, Indonesia and the Philippines in the southwest. Majority of the arid part, which is present in the west of the Indus River is included in the Palaearctic region, while the high deserts fall in the Ethiopian region.

Life forms and Climatic Biomes

The majority of Oxyinae are herbicoles and some species are gramnicoles. Herbaceous species are found in small trees or bushes. According to their habitat, their body structure is in relation to the thickness of the flora. These types of species live in open habitats and thick grasses, so according to their living style the freely living species mostly are broader and shorter in size and those inhabiting thickets are slightly longer and cylindrical in shape. While gramnicoles Oxyinae hoppers primarily live in the grasses, so their body structure is compressed, width and height are smaller than herbicoles species and face is oblique in shape. Recent survey and ecological data showed that the short, bodied grasshoppers occur in short and long grasses, while long bodied grasshoppers are restricted to long grasses only. Gramnicoles species are greenish, grey or straw-yellow in color, analogous with shades of the grasses.

Zoogeographically, Pakistan is divided into ten major zones, i.e., Temperate, Tundra, Taiga, Mixed and deciduous forests, Wooded meadow – steppe and steppe grassland and semi-desert, desert, hilly mountainous forests and tropical rain forests zone. Several Acrididae herbicoles species are found from mixed and deciduous

forests and gramnicoles from wooded meadow-steppe and steppe and genus *Oxya* from the desert of Sindh. Sindh is situated in subtropical region and according to the climatic condition Sindh is divided into three regions, i.e., upper region (center Jacobabad), middle region (center Hyderabad) and lower region (center Karachi), the climatic conditions of these regions are moderate, with the temperature frequently rising above the 46℃ from May to August and 2℃ recorded during the months of December to January. Average rainfall in Sindh is 20 – 31 cm in a year.

MATERIAL AND METHODS

Sampling Sites

The data collection and sampling were done from the irrigated, non-irrigated area and grassland of different districts of Sindh, during the year 2021 to 2023, 17 study sites were selected for the determination, distribution and zoogeographic position of Oxyinae hoppers. A total of 917 specimens were randomly collected from the sites shown in table 1.

Table 1: Data of different study sites

Area name	Latitude	Longitude
Matiari	25.5922º N	68.444º E
Jamshoro	25.4303º N	68.2809º E
Hyderabad	25.3960º N	68.3578º E
Tando Allah yar	25.4570º N	68.7215º E
Tando. M. Khan	25.1256º N	68.5426º E
Badin	24.6459º N	68.8467º E
Saanghr	27.9570º N	68.6380º E
Shikarpur	26.0436º N	68.9480º E
Larkana	27.5570º N	68.2028º E
Mirpur Khas	25.5256º N	69.0136º E
Khairpur	27.5256º N	68.7551º E
Dadu	26.7341º N	67.7795º E
Thatta	24.7475º N	67.9106º E
Sukkar	27.7244º N	68.8228º E
Qambar Shahdadkot	27.5859º N	68.0060º E
Noushehro Feroze	26.8463º N	68.1253º E
Sujawal	24.6042º N	68.0776º E

Collection and preservation of specimens

All grasshoppers collected from distinct localities were captured using two methods: hand-picking and netting (net diameter 8.9 cm and length 51 cm). The collected specimens were placed in jars and killed using potassium cyanide (KCN) following standard entomological methods described by Vickery and Kevan (1983). After killing, the specimens were transferred from the cyanide bottles to preserving boxes containing 70% alcohol and a few drops of glycerin for further analysis. The identification of the specimens was carried out using a stereoscopic dissecting binocular microscopic (Olympus SZX7, SZ2- ILST), following the taxonomic keys and descriptions of Hollis (1971, 1975). Morphometric measurements were taken in millimeters using scales, ocular squares, reticules, and dividers. All collected material was preserved in preserving boxes with their ID number, genus, species name and the name of the host plant from which the Oxyinae hoppers were captured. The specimens were stored in the Sindh Entomological Museum (SEM) at the Department of Zoology, University of Sindh, Jamshoro.

RESULTS AND DISCUSSION

***Oxya hyla* Serville, 1831**

Morphological Characteristics

Female specimens of this species are larger and stouter, while male species is moderate in size. The body is pale green or reddish brown in color. Antennae filiform, with 24 to 27 segments. Female antennae shorter in length and male antennae larger in size as compared to the combined length of head and pronotum. Eyes oval, fastigium of vertex short, broad, wide and obtusely angular. The pronotum sub cylindrical in shape, with white broad band lined and dorsally possess two black bands. Metazona is shorter than prozona. Tegmina are fully developed and larger in size than wings, few tegmina have short bristles on anteriorly. Wings are hyaline. Femur light green in color. Male cercus conical in shape (Table 2).

Table 2: Measurement of various body parts of *Oxya hyla*

Body parameters	Male (n=15)		Female (n=15)	
	Mean ±SD (mm)	Range	Mean ±SD (mm)	Range
Length of antenna	6.76 ± 0.31	6.3 -7.1	6.79 ± 0.51	5.59-7.29
Distance between eyes	0.50 ± 0.07	0.4-0.7	0.78 ±0.08	0.69-0.9
Length of head	2.76 ± 0.28	2.1-3.3	3.39 ±0.35	2.9-3.7.1
Length of pronotum	3.91 ± 0.30	3.5-4.5	5.04 ±0.61	4.3-5.02
Length of Tegmina	19.70 ± 0.81	19-22	24.3 ±2.12	19.7-30
Width of Tegmina	3.35 ± 0.80	3.0-5.0	4.31 ±0.63	3.001-5.2
Length of wings	18.5 ± 0.10	17-21	22.04 ±2.03	20-26.01
Width of wings	8.5 ± 0.7	7.0-9.0	9.97 ±0.83	9.02-11
Length of femur	12.34 ± 0.8	11-14	15.01 ±1.39	13.2-16.7
Width of femur	3.4 ± 0.45	3.0-4.0	3.75 ±0.41	3.02-04
Length of tibia	10.77 ± 0.61	10-12	12.72 ±1.32	11.03-15
Total body length	20.97 ±1.25	19-23	26.7 ±3.06	22.5-31

Material Examined

PAKISTAN: Sindh province. 21♂, 32 ♀, Tando Muhammad Khan (25.1256º N, 68.5426º E), 17 June 2021, Sadaf. 7 ♂, 14 ♀, Badin (24.6459º N, 68.8467º E) 27 March 2021, Sadaf and Seema. 27 ♂, 42 ♀, Shikarpur (26.0436º N, 68.9480º E) 03 June 2022, Sadaf. 5♂, 7♀, Sukkar (27.7244º N, 68.8228º E), 14 July 2021, Sadaf. 18♂, 24♀, Matiari (25.5922º N, 68.444º E) 19 August 2022, Sadaf. 9♂, 19♀, Jamshoro (25.4303º N, 68.2809º E), 7 May 2022, Sadaf. 13♂, 16♀ Khairpur (27.5256º N, 68.7551º E), 22 April 2023, Sadaf. 17♂, 19♀, Thatta (24.7475º N, 67.9106º E), 11 March, 2023, Sadaf. 14♂, 25♀ Hyderabad (25.3960º N, 68.3578º E), 8 September 2022, Sadaf (Fig. 1a and 1b).

Fig. 1a. *Oxya hyla* ♂ (Dorsal view)

Fig. 1b. ♀ (Dorsal view)

Habitat

The majority of Oxyinae species were found in thick grasses (*Cynodon dactylon)*, in roadside vegetation and some other agricultural fields. It was observed that some specimens of this species were present in rice (*Oryza sativa)*, maize (*Zea mays*) and jowar (*Sorghum vulgare).* Oxyinae are very harmful and damage economically important crops.

Geographical Distribution

Oxya hyla grasshoppers have greater geographical range and coupled with this feature, which is excessively variable in its general size and morphological appearances. According to Sergeev (1995), *Oxya* species are terrestrial insects, they are found in Pakistan and some other countries i.e. Africa, Afghanistan, Bangladesh, India, Nepal, Sri Lanka and Kenya. Zoogeographically Pakistan lies in the Indomalayan, this region connected with Sindh, Punjab and Khyber Pakhtunkhwa. The oriental fauna zone is bounded on the west by the river Indus, while Himalayas (north), China, Indonesia and Philippines with southeast, reported by Sultana and Wagan 2015. Their presence has been confirmed from Tando Muhammad Khan, Badin, Shikarpur, Sukkar, Matiari, Jamshoro, Khairpur, Thatta, Hyderabad and some other cultivated areas. At the present *Oxya hyla* was found abundantly from rice field and observed that the male and female specimens of this species are the major pest of many cultivated areas.

Species: *Oxya velox* (Fabricius, 1787)

Morphological Characteristics

Body medium to large, with pale to paler greenish color. Antennae and Tegmina both are fully developed. Antennae are wooden brown in color while tegmen with yellow brownish in color at basal parts. The edges of the vertex and eyes are dark brownish in color. Wings are hyaline. The inner and lower part of hind femur is yellowish green. Female is larger in length than male specimens. Fastigium of vertex short, weakly concave, less widened with apex obtusely parabolic and transverse furrows absent. Metazona flattened and weakly flattened prozona. Hind tibia with two rows, 39 dorsal black tipped spines, 09 external, while 11 internal (Table 3).

Table 3: Measurement of various body parts of *Oxya velox*

Body parameters	Male (n=15) mm		Female (n=15) mm	
	Mean ±SD	Range	Mean ±SD	Range
Length of antenna	6.65 ± 0.32	6.61-7.4	6.37 ±0.70	5.5-7.4
Distance between eyes	0.39 ±0.04	0.42-0.7	0.69 ±0.06	0.7-0.9
Length of head	2.61 ±0.20	2.41-2.1	3.30 ±0.14	03-3.6
Length of pronotum	3.69 ±0.20	3.4-4.3	4.74 ±0.40	3.81-5.3
Length of Tegmina	18.75 ±0.86	18.2-20	23.87 ±1.16	22-25.1
Width of Tegmina	4.09 ±0.60	3.02-5.1	4.39 ±0.46	4.02-5.01
Length of wings	17.39 ±1.36	16.1-20	22.15 ±1.39	20-23.5
Width of wings	8.81 ±0.74	8.49-10	10.15 ±0.81	9.03-13
Length of femur	11.06 ±0.80	10.2-11	13.89 ±1.60	10.5-17
Width of femur	3.49 ±0.60	3.01-4.2	3.70 ±0.74	3.03-5.3
Length of tibia	10.38 ±0.51	10.2-10	13.08 ±1.30	11.0-14
Total body length	20.42 ±0.86	21-23	26.17 ±1.96	23-31

Material Examined

PAKISTAN: Sindh province. 36♂, 55 ♀, Tando Muhammad Khan (25.1256º N, 68.5426º E), 2 March, 2021, Sadaf. 28♂, 40♀, Matiari (25.5922º N, 68.444º E) 7 August 2023, Sadaf. 22♂, 31♀ Hyderabad (25.3960º N, 68.3578º E), 29 September 2023, Sadaf (Fig. 2a and 2b).

Fig. 2a. *Oxya velox* ♂ (Dorsal view)

Fig. 2b. *Oxya velox* ♀ (Dorsal view)

Habitat

Oxya velox is a rare species. During field survey specimens were collected from the rice field in abundant form and few specimens were captured from grasses.

Geographical Distribution

This herbivores species is distributed in Eastern and Western Pakistan, Burma, India and some irrigation fields of Himalayas. Ahmed (1980) and Baloach (1966) reported this species from the irrigated areas of Sindh, i.e., Thatta, Jacobabad and Larkana divisions.

Species: *Oxya fuscovittata* (Marschall, 1836)

Morphological Characteristics

Female specimens are larger and more robust than male. Antennae brown in color and filiform with 25 to 28 segments, in female antennae size is shorter than male specimens as compared to the combined size of head and pronotum. The wings are fully developed and hyaline. Fastigium of vertex concave with obtusely parabolic apex, wide and short. Transverse furrow totally absent. Tegmina fully developed, weakly spinose at interior margin, extending by abdomen, broad basally, hyaline, while in distal half it is narrowed. The hind tibia has two rows, these rows covered with the black tipped spines at dorsal, nine spines at dorso-external side while at dorso-internal side having ten spines. Body greenish in color. The head and pronotum both are light green color with dark green patches (Table 4).

Table. 4: Measurement of various body parts *O. fuscovittata*

Body parameters	Male (n=15) mm		Female (n=15) mm	
	Mean ±SD	Range	Mean ±SD	Range
Length of antenna	6.20±0.31	5.7-6.8	6.10±0.30	6.5-7.7
Distance between eyes	0.50±0.12	0.40-0.6	0.67±0.08	0.49-0.6
Length of head	2.79±0.29	2.41-2.79	3.18-0.47	03 -3.9
Length of pronotum	3.80±0.39	3.41-3.08	4.59±0.89	3.21-5.10
Length of Tegmina	19.70±1.10	18.5 -22.05	24.19±1.23	23.7-25.3
Width of Tegmina	3.51±0.49	3.01-4.03	4.49±0.61	4.02-6
Length of wings	18.38±0.69	16.9-18.2	23.40±1.19	22.2-24.9
Width of wings	8.51±0.57	8.01-9.02	10.6±0.59	10.7-10.5
Length of femur	12.49±0.1	11.4-14.98	14 ±1.37	12-15.9
Width of femur	3.39±0.49	3.1-4.3	4.50 ±0.49	4.03-6
Length of tibia	10.9±0.70	11-12.3	12.9±1.07	10.9-13.6
Total body length	21.50±1.50	20.5-24.9	24.08±0.80	23.8-25.9

Material Examined

PAKISTAN: Sindh province. 9♂, 13♀, Sukkar (27.7244º N,

68.8228º E), 22 July 2023, Sadaf. 16♂, 31♀, Jamshoro (25.4303º N, 68.2809º E), 28 August 2022, Sadaf. 29♂, 48♀, Thatta (24.7475º N, 67.9106º E), 11 March, 2021, Sadaf. 25♂, 27♀ Hyderabad (25.3960º N, 68.3578º E), 15 September 2023, Sadaf (Fig. 3a and 3b).

Fig. 3a. *Oxya fuscuvittata* ♂ (Dorsal view)

Fig. 3b. *Oxya fuscuvittata* ♀ (Dorsal view)

Habitat

Oxya fuscovittata specimens were collected from the agricultural fields of Sindh, it is found abundantly in maize, rice and wheat crops of Sindh. This species is widely distributed in grass and is a major pest of paddy areas.

Geographical Distribution

Geographically, this species is distributed in Pakistan and India. Records from India by Usmani and Nayeem (2012), include only the females. During present attempt we found both male and female specimens abundantly from different cultivated areas of Sindh. These are herbivores and included in the Indomalayan region zoogeographically, by Sultana and Wagan 2015.

Species: *Oxyina bidentata* (Willemse, 1925)

Morphological Characteristics

Female larger in size than male specimens. Antennae brown in color with 23 – 25 segments. In male, antennae longer in length than female as compared to the length of head and pronotum combined. Body green in color. Eyes and vertex of adages brownish in color. Fastigium of vertex wide, short and concave with obtusely parabolic apex. Abdomen yellowish brown in color. The wings are fully developed and hyaline. Pronotum compressed, light greenish and dark green patches are present on dorsum. Tegmina is well developed. Hind tibia with two rows of black-tipped at dorsally and nine externally while internally with ten spines (Table 5).

Table 5: Measurement of various body parts of *O. bidentata*

Body parameters	Male (n=15) mm		Female (n=15) mm	
	Mean ±SD	**Range**	**Mean ±SD**	**Range**
Length of antenna	6.81±0.79	5.1-09	6.6±0.89	5.09-09
Distance between eyes	0.39±0.06	0.5-0.61	0.60±0.06	0.8-0.7.5
Length of head	2.79±0.19.7	2.43-3.10	3.07±0.16	2.78-3.19
Length of pronotum	3.90±0.21.9	3.7-4.7	4.60±0.67	3.9-6
Length of Tegmina	18.80±0.80	17.5-23	22.69±1.40	20.8-24.7
Width of Tegmina	3.49±0.58	3.06-4.03	4.06±0.90	3.10-6
Length of wings	17.7±0.10	16.1-20	20.50±1.40	19.75-29
Width of wings	8.3±0.80	7.01-9.02	9.6±0.77	9.02-10.9
Length of femur	11.7±0.80	10.7-12.9	12.30±1.41	10-13.8
Width of femur	2.10±0.09	2.10-3.17	3.69±0.69	3.02-5.07
Length of tibia	9.54±0.49	9.01-10.07	12.29±0.90	11.6-17
Total body length	20.40±0.79	19.4-19.9	23.7±0.90	21.9-24.7

Material Examined

PAKISTAN: Sindh province. 10♂, 12♀, Tando Allah Yar (25.4570º N, 68.7215º E), 6 March, 2022, Sadaf. 5 ♂, 9 ♀, Sanghar (27.9570º N, 68.6380º E) 27 September 2022, Sadaf and Seema. 7 ♂, 18 ♀, Larkana (27.5570º N, 68.2028º E) 03 June 2023, Sadaf. 13♂, 16♀, Noushahro Feroz, (26.8463º N, 68.1253º E), 23 June 2021, Sadaf. 26♂, 32♀, Sujawal (24.6042º N, 68.0776º E) 10 August 2023, Sadaf. 11♂, 28♀, Mirpur khas (25.5256º N, 69.0136º E), 17 May 2022, Sadaf (Fig. 4a, 4b).

Fig. 4a. *Oxyina bidentata* ♂ (Dorsal view)

Fig. 4b. *Oxyina bidentata* ♀ (Dorsal view)

Habitat

Ecological studies show that this species lives in a variety of habitats. Specimens of this species were collected from different agricultural fields and from herbs and shrubs.

Geographical Distribution

Oxyina bidentata widely distributed all around the Asia-tropical, Indian subcontinent, including Pakistan. This species

was reported by Ahmed (1980) from the irrigated areas of Khyber Pakhtunkhwa and Punjab, from Sindh it was reported by Soomro at al. (2015). Recently, natural habitat and interaction of related species was worked by Usmani and Nayeem (2012).

CONCLUSION

Extensive surveys in different localities of Sindh from 2021 to 2023 resulted in the collection of about 917 specimens. These surveys aimed to study the taxonomic composition, zoogeographical status, and distribution of Oxyinae in various agricultural fields. Oxyinae grasshoppers, observed in habitats such as herbs, shrubs, trees, and fields of maize, jowar, wheat, rice, and sugarcane, prefer rice as their primary diet. The specimens were sorted into four species: *Oxya hyla* (Serville), *O. velox* (Fabricius), *O. fuscovittata* (Marschall), and *Oxyina bidentata* (Willemse). *Oxya hyla* was the most dominant species, especially from May to July, while *Oxyina bidentata* was less common. The highest populations of Oxyinae hoppers were recorded during these months. This study, the first to examine the zoogeographical affinities of Oxyinae in this region, found these grasshoppers in both irrigated and non-irrigated areas of Sindh, where they significantly damage economically important crops, particularly rice.

ACKNOWLEDGEMENT

The first author is highly thankful to the farmers and landlords who allowed and assisted me during the field visits. I am grateful to my parents for their support and motivation.

CONFLICT OF INTERESTS

The authors declare no conflict of interest.

REFRENCES

1. Ahmed FU (1980). Survey of grasshopper in arid and semi-arid region of Pakistan. Final Rep., Pl-480 No. P.K-ARS-20 (FG-Pa-21): 500.
2. Baloach HA (1966). Taxonomy of Pyrgomorphidae and sub-families Hemiacridianae, Oxyinae, Crytacanthacridianae, Eyprepocnemidinae and Catantopinae of Acrididae of Hyderabad and its adjoining areas. M.Sc. Thesis, Uni. of Sindh. 1-66.
3. Dirsh VM (1956). The phallic complex in Acridoida (Orthoptera) in relation to taxonomy. Transactions of the Entomological Society, London. 108 (7): 223-356.
4. Harz K (1975). The Orthoptera of Europe, Series of Entomologia, The Hague. 11: viii+-939.
5. Hollis D (1971). A preliminary revision of the genus *Oxya* (Orthoptera:Acridoidea). Bull. Brit. Mus. (Nat. His), Ent. 26 (7): 267-343.
6. Hollis D (1975). Review of the sub-family Oxyinae (Orthoptera: Acridoidea). Bull.

Brit. Mus. (Nat. His), Ent. 31: 189- 234.

7. Karim S, Riazuddin S (1999). Rice insects' pests of Pakistan and this control: A lesson from past for suitable integrated pest management. Paki. J. Bot. 2 (2): 261-276.

8. Kumar S, Sultana R, Wagan MS (2013). Susceptibility of developmental stages of *Oxya velox* (Orthoptera: Acrididae) to Aspergillus species from Sindh. 33rd Pakistan Congress of Zoology (International) at Islamabad, 2nd - 4th April: 173.

9. Ma E, Guo Y, Zheng Z (1994). Cytotaxonomic study of *Oxya* species in China (Orthoptera: Acridoidea). Entomol. Sin. 1: 101 – 109.

10. Mohan N, Manoharan T (1987). Population distribution and control of small Rice grasshopper *Oxya nitidula*. Madras Agric J. 74: 328-329.

11. Sultana R, Soomro N, Kumar S, Samajo AA, Soomro S (2020a). A Comparative Study of the Egg-pod Morphology in two genera of Oxyinae (Acrididae: Orthoptera) Pak. J. Zool. 52(4):1327-1332.

12. Sultana R, Soomro N, Wagan MS (2020b). Description of new species with comparison to close allies (Oxyinae: Acrididae: Orthoptera). Paki. J. Zool. 1-6.

13. Sultana R. Soomro N, Kumar S, Samajo AA (2021). Comparison of Mating Behavior of four species of Oxyinae (Acrididae: Orthoptera). Paki. J. Zool. 53(3): 1181-1184.

14. Sultana R, Bughio AB, Waheed AP, Haji K (2012). Studies on the Immature Stages of *Oxya velox*. A rice grasshopper from district Jamshoro. FUUAST J. Biol. 2(1): 57-62

15. Sultana R, Wagan MS (2015). Grasshoppers and Locusts of Pakistan. Higher Education Commission of Pakistan. ISBN: 978-969-417-180-7: 1-180.

16. Sultana R, Abbas W, Bughio BA (2013). Preliminary studies on the occurrence of orthoptera from district Jamshoro. FUUAST J. Biol. 3 (2): 111.

17. Soomro N, Sultana R, Wagan MS, Abbasi AR, Solangi BK (2015). Occurrence of *Oxya* Species (Oxyinae: Acrididae: Orthoptera) from Sindh. Sindh Uni. Research J. 47 (2): 251-254

18. Soomro N, Sultana R, Wagan MS (2016). Biology of *Oxya* species (Oxyinae: Acrididae: Orthoptera) under laboratory conditions. 36th Pakistan Congress of Zoology (International) held at Uni. of Sindh, Jamshoro. Feb. 16-18: 133-34.

19. Soomro N, Sultana R, Wagan MS (2017). Comparative study on the immature stages of *oxya* (Oxyinae: Acrididae: Orthoptera). 37th Congress of Zoology (International) at Govt. Coll. Uni. Faisalabad. 210.

20. Soomro N, Sultana R, Wagan, MS (2018). Morphological and behavioral description of *Oxya hyla hyla* under laboratory conditions. 38th Pakistan Congress of Zoology (International) at University of the Punjab, Lahore, Feb. 27- March 1: 221.

21. Sergeev MG (1995). Biodiversity of insects of Arid and semi-arid lands of Eurasia Sino-Russian workshop on the study of Animal Biodiversity of major

ecosystem of Eurasia held in Beijing: 57-66.
22. Samejo AA and Sultana R (2019). Morphology of immature stages of *Schistocerca gregaria* with special references to its size variations. Pak. J. Zool. 51: 1221 - 1226.
23. Usmani MK, Nayeem M (2012). Studies on taxonomy and distribution of Acridoidea (Orthoptera) of Bihar, India. J. Threat. Taxa. 4(13): 3190-3204.
24. Uvarov BP (1926). Notes on the *Oxya* (Orthoptera: Acridoidea). Bull. Ento. Res. 17: 45-48.
25. Vickery VR, Kevan DK McE (1983). A monograph of the Orthopteroid insects of the Canada and adjacent regions. Lyman Ent. Mus. Res. Lab. Mem. (13): 680-1462.
26. Willemse C (1925). Contribution a la faune des Orthopteres des Nouvelles Hebrides. Transactions of the Entomological Society of London. 3 (4): 513-525.
27. Xu S, Liu Z and Zheng Z (1997). A cladistics study on karyotype characters of some species of genus *Oxya* (Orthoptera: Acridoidea). J. Shaanxi Normal Univ. 25: 70-73.
28. Yusuf M (1996). Taxonomic studies on Grasshoppers and Locust (Acridoidea: Orthoptera) of Pakistan. Final Techenical Report: Pakistan Sci. Foundation, Project S/Bio: 1-158.

LGU Journal of

LIFE SCIENCES

LGU Society of Life Sciences

DOI: https://doi.org/10.54692/lgujls.2024.0803348

Paper Submission: 9th Jan 2024; Paper Acceptance: 10th July 2024; Paper Publication: 10th Sep 2024

Research Article | LGU J. Life. Sci

Vol 8 Issue 3 July- Sep 2024 | ISSN 2519-9404

eISSN 2521-0130

Molecular Docking and Simulation of Azo Dye Binding with Laccase, Peroxidase, and Oxidoreductase in Acinetobacter junii

Sidra Ishaque[1], Hina Batool[1], Muhammad Zaid[1], Hareem Mohsin[1], Mahnoor Mushtaq[2], Syeda Sheher Bano[1], Kaneez Fatima*[1]

1. Department of Life Sciences, School of Science, University of Management and Technology, Lahore Pakistan
2. School of Biochemistry and Biotechnology, University of the Punjab, Lahore

Corresponding Author's Email: kaneezfatima77@yahoo.com

ABSTRACT: *The incorporation of omics approach in the field of bioremediation is an exciting venture to research. It will significantly reduce the screening time. Therefore, this study employs a computational strategy to compare the azo dye degrading potential of three prominent enzymes from Acinetobacter junii, i.e. oxidoreductase, laccase, and peroxidase. For this purpose, six azo dyes, Acid violet 7, Acid orange 19, Congo red, disperse red 1, Disperse red 13, and Reactive brilliant red, were considered for the analysis of molecular interactions with the three enzymes. After 3D structure modeling through I-TASSER and validated by RAMPAGE, the enzymes were docked with the azo dyes by using auto dock vina, and their binding energies and molecular interactions were evaluated. The comparative analysis of enzymes-dye complexes revealed that both oxidoreductase and laccase formed highly stable complexes with all azo dyes, showing strong binding affinities (>-5kcal/mol). Moreover, NAMD used for the molecular dynamic simulations have revealed the minimum conformational deviations for oxidoreductase and laccase compared to the docked complex of peroxidase. These findings suggest that oxidoreductase and laccase of A. junii are highly promising for efficient remediation of toxic azo dyes. However, these enzymes need further experimental characterization before their use in large-scale setups.*

Keywords: *Acinetobacter junii*, Azo dyes, Bioinformatics, Dye-degradation, Laccase, Molecular Docking

INTRODUCTION

Textile industry plays a pivotal role in augmenting the economic growth of the country, but it is also known for significant environmental concerns, including soil, air and water pollution. Among various types of dyes used in textile industry, synthetic azo dyes impart vibrant and long-lasting colors to products (Ajaz et al., 2020; Samsami et al., 2020). However, their widespread usage and the release of untreated dye effluents in the lakes, rivers and other aquatic bodies is posing a threat to aquatic life, human health as they can persist in the environment for a longer period (Okafor et al., 2021; Godswill et al., 2020).

Bioremediation of azo dyes is considered as an appealing, environmental-friendly, cost-efficient, and functionally simple approach compared to physicochemical strategies (Misal et al., 2018; Majumdar et al., 2022). It involves the screening and utilization of bacterial and fungal enzymes such as laccases, peroxidases, and oxidoreductase, which reduce the azo bonds (–N=N–) using flavin containing NADH/NADPH to colorless amines (Singh and Biotechnology, 2022). The enzyme laccases (EC 1.10.3.2) belong to copper oxidases family, which plays a significant role in oxidative bioremediation of contaminated environment. On the other hand, enzymes belonging to the oxidoreductase family catalyze the NAD(P)H-dependent azo bond reductive cleavage. These enzymes contribute to the metabolic breakdown of azo dyes within bacterial cells.

However, microbial screening for dye degradation is tedious and a time taking process. Modern system biology offers robust and fast mode of screening the target microorganism for bioremediation. *In silico* approaches including structure modelling, molecular docking analysis, and molecular dynamic simulations help in predicting the 3D structure (Pinheiro et al., 2020; Tülek et al., 2021; Rathour et al., 2023) and assessing the binding affinities of azo dyes with bacterial enzymes (Kumar et al., 2020; Meghwal et al., 2020) saving the time and reduing experimental costs in future. Although molecular docking analysis has been extensively used in drug discovery but its applications in determining targets for bioremediation will provide a new impact.

The present study employs a computational strategy to explore the potential of enzymes laccase, peroxidase, and oxidoreductase from *Acinetobacter junii* to degrade the toxic azo dyes by

assessing their molecular interactions with disperse red 13, acid violet 7, acid orange 19, disperse red 1, Congo red, and reactive brilliant red. For this purpose, molecular docking analysis was performed to recognize the suitable dye and enzyme arrangement while MD (Molecular Dynamic) simulations revealed the conformational stabilities of enzyme-dye complexes. This study can be an effective approach in early screening of suitable dye degrading enzymes which can further be used in remediation of textile effluent.

MATERIALS AND METHODS

Azo Dyes and Bacterial Strain

Six textile azo dyes, namely, acid violet 7, disperse red 1, acid orange 19, Congo red, disperse red 13, and reactive brilliant red, were used in present study. *A. junii* was chosen due to its presence in wastewater samples.

Bacterial Enzymes

The database NCBI (https://www.ncbi.nlm.nih.gov/) was employed to recover the amino acid sequence of the A. junii enzymes (laccase, peroxidase, and oxidoreductase).

Physicochemical Characterization of Enzymes

To analyze the physical and chemical properties of three selected enzymes, ProtParam tool (http://web.expasy.org/protparam/) was used. This tool provides insights into several key parameters including molecular weight, stability, aliphatic index (AI), theoretical isoelectric point (pI), grand average of hydropathicity (GRAVY), and instability index (II) (ProtParam, 2017).

Structure Modelling

The three-dimensional structures of three selected enzymes were built using online I-TASSER (http://zhanglab.ccmb.med.umich.edu/I-TASSER) server, followed by the selection of precise protein mockups on the basis of RMSD values, TM score, and C-score. Furthermore, the quality of protein models was evaluated through Ramachandran plots that were designed using RAMPAGE software (Wang et al., 2016). Likewise, the three-dimensional structures of selected azo dyes were fetched in SDF format from the PubChem database (pubchem.ncbi.nlm.nih.gov). PubChem database presents the repository of small molecules, substances, and compounds along with their molecular information (Kim et al., 2016).

Protein and Ligand Preparations

The protein and ligand preparation are a prerequisite for molecular docking analysis (Madhavi et al., 2013). This involves the conversion of 3D structures to the PDBQT format using AutoDock Vina. In the case of proteins,

Discovery studio was used to remove potential clashes and water molecules. Missing residues, gap-filling, and optimization of hydrogen-bonding networks were also incorporated by Discovery studio (Huang et al., 2006).

Molecular Docking Analysis

The docking of selected enzymes (laccase, peroxidase, and oxidoreductase) with each of the six selected azo dyes was accomplished using Autodock Vina. The most appropriate binding position and binding energies ($kcalmol^{-1}$) for each docked complex was calculated (Li et al., 2019).

Molecular Dynamic Simulations

Finally, stabilities of docked complexes were assessed using MD simulations that were executed via NAMD software and QwikMD interface plugin in VMD (Alonso et al., 2006; Sung, 2011). The simulations were carried out using equilibration phase of 2 ns and production phase of 10 ns at 315 K. The conformational trajectories were analyzed based on the RMSD (Root Mean Square Deviations) and RMSF (Root Mean Square Fluctuations) (Martínez, 2015).

RESULTS

Azo Dye Degrading Enzymes

The amino acid sequences of three enzymes, oxidoreductase, laccase, and peroxidase were retrieved from NCBI using SUU15883.1, SUU18727.1, and ATU46662, accession IDs for these three enzymes, respectively.

Physicochemical Characterization

The isoelectric point of oxidoreductase, laccase, and peroxidase were 8.02, 5.85, and 4.55, respectively. The GRAVY value for all three enzymes was negative. The Instability Index (II) of oxidoreductase, laccase, and peroxidase were 29.54, 23.00, and 38.08, respectively. The aliphatic index of oxidoreductase (93.07), laccase (84.11), and peroxidase (87.39) proclaim them as thermally stable (Table 1). These features have marked the stable nature of the three selected enzymes.

Table 1: The physiochemical parameters of laccase, oxidoreductase and peroxidase enzymes of *Acinetobacter junii* were evaluated through ProtParam tool

Enzymes	A. A	MW	pI	AI	GRAVY	S/IS	II
Laccase	246	27287.15	5.85	84.11	-0.084	S	23.00
Oxidoreductase	551	61014.34	8.02	93.07	-0.113	S	29.54
Peroxidase	306	34337.61	4.55	87.39	-0.228	S	38.08

A. A= No. of amino acid residues; MW= Molecular Weight; pI=Isoelectric point; AI=Aliphatic Index; GRAVY= Grand Average of Hydropathicity; S/IS= Stable/Instable; II= Instability index

Structural Modelling

I-TASSER was used to model the three structures of enzymes followed by the model selection based on RMSD values, C and TM score (Figure 1).

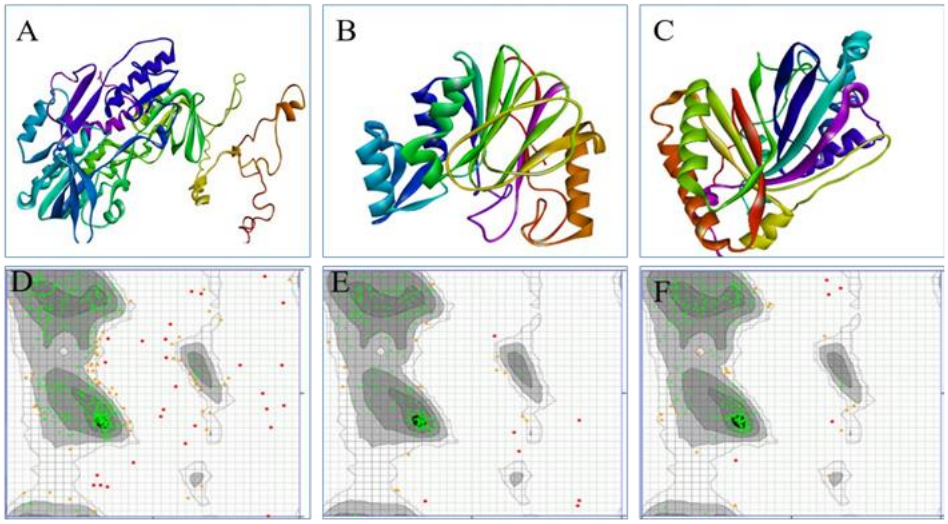

Fig. 1: Three-dimensional structures of enzymes (A) Oxidoreductase, (B) Laccase, and (C) Peroxidase designed through I-TASSER. The Ramachandran plots of (D) Oxidoreductase, (E) Laccase, and (F) Peroxidase generated via RAMPAGE shows the percentage of amino acid residues in favored regions of plot.

The confidence score (C-score) is used to estimate the quality of protein model. The higher value of this score indicates the good quality models. The 3D structures of enzymes oxidoreductase, laccase, and peroxidase with C-score values of -1.91, 1.15, and 1.43 were found to be good quality models. Similarly, the TM score (0.49±0.15, 0.87±0.07, and 0.91±0.06) and RMSD values (12.1±4.4Å, 12.1±4.4Å, and 3.3±2.3Å), of oxidoreductase, laccase, and peroxidase were within the acceptable ranges, further affirming the fidelity of protein structures.

Finally, the Ramachandran plots revealed the 83.298%, 89.815%, and 91.513% residues of oxidoreductase, laccase, and peroxidase in the favorable and acceptable areas of the plot (Figure 1).

Molecular Docking Analysis

The molecular interactions of enzymes laccase, peroxidase, and oxidoreductase with six azo dyes are shown in Figure 2, 3, 4 respectively.

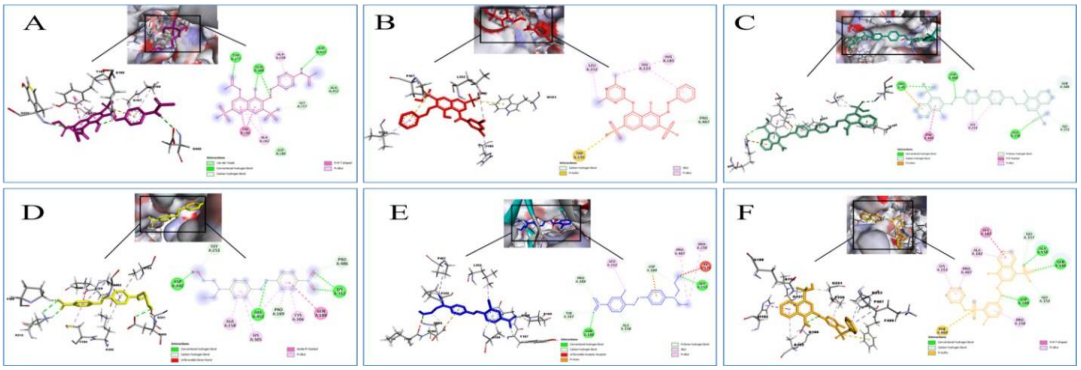

Fig. 2: The molecular interactions of enzyme oxidoreductase with the azo dyes (A) acid violet 7 (B) brilliant red (C) congo red (D) disperse red 1 (E) disperse red 13 (F) acid orange 19.

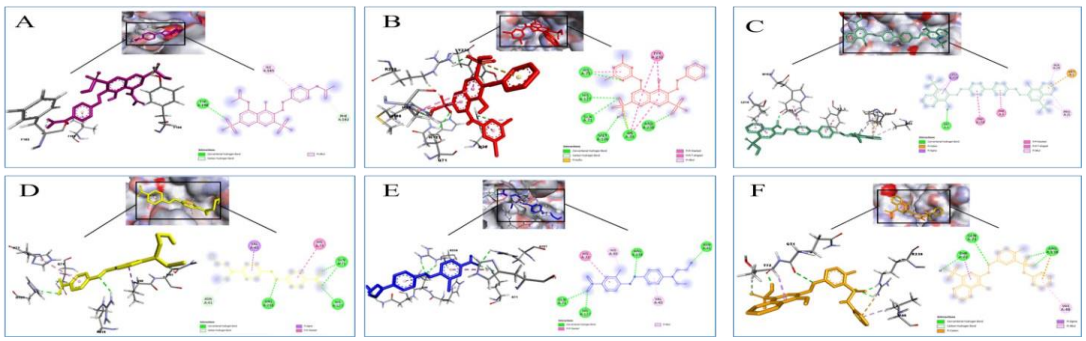

Fig. 3: The molecular interactions of enzyme laccase with (A) acid violet 7 (B) brilliant red (C) congo red (D) disperse red 1 (E) disperse red 13 (F) acid orange 19.

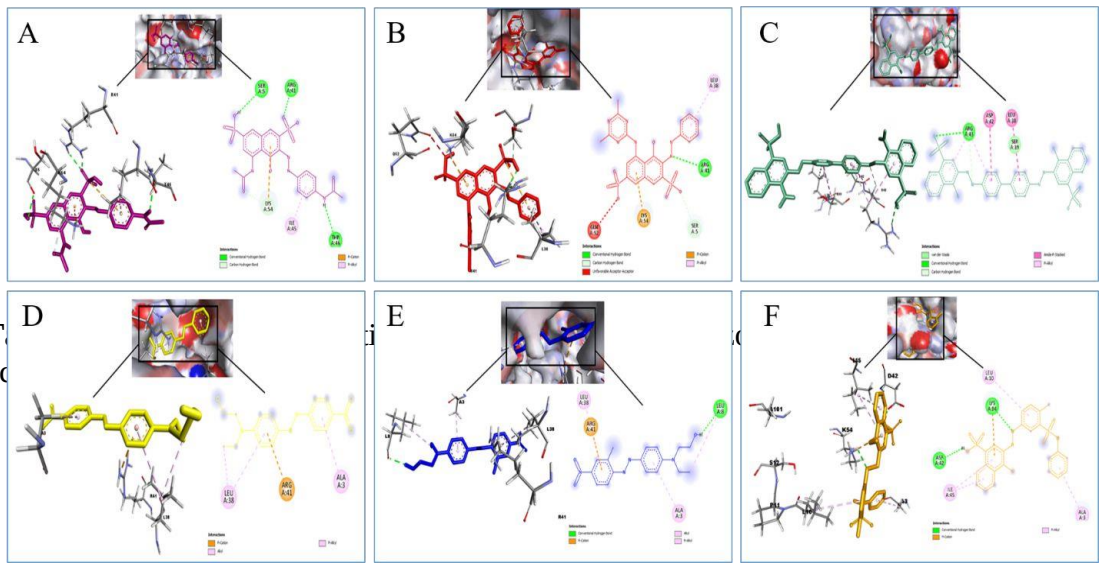

Fig. 4: The molecular interactions of enzyme peroxidase with (A) acid violet 7 (B) brilliant red (C) congo red (D) disperse red 1 (E) disperse red 13 (F) acid orange 19.

Name of dye	Binding Affinities (kcal/mol)		
	Laccase	**Oxidoreductase**	**Peroxidase**
Acid Violet 7	-6.2	-8.5	-6.3
Acid Orange19	-7.1	-9.0	-6.6
Congo Red	-7.5	-8.9	-6.9
Disperse Red 1	-5.9	-7.9	-4.3
Disperse Red 13	-6.0	-7.3	-4.9
Reactive Brilliant Red	-6.8	-9.1	-6.6

Consequently, the order of best interactions is oxidoreductase > laccase > peroxidase. Furthermore, the analysis of hydrogen bonds indicates that laccase and oxidoreductase establish a greater number of hydrogen bonds with the azo dyes, creating more stable complexes (Table 3).

Table 3. The details of amino acid residues from the selected enzymes of Acinetobacter junii forming H-bonds with azo dyes

	Laccase	**Oxidoreductase**	**Peroxidase**
Acid Violet 7	Y198	Q188, Y277, D442	S5, R41, T46
Acid Orange19	Q71, T72, R238	A158, D180, Q188	L54, D42
Congo Red	G6	R95, A158, D408	R43
Disperse Red 1	Q71, H127, R238	L312, D442, A452	0
Disperse Red 13	N41, Q73, H127, R238	G155, Q188	L8
Reactive Brilliant Red	H39, Q71, H73, M106, H127, R238	0	R41

Molecular Dynamic Simulations

The docked complexes of laccase, oxidoreductase, and peroxidase with azo dye acid orange 19 were further analyzed by the MD simulations. The conformational deviations of these complexes were analyzed based on the RMSD and RMSF (Figure 5).

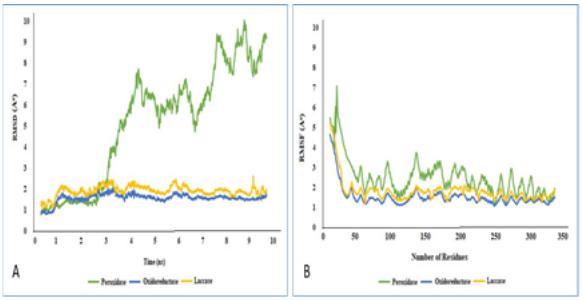

Fig. 5: Molecular Dynamic Simulation analysis of laccase, oxidoreductase, and peroxidase of *Acinetobacter junii* docked with the azo dye acid orange 19. **(A)** RMSD values of the docked complexes shows the minimum conformational deviations for oxidoreductase and laccase (yellow and blue), while the peroxidase (green) shows conformational deviations over most of

The trajectory analysis revealed that the enzyme oxidoreductase and laccase show minimum conformational deviations over the time compared to the peroxidase. These results indicate that the enzyme oxidoreductase and laccase from *Acinetobacter junii* forming the stable complexes with dyes can be used for the degradation of azo dyes.

DISCUSSION

The textile industry plays a pivotal part in the economy of Pakistan, however, the extensive use of azo dyes in this industry has raised significant environmental concerns (Hashemi and Kaykhaii, 2022). These dyes find their way into the water bodies where they block light penetration resulting in the inhibition of photosynthesis, resulting in an increase in the chemical and biological oxygen demands (Mehmood et al., 2016; Meghwal et al., 2020). Despite the availability of different wastewater treatment options, biological treatment using microbial enzymes appears to be the most promising method for clean degradation of azo dyes (Mishra et al., 2020). Numerous microbial enzymes have been reported for their ability to effectively decolorize and degrade azo dyes. Among these, peroxidases, laccases, and oxidoreductase are the most promising enzymes (Mahmood et al., 2017).

Recently the *Acinetobacter junii* has been identified in the wastewater samples of various regions in Pakistan (Fatima et al., 2015). The natural occurrence of this microorganism in wastewater underscores the potential of its enzymes to degrade the toxic azo dyes. However, the efficacy of this degradation depends upon the binding affinities of its enzymes with the azo dyes (Raj et al., 2014; Medfu et al., 2020). The present study is focused on analysis of molecular interactions and binding affinities of three enzymes: azoreductase, laccase, and peroxidase from *A. junii* with the six azo dyes, acid violet 7, acid orange 19, congo red, disperse red 1, disperse red 13, and reactive brilliant red. The rationale behind the selection of these three enzymes from *A. junii* lies in their well-established potential to degrade organic pollutants. To assess the molecular interactions of these enzymes with azo dyes, the three-dimensional structures of the selected enzymes were built using I-TASSER. As they lack experimentally determined 3D structures, so the structures of

respective enzymes predicted by software-based modelling by using an ab initio method (Chopra et al., 2023; Xuejiao et al., 2023). The quality of resulting protein models was rigorously assessed through a variety of parameters, including the Ramachandran plot, C-score, TM score, and RMSD values. In the absence of experimental structures, the model quality estimation is crucial to determine its potential applications for the further analysis (Zhang, 2008; Wang et al., 2016). The outcomes of these quality evaluators have revealed that the protein models exhibit a high level of accuracy and are suitable for subsequent analysis (Kim et al., 2016). Subsequently, the three-dimensional structures of enzymes and azo dyes were prepared for the molecular docking analysis through AutoDock Vina. This preparation step ensures that proteins and ligands are in appropriate formats for studying their molecular interactions.

The molecular docking analysis calculates the binding energies of each enzyme-dye complex in kcal/mol, providing insight into the affinity of each enzyme for the azo dyes. The more negative binding energy suggests the more stable complex where enzymes form stable interactions with the azo dyes and can degrade it effectively (Henrich et al., 2010). The results of molecular docking analysis revealed that enzyme oxidoreductase has the highest binding affinities towards all six selected azo dyes, followed by laccase, and peroxidase as indicated in Table 3. This suggests that oxidoreductase from *A. junii* is the most suitable enzyme for degrading the chosen azo dyes, followed by laccase and peroxidase. In addition to strong binding affinities, oxidoreductase and laccase also formed more stable complexes with azo dyes forming more H-bonds compared to peroxidase (Tables 2 and 3) (Figures 2, 3 and 4). While the various types of interactions contribute to the protein-ligand interactions, hydrogen bonding is the most stable, contributing stability to the complex (Kumar et al., 2016; Bitencourt-Ferreira et al., 2019). Consequently, the enzyme making the highest number of hydrogen bonds with azo dyes is expected to form the most stable complexes resulting in effective degradation (Chen et al., 2016).

Molecular docking analysis, due to its static nature, may not provide the comprehensive representations of protein-ligand interactions alone, as it overlooks the dynamic interplay between the protein and ligands (Tkaczyk et al., 2020). Therefore, the stability of protein-ligand complexes was further assessed through molecular dynamic simulations that provides insight to the into atomic-level

conformational patterns of protein-ligand complexes (Du et al., 2016; Fu et al., 2018; Haghshenas et al., 2016). The analysis of conformational deviations of the docked complexes, based on RMSD and RMSF values (Figure 5), revealed that the complexes of oxidoreductase and laccase with the chosen azo dyes exhibited minimal conformational deviations. This finding indicates that these two enzymes are better suited for forming stable complexes with the prevalent and toxic azo dyes present in wastewater, compared to peroxidase.

CONCLUSION

Our study demonstrates that oxidoreductase and laccase from *A. junii* can be considered for bioremediation applications in the treatment of textile and paper mill effluent based on binding affinities and molecular interactions with azo dyes. However, further wet-lab experimentation is imperative to determine the suitability of these enzymes for efficiently addressing the environment required for the elimination of azo dyes using biological tools.

ACKNOWLEDGEMENTS

This research is self-supported by the authors.

CONFLICT OF INTERESTS

The authors declare no conflict of interest.

REFERENCES

1. Ajaz M, Shakeel S, Rehman AJIM (2020). Microbial use for azo dye degradation-a strategy for dye bioremediation. Int. Microbiol. 23:149-159.
2. Bitencourt-Ferreira G, Veit-Acosta M, Azevedo WF (2019). Hydrogen bonds in protein-ligand complexes. In Docking screens for drug discovery, Springer. pp. 93-107
3. Chen A, Yang B, Zhou Y, Sun Y, Ding CJRS (2018). Effects of azo dye on simultaneous biological removal of azo dye and nutrients in wastewater. Royal Soci Open Sci. 5:180795.
4. Chen D, Oezguen N, Urvil P, Ferguson C, Dann SM, Savidge TC (2016). Regulation of protein-ligand binding affinity by hydrogen bond pairing. Sci. Adv. 25:e1501240.
5. Chopra NK, Singhal D, Saini R, Sondhi S (2023). Structure analysis and molecular docking studies of laccase from "*Bacillus licheniformis* NS2324." Sustainable Chem. Environ. 1:100004.
6. Du X, Li Y, Xia YL, Liang J, Sang P, Liu SQ (2016). Insights into protein-ligand interactions: Mechanisms, models, and methods. Int. J. Mol. Sci.17:144.

7. Fatima K, Afzal M, Imran A, Khan QMJB, Toxicology (2015). Bacterial rhizosphere and endosphere populations associated with grasses and trees to be used for phytoremediation of crude oil contaminated soil. Bull. Environ. Contam. Toxicol. 94:314-320.
8. Fu Y, Zhao J, Chen ZJC, Medicine MMI (2018). Insights into the molecular mechanisms of protein-ligand interactions by molecular docking and molecular dynamics simulation: A case of oligopeptide binding protein. Comput. Math. Methods Med.1: 3502514
9. Godswill AC, Gospel AC, Otuosorochi AI, Somtochukwu IV. (2020). Industrial and community waste management: Global perspective. Am. J. Phys.1:1-16.
10. Haghshenas H, Kay M, Dehghanian F, Tavakol HJJ, Dynamics (2016). Molecular dynamics study of biodegradation of azo dyes via their interactions with AzrC azoreductase. J. Biomol. Struct.Dyn. 34: 453-462.
11. Hashemi SH, Kaykhaii M (2022). Azo dyes: sources, occurrence, toxicity, sampling, analysis, and their removal methods. In Emerging freshwater pollutants, Elsevier, pp. 267-287
12. Henrich S, Feierberg I, Wang T, Blomberg, Wade RC (2010). Comparative binding energy analysis for binding affinity and target selectivity prediction. Proteins: Struct. Funct. Bioinf.78:135-153.
13. Huang GB, Zhu QY, Siew CKJN (2006). Extreme learning machine: Theory and applications. Neurocomputing. 70:489-501.
14. Kim S, Thiessen PA, Bolton EE, Chen J, Fu G, Gindulyte A, Shoemake, BAJN (2016). PubChem substance and compound databases. Nucleic Acids Res. 44:D1202-D1213.
15. Kumar P, Kumar AJS, Research QE (2020). *In silico* enhancement of azo dye adsorption affinity for cellulose fibre through mechanistic interpretation under guidance of QSPR models using Monte Carlo method with index of ideality correlation. SAR QSAR Environ. Res. 31:697-715.
16. Kumar SS, Shantkriti S, Muruganandham T, Murugesh E, Rane N, Govindwar SPJE (2016). Bioinformatics aided microbial approach for bioremediation of wastewater containing textile dyes. Ecol. Infor. 31:12-121.
17. Li J, Fu A, Zhang LJIS (2019). An overview of scoring functions used for protein-ligand interactions in molecular docking.

Computational Life Sci. 11:320-328.
18. Madhavi Sastry G, Adzhigirey M, Day T, Annabhimoju R, Sherman WJJ (2013). Protein and ligand preparation: Parameters, protocols, and influence on virtual screening enrichments. J. Comput Aided Mol. Des. 27:221-234.
19. Mahmood F, Shahid M, Hussain S, Shahzad T, Tahir M, Ijaz M, Babar SAKJB (2017). Potential plant growth-promoting strain Bacillus sp. SR-2-1/1 decolorized azo dyes through NADH-ubiquinone: oxidoreductase activity. Bioresour. Technol. 235:176-184.
20. Mahmood S, Khalid A, Arshad M, Mahmood T, Crowley DEJC (2016). Detoxification of azo dyes by bacterial oxidoreductase enzymes. Crit. Rev. Biotechnol. 36:639-651.
21. Majumdar R, Shaikh WA, Chakraborty S, Chowdhury SJMB (2022). A review on microbial potential of toxic azo dyes bioremediation in aquatic system. Microbial Biodeg. Biorem. 1:241-261.
22. Martínez LJ. (2015). Automatic identification of mobile and rigid substructures in molecular dynamics simulations and fractional structural fluctuation analysis. *10*(3), e0119264.
23. Medfu Tarekegn M, Zewdu Salilih F, Ishetu AIJCF (2020). Microbes used as a tool for bioremediation of heavy metal from the environment. Cogent Food Agric. 6:1783174.
24. Meghwal K, Kumawat S, Ameta C, Jangid NK (2020). Effect of dyes on water chemistry, soil quality, and biological properties of water. In Impact of Textile Dyes on Public Health and the Environment. IGI Global, pp. 90-114
25. Misal SA, Gawai KRJB (2018). Azoreductase: A key player of xenobiotic metabolism. Bioresour. Technol. 5:1-9.
26. Mishra S, Nayak JK, Maiti AJCT, Policy E (2020). Bacteria-mediated bio-degradation of reactive azo dyes coupled with bio-energy generation from model wastewater. Clean Technol. Environ. Policy 22:651-667.
27. Okafor CC, Madu CN, Ajaero CC, Ibekwe JC, Nzekwe CA, Okafor C, Nzekwe CJ (2021). Sustainable management of textile and clothing. Clean Technol. Recycl. 1:70-87.
28. Pinheiro LRS, Gradíssimo DG, Xavier LP, Santos AVJS (2022). Degradation of azo dyes: bacterial potential for bioremediation. Sustainability. 14:1510.
29. Raj A, Kumar S, Haq I, Singh SKJE (2014). Bioremediation and toxicity reduction in pulp and paper mill effluent by

newly isolated ligninolytic *Paenibacillus* sp. Ecol Eng. 71:355-362.
30. Rathour R, Patel DH, Madamwar D, Desai C (2023). Metagenomic analysis of a bioreactor biofilm treating raw textile effluent and biochemical characterization of a novel azoreductase gene. Agric.Biotechnol. 53:102876.
31. Samsami S, Mohamadizaniani M, Sarrafzadeh MH, Rene ER, Firoozbahr MJP (2020). Recent advances in the treatment of dye-containing wastewater from textile industries: Overview and perspectives. Process Saf. Environ. Prot. 143:138-163.
32. Singh PJJ (2022). Bioremediation of hazardous azo dye methyl red by a newly isolated *Enterobacter asburiae* strain JCM6051 from industrial effluent of Uttarakhand regions. J. Appl. Biol. Biotech. 10:64-72.
33. Tkaczyk A, Mitrowska K, Posyniak AJS (2020). Synthetic organic dyes as contaminants of the aquatic environment and their implications for ecosystems: A review. Sci. Tot. Environ. 717:137222.
34. Tülek A, Karataş E, Çakar MM, Aydın D, Yılmazcan Ö, Binay B (2021). Optimisation of the production and bleaching process for a new laccase from *Madurella mycetomatis*, expressed in *Pichia pastoris*: From Secretion to Yielding Prominent. Mol. Biotech. 63:24-39.
35. Wang W, Xia M, Chen J, Deng F, Yuan R, Zhang X, Shen FJD (2016). Data set for phylogenetic tree and RAMPAGE Ramachandran plot analysis of SODs in *Gossypium raimondii* and *G. arboreum*. Data Brief. 1:345-348.
36. Xuejiao A, Yi C, Ningjian L, Shulin Z, Liuwei W, Qinghua Z (2023). Green and sustainable approach for decoloration and detoxification of azo dye by bacterial-mediated thermo-halotolerant dye-decolorizing peroxidase (DyP). Process Biochem.130:334-346.
37. Zhang YJB (2008). I-TASSER server for protein 3D structure prediction. BMC Bioinformatics. 9:1-8.

LGU Journal of
LIFE SCIENCES

LGU Society of Life Sciences

DOI: https://doi.org/10.54692/lgujls.2024.0803349

Paper Submission: 4th Oct 2022; Paper Acceptance: 10th July 2024; Paper Publication: 10th Sep 2024

Research Article | LGU J. Life. Sci
Vol 8 Issue 3 July- Sep 2024 | ISSN 2519-9404
eISSN 2521-0130

Impact of Natural Polysaccharides Based Edible Coatings on Postharvest Physiology and Bioburden of Lycopersicon Esculentum

Hina Qaiser*[1,2], Mehlil Khalid[2], Farah Noreen[2]

1. School of Biological Sciences, University of the Punjab, Lahore, Pakistan
2. Department of Biology, Lahore Garrison University, Lahore, Pakistan

Corresponding Author's Email: hinaqaiser@lgu.edu.pk

ABSTRACT: *Edible coatings are a promising postharvest quality management treatment for shelf-life enhancement and marketability of the agriculture products. This study aims to evaluate the effects of polysaccharide based edible coatings on the mean life of un-ripened tomatoes (Lycopersicon esculentum). Fruits were treated with three different edible coatings Aloe vera gel (T1), tragacanth gum (T2) and Aloe vera gel-tragacanth gum (T3) for postharvest preservation and the mean life was analyzed at 20°C. They were then examined for various physiological, physiochemical and microbiological changes. The results revealed that all the applied formulations could retard the metabolic processes involved in tomato ripening. However, the combined effects of Aloe vera gel and tragacanth gum (T3) were most successful in positively maintaining the tomatoes since the fruits in this category recorded comparatively superior results for most of the analyzed parameters. They reached full maturity in 45 days compared to the control set which ripened in 14 days. This treatment led to a substantial postponement in weight loss, disease incidence, microbial growth and ripening index of tomatoes. A significant difference was observed in rate of colour change among treated and untreated samples (P <0.05). For decay assessment, Uncoated samples decayed after 4 weeks while coated samples (T-3 tomatoes) remained healthy for 60 days. For weight loss assessment, the samples receiving treatments T1, T2, and T3 showed 16.23%, 14.45%, and 10.23 % weight loss at 20°C respectively. Thus, storage life and safety of tomatoes can be extended using Aloe vera-tragacanth gum based edible coating which has the potential to be used as natural preservative.*

Keywords: *Tomatoes; Aloe vera; Tragacanth gum; Shelf Life; Edible coating; Postharvest*

INTRODUCTION

Tomatoes are quite rich in minerals, vitamins, vital amino acids, sugars and dietary fibers. They harbor ample amount of lycopene (71.6%), vitamin C (12.0%), pro vitamin A carotenoids (14.6%) and vitamin E (6.0%) (García-Closas et al., 2004). Lycopene, primarily accountable for the distinctive deep red color, holds strong antioxidant properties hence able to reduce the risk of certain human cancers related to prostate, lung and stomach and chronic ailments such as cardiovascular disease (Heber, 2004). As per World Health Organization (WHO) estimates, lower consumption of fruits and vegetables is among the highest risk factors contributing to the mortality rates of 2.7 million deaths each year (Hartley et al., 2013). Preservation of vegetables and fruits is a great challenge for the world. According to rough estimates about 30-40% of vegetables/fruits are wasted due to improper and deficient processing facilities (Tiwari and Cummins, 2013). Being a climacteric fruit, respiration and transpiration primarily determine its storage life and quality of tomatoes. However, effects of these processes can be curtailed using a physical barrier for oxygen diffusion and moisture migration. Storage at low temperatures is the traditional strategy used to postpone and/or decrease ethylene synthesis, yet this approach may result in chilling harm (Singh and Shalini, 2016). In order to lower pathogen levels, pesticides and sanitizers are frequently used; however, their application can leave residues that could beyond the maximum permissible limits, which could be extremely harmful to human health (Singh and Shalini, 2016).

Recent studies have concentrated on investigating better and more effective postharvest processing and preservation methods to overcome these issues. Applying edible coatings has been a popular substitute among these methods for prolonging the postharvest shelf life of tomato fruit (Yaashikaa et al., 2023).

Edible coatings are a promising postharvest quality management treatment for marketability of the agriculture produce. Minimization of post-harvest losses would reduce the production cost, trade and distribution, increasing the farmer’s income and lowering the price for the consumers (Kiaya, 2014). Moreover, , two fungi that

can colonize damaged fruits during harvesting and handling and quickly spread to neighbouring fruits, causing large losses, are capable of attacking tomatoes (Tahmasebi et al., 2020*)*. When tainted tomatoes are consumed, bacterial illnesses, such as *Escherichia coli*, can also be harmful to human health. Currently, edible coatings are becoming a popular treatment when it comes to keeping intact the quality factors of fruits (Galgano, 2015). They provide a semi-permeable barricade for carbon dioxide and oxygen transfer, moisture and the movement of solute, thereby plummeting respiration, water loss and oxidation. This supports in regulating the quality control of the fruits (Mahfoudhi and Hamdi, 2015). The leeway in postharvest life of the fruits and vegetables and their quality critically depends upon reduction in desiccation, decline in physiological processes of maturation and senescence and slower rates of microbial growth (Rico et al., 2007). In addition, another important benefit is the decreased synthetic packaging waste since the coatings are made up of biodegradable raw material. The potential of *Aloe vera* and tragacanth based edible coatings in food preservation has been highlighted by recent studies. et al. Tarangini (Hadi et al., 2022; Mohebbi et al., 2014; Mohebbi et al., 2012).

In this study, three different edible coating viz., *Aloe gel*, tragacanth gum and *Aloe Vera* gel/tragacanth gum-based formulations have been used with the aim to enhance the shelf life of tomatoes with preserving the organoleptic quality.

MATERIALS AND METHODS

Sample Collection

Fresh tomato fruits (*Lycopersicum esculentum*) harvested at mature green stage were taken from a commercial market in Lahore, Pakistan. The fruits were selected based upon their size, weight, color, and physical appearance to maintain the uniformity in the sampling.

Preparation of the natural extracts

Aloe vera (*Aloe barbadensis*) leaves were washed with chlorine water (25%) and colorless hydro parenchyma was taken out. The excised gel matrix was grinded, and the solution was filtered to remove fibers. The extract was pasteurized and stored at ambient temperature. The tragacanth gum

(*Astragalus gummifer*) crystals were pulverized and sieved to get fine powder. 0.5% gum solution was prepared in distilled water and heated at 40°C for 10 mins and kept overnight under ambient conditions to fully hydrate. Next day, it was pasteurized and stored in an amber bottle.

Edible coating formulations and treatment

After extracts preparation, three different types of coating solutions were formulated as T1 (20 ml of *Aloe vera* gel extract, 0.5 g of CaCl2, 5 ml of lemon juice), T2 (20 ml of Tragacanth gum extract, 0.5 g of CaCl2, 5 ml of lemon juice) and T3 (10 ml of *Aloe vera* gel extract, 10 ml of tragacanth gum extract, 0.5 g of CaCl2, 5 ml of lemon juice). 1% agar was added to each of the above-mentioned coating formulations which were then heated slightly to dissolve it.

The experimental group of tomatoes were first dipped in the neem water followed by immersion in each edible coating formulation for 5 mins, air dried, packaged into zip locked polyethylene bags and stored at 20°C.

Parameters and Analysis

Evaluation was carried out of microbiological, physiochemical and sensory attributes. Tomatoes were observed for 3 days interval for their organoleptic qualities and 14 days interval for microbial load till 8 weeks.

Physiological studies

Physiological factors such as fruit color, firmness, weight loss and decay percentages were explored as an index of fruit quality during storage post treatments. The variations in the skin color were logged by comparing with a standard color chart (Royal Horticultural Society color chart).

Weight loss was determined as the percentage loss of the initial fresh weight using the method of Athmaselvi et al. (2013). Firmness was estimated through the reduction in girth size of coated and uncoated tomatoes. A measuring tape was used to measure the same at weekly intervals (Goyal et al., 2017). The decay incidence was recorded based on visual inspection of each fruit for infection and their percent decay using (Abdullah et al., 2017).

Physiochemical Studies

Physiochemical changes in pH, titratable acidity and reducing sugars were examined to study the

progression of ripening. The pH of the juice was measured after every 7 days via pH meter. Titratable acidity was estimated by titrating 5 ml of tomato juice in 10 ml distilled water against 0.1 N NaOH (Abebe et al., 2017). The amount of reducing sugar present in tomatoes was determined by DNS (3,5 Dinitrosalicylic acid) method (Miller, 1959).

Microbiological Studies

A serial dilution method was used for microbiological studies. The total viable microbial count was observed on Nutrient agar, MacConkey agar and Potato Dextrose agar.

Statistical Analysis

The results were validated by Costat 6.4 using a completely randomized block design. The means were compared using ANOVA and Duncan's New Multiple Range test at $p \leq 0.05$ with three replicates.

RESULTS AND DISCUSSION

Physiological Parameters

Color and physical transformations of tomatoes during storage

Color is an important index of fruit ripening and consumer acceptability. The tomato fruit undergoes color transitions due to chlorophyll degradation and formation of carotenoids (Abebe et al., 2017). In this study, mature green tomatoes turned tarnished yellow to red in color indicating the progression of ripening (Fig. 1a). A significant difference was observed in rate of color change among treated and untreated samples ($P < 0.05$). Control group changed color more rapidly than the experimental group and reached the 6^{th} stage of maturity within 20 days at 20°C. *Aloe vera* gel (T1) coated fruits ripened within 35 days in storage while tragacanth gel (T2) coated samples turned red (6^{th} stage) after 40 days. However, the combination of both gel formulations (T3) retarded color and physiological changes at maximum since the fruits receiving this treatment ripened in 45 days. Investigations carried out by Bhatnagar (2018) also indicated retardation in color development of tomatoes treated with *Aloe vera* gel based coatings as per the slow rate of respiration and decreased ethylene production. The altered atmosphere in the fruit formed by the edible coatings delimited the respiration rate deferring color variation. Preeminent CO_2 levels (>1%) in fruit tissues attained by

coating materials may also slow down fruit ripening by constraining ethylene production (Zapata et al., 2008).

Fruit firmness also dictates the postharvest life and fruit quality. The degradation of cell wall components may render the fruit susceptible to different postharvest handling factors. The loss in width diameter was taken as an index of decrease in fruit firmness during ripening (Fig. 1b).

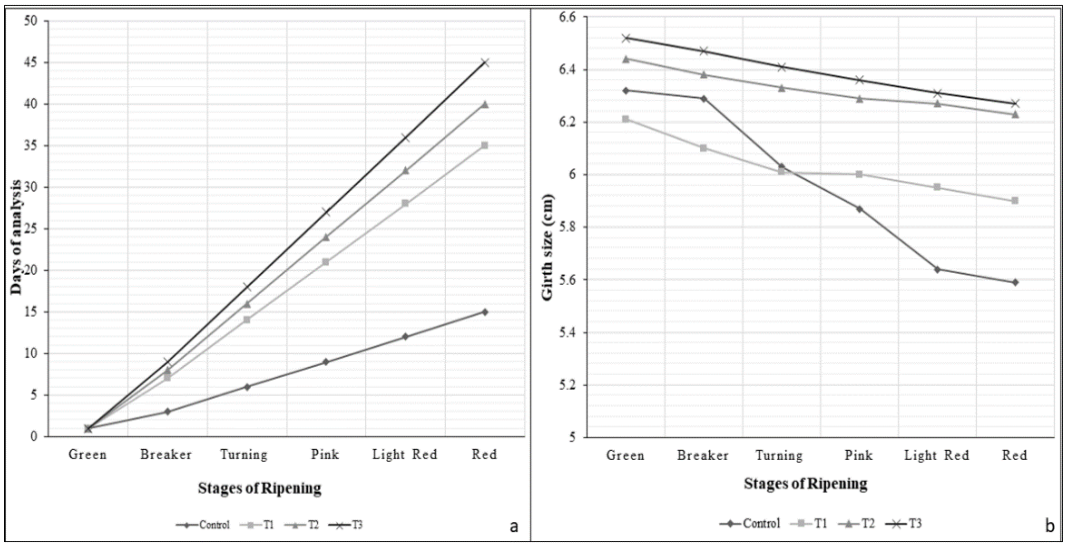

Fig. 1. Comparative analysis of ripening behavior and fruit firmness of Tomatoes following edible coating treatments (a) Progression of ripening in treated and control tomatoes (b) Changes in the girth size of treated and control tomatoes

The coated tomatoes were significantly firm for a longer period than the controls ($P < 0.05$) which indicated a 12% loss in width diameter till mature red stage. In contrast, the treated samples sustained a high degree of firmness with only 4 to 5% decrease in width diameter until red stage. The decrease in firmness results from the breakdown of pectin and starch present in the cell wall by enzymes such as hydrolases, pectin esterase, and polygalacturonase produced during ripening (Jahanshahi et al., 2018). The above findings are in line with the previous studies in which *Aloe vera* gel and tragacanth gum based edible coatings were able to cause firmness retention in cherries, grapes and strawberries

(Emamifar and Bavaisi, 2017, Martínez-Romero et al., 2006).

Decay Assessment

Both coated and uncoated samples showed zero decay percentage up to 18 days (Table 1).

Table 1. Effect of edible coatings on the spoilage rate of tomatoes stored at 20°C

Days of storage	Percentage of spoilage (%)			
	Control	T1	T2	T3
1	0	0	0	0
5	0	0	0	0
10	0	0	0	0
15	0	0	0	0
20	0	0	0	0
25	65.3	0	0	0
30	D	0	0	0
35	-	0	0	0
40	-	16.5	0	0
45	-	67.8	0	0
50	-	D	0	0
55	-	-	14.8	0
60	-	-	57.5	0

Uncoated samples decayed after 4 weeks while coated samples (T-3 tomatoes) remained healthy for 60 days. The antagonistic action of the edible coatings used against the decay causing microorganisms are primarily attributed to the presence of compounds such as polysaccharides, mannans, anthraquinones, and lectins (Monjezi et al., 2019, Thiruppathi et al., 2010). Mohebbi et al (2012) has also reported that the synergistic application of the *Aloe vera* and tragacanth gum based edible coating was most effective in positively maintaining the quality of button mushrooms.

Weight Loss

This quality parameter is crucial since every loss in weight can be translated into economic loss. Fig. 2 shows the percentage weight loss of the coated and uncoated samples.

The results revealed that weight loss occurred at a faster rate in case of controls. The samples receiving treatments T1, T2, and T3 showed 16.23%, 14.45%, and 10.23 % weight loss at 20°C respectively. This was significantly different compared to 23.61% weight loss in the control tomatoes at this temperature ($P < 0.05$).

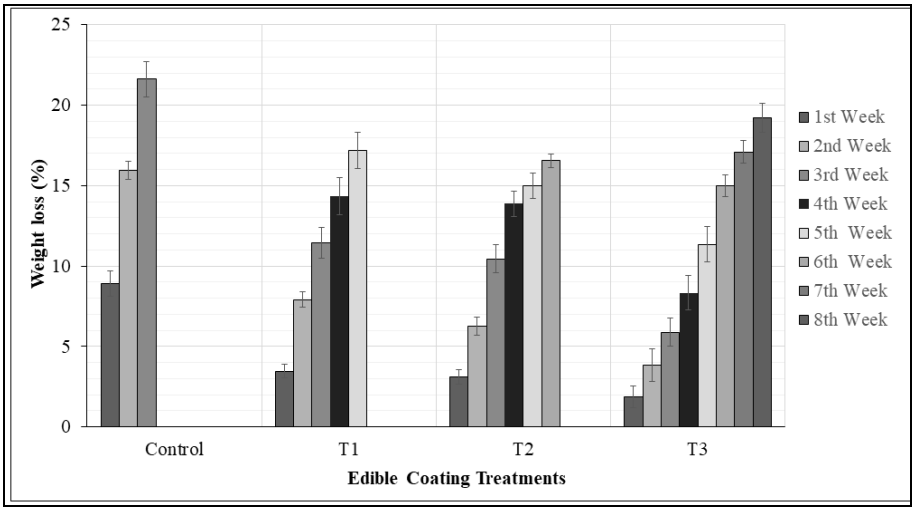

Fig. 2. Comparative analysis of % weight loss between coated and control tomatoes

The post-harvest weight losses generally results from water loss through transpiration (Ergun and Satici, 2012). The guard cells and stomata present in the epidermal layers control the gaseous exchange and loss of moisture from the fruit surface. The covering formed by the edible coatings provides a semi permeable physical barrier to limit the moisture loss (Toğrul and Arslan, 2004). This may also interferes with the level of oxygen uptake by the fruit, retarding the rate of respiration and its associated weight loss (Abbasi et al., 2009). The previous investigation carried out by Emamifar and Bavaisi (2017) also supported the present study and described that *Aloe vera*-tragacanth gum treatment expressively reduced the weight loss levels in strawberries.

Physiochemical Parameters

Effect on pH, titratable acidity and reducing sugar content

Acidity constitutes a crucial quality aspect that greatly affects the fruit taste. The effect of different coating formulations on the pH of tomato fruits is presented in Fig. 3a. The pH value is mainly dependent upon the acid content of the fruit. The pH value showed a progressive increase with the advancement in maturity during the storage period. The control set had the highest pH value of 4.19 after 3rd week of storage. In contrast, all the treated fruits had lower pH values in that period. The fruits receiving the

treatment T3 had the lowest pH value of 4.09 when they reached the red stage of maturity after the 8th week of storage. Low pH values related to higher acidity in coated fruits might be accounted by reduced respiration rates due to restricted oxygen availability (Jiang and Li, 2001). Athmaselvi et al (2013) and Abebe et al (2017) also stated that, aloe vera treated tomato fruits were superior in keeping pH and exhibited a healthier response in contrast with untreated fruit.

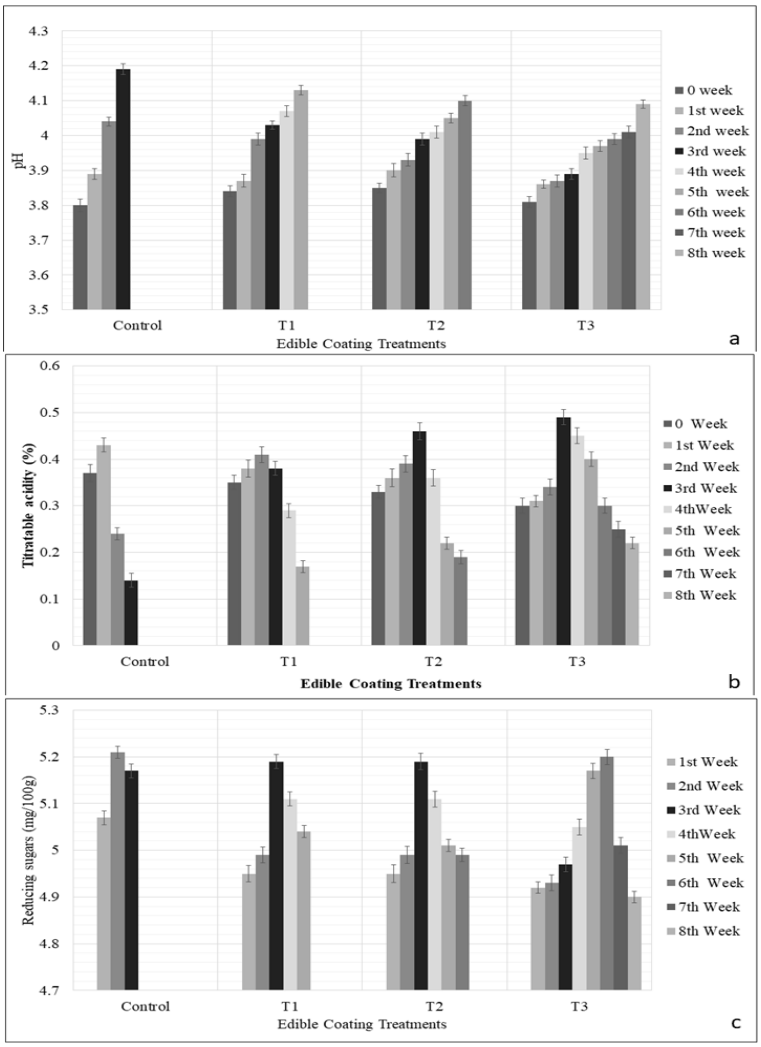

Fig. 3. Comparative analysis of (a) pH, (b) titratble acidity and (c) reducing sugar content between coated and control tomatoes

Tomatoes are highly susceptible to after harvest respiration activity because the organic acid, especially citric acid, undergoes metabolism to provide mediators to the tricarboxylic acid cycle with a rise in respiration. Tomato titratable acidity decreases during ripening. Coated tomatoes showed a statistically higher titratable acidity during the experiment (P = 0.05). Titratable acidity of the tomatoes decreases with storage time (Fig. 3b). The acid content peaks as the tomatoes undergo transition from mature green to turning stage but thereafter shows a decline with the onset of light red stage. The uncoated tomatoes experienced significantly ($p < .05$) greater reduction in acidity from initial day (0) to end day of storage (12) and the value drops from 1.01% to 0.22%. The coated tomatoes showed a slower decline in acidity. The slower decline in acidity values in samples that were coated indicated a decrease in the rate of transpiration due to a decreased accessibility of organic acids, that is important for acidity in fruits. The gradual change in the acid concentrations of the experimental groups compared with the control indicated that edible coatings were effective in delaying the metabolic changes occurring in the treated fruits. The uncoated fruits showed reduced TA values for the ripened stage (0.14%) because of the rapid conversion of organic acids into sugars. The degrees of titratable acidity in coated fruits were considerably maintained with T3 (0.22%) exhibiting the most positive results. It has been reported that tragacanth and *Aloe vera* gum worked well to maintain the titratable acidity of coated strawberries in comparison to the controls (Nasar et al., 2023). As the ripening progresses, the acids present in the fruit might be converted into sugars, used in respiration or other cellular activities. The edible coatings slow down the rate of acid metabolism. Since organic acids (malic or citric acid) can be utilized as primary substrates for respiration, a decrease in acidity is seen in terms of upsurge in respiration of cells of fruits.

During the storage, total reducing sugar rose markedly from mature green stage to the onset of yellow pigmentation with the propensity to decrease as the ripening progressed (red stage) (Fig. 3c). These changes were analogous to both control and experimental

groups however the transition was slow with the treated tomatoes since the process of ripening had been retarded by the edible coatings. The tomatoes in all the three treatments T1, T2 and T3 showed the lowest reducing sugar content values i.e., 5.01, 4.95 and 4.93 mg/ml respectively than the control group (5.14 mg/ml) as they ripened completely.

Microbiological Analysis

Aloe vera and Tragacanth gum have both received attention as a food preservative due to their antimicrobial activity against a wide range of bacteria, yeast and fungi. There may be synergistic benefits when using tragacanth gum and aloe vera. The direct antibacterial action of *Aloe vera* is complemented by the protective layer that tragacanth gum helps build for efficacy. The antagonistic action of *Aloe vera* gel against microorganisms has been credited to the presence of natural anthraquinones (Reynolds and Dweck, 1999). The geraniol and carvacrol of tragacanth also exhibit broad spectrum antimicrobial effects (Jahanshahi et al., 2018). The antimicrobial constituents of the edible *Aloe vera* and Tragacanth-based coatings retards the growth rate of microorganisms that directly affect the quality of tomatoes. The coatings serve to limit the gaseous exchange along with the moisture and nutrients availability which are the stakeholders of microbial development. Furthermore, protective coatings prevent the subsequent microbial contamination during storage (Rong-yu and Yao-wen, 2003). The significant effect of applied edible coatings on total viable bacterial and fungal counts of tomato fruits obtained on nutrient agar, MacConkey agar and Potato Dextrose agar is shown in fig. 4.

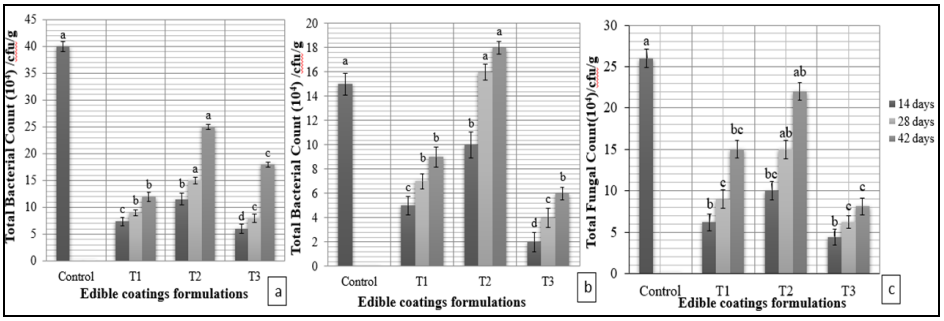

Fig. 4. Comparative analysis of bioburden exhibited by coated and control tomatoes (a) Total viable bacterial count observed on Nutrient agar (b) Total bacterial count observed on MacConkey agar (c) Total fungal count observed on Potato dextrose agar

All the applied coatings exhibited antagonist behavior against bacteria and fungi as observed by the lesser bioburden isolated from treated fruits in comparison to that of control fruits. The bacterial count increased gradually as the days progressed in the case of coated tomatoes but remained low in comparison to the control tomatoes. For instance, after six weeks of storage T3 registered the total viable bacterial count of 8.1 $\times$ 10^4cfu/g (nutrient agar), less than the one for the control tomatoes after 2 weeks. A significant growth inhibition of gram-negative bacteria was witnessed for T3 as seen on MacConkey agar. The effects of all the treatments on total viable bacterial count vary significantly from each other at $p \leq 0.05$. The ability of edible coatings to retard the fungal growth depended upon the nature of applied coatings. The data clearly showed that the fungal load of tomato fruits was considerably higher than that seen for the total bacterial load. A significant reduction was deployed by the T1 and T2. However, the most effective results were noted for the T3 since maximum fungal growth inhibition was registered by the T3 treatment. The effects of all the treatments on total viable fungal count vary significantly from each other at $p \leq 0.05$.

CONCLUSION

The comparative analysis of physical, physiochemical and microbiological parameters revealed that *Aloe vera*-Tragacanth coating (T3) was proven to be the most efficient natural treatment to extend the shelf life of tomatoes up to 8 weeks. *Aloe vera* and tragacanth gum are being investigated as preservatives in fruits, vegetables, meats, and other perishable foods because of their natural origins and proven antibacterial activity. Although these natural ingredients have a lot of potential, more study is required to determine their safety and effectiveness for a range of food preservation applications.

Edible coating offers a layer of defense that prevents food from spoiling in addition to fixing surface damage to the fruit. Natural polymers for bio-preservation of fruits appears to be a low cost, ecofriendly alternative to conventional physical and chemical treatments and would be reasonable for building up a biological process for large scale production.

ACKNOWLEDGEMENT

N/A

CONFLICT OF INTEREST

Authors declare no conflict of interest.

REFERENCES

1. Abbasi NA, Iqbal Z, Maqbool M, Hafiz IA (2009). Postharvest quality of mango (Mangifera indica L.) fruit as affected by chitosan coating. Pak. J. Bot. 41(1):343-57.

2. Abdullah R, Qaiser H, Farooq A, Kaleem A, Iqtedar M, Aftab M, Naz S (2017). Evaluation of microbial potential and ripening behaviour of preclimacteric bananas following gamma irradiation. Biosci. J. 33(1).

3. Abebe Z, Tola YB, Mohammed A (2017). Effects of edible coating materials and stages of maturity at harvest on storage life and quality of tomato (Lycopersicon esculentum Mill.) fruits. Afr. J. Agric. Res. 12(8): 550-65.

4. Athmaselvi K, Sumitha P, Revathy B (2013). Development of Aloe vera based edible coating for tomato. Int. Agrophys. 27(4):369-75.

5. Bhatnagar T (2018). Studies to enhance the shelf life of tomato using Aloe vera and neem based herbal coating. J. Postharvest Technol. 6(2): 21-28.

6. Emamifar A, Bavaisi S (2017). Effect of mixed edible coatings containing gum tragacanth and Aloe vera on postharvest quality of strawberries during storage. Iran Sci Technol Res. 13(3):39-54.

7. Ergun M, Satici F (2012). Use of Aloe vera gel as biopreservative for ‘Granny Smith’ and ‘Red Chief’ apples. J. Anim. Plant Sci. 22(2):363-68.

8. Galgano F (2015). Biodegradable packaging and edible coating for fresh-cut fruits and vegetables. Ital. J. Food Sci. 27(1):1-20.

9. García-Closas R, Berenguer A, Tormo MJ, Sánchez MJ, Quiros JR, Navarro C, et al. (2004). Dietary sources of vitamin C, vitamin E and specific carotenoids in Spain. Br. J. Nutr. 91(6):1005-11.

10. Goyal K, Chawla A, Grover P, Prakash S (2017). Increasing the shelf life of tomato using Aloe vera. J. Biospectra. 2(1):25-27.

11. Hadi A, Nawab A, Alam F, Zehra K (2022). Alginate/aloe vera films reinforced with

tragacanth gum. Food Chem Mol Sci. 4:100-5.

12. Hartley L, Igbinedion E, Holmes J, Flowers N, Thorogood M, Clarke A, et al. (2013). Increased consumption of fruit and vegetables for the primary prevention of cardiovascular diseases. Cochrane Database Syst Rev. 2013;(6)

13. Heber D (2004). Vegetables, fruits and phytoestrogens in the prevention of diseases. J Postgrad Med. 50(2):145.

14. Jahanshahi B, Jafari A, Vazifeshenas MR, Gholamnejad J (2018). A novel edible coating for apple fruits. J Hortic Postharvest Res. 1(1):63-72.

15. Jiang Y, Li Y (2001). Effects of chitosan coating on postharvest life and quality of longan fruit. Food Chem. 73(2):139-43.

16. Kiaya V (2014). Post-harvest losses and strategies to reduce them. Technical Paper on Postharvest Losses, Action Contre la Faim (ACF). 25L1-25.

17. Mahfoudhi N, Hamdi S (2015). Use of Almond Gum and Gum Arabic as novel edible coating to delay postharvest ripening and maintain sweet cherry (Prunus avium) quality during storage. J Food Process Pres. 39(6):1499-1508.

18. Martínez-Romero D, Alburquerque N, Valverde J, Guillén F, Castillo S, Valero D, et al. (2006). Postharvest sweet cherry quality and safety maintenance by Aloe vera treatment: a new edible coating. Postharvest Biol Technol. 39(1):93-100.

19. Miller GL (1959). Use of dinitrosalicylic acid reagent for determination of reducing sugar. Anal Chem. 31(3):426-28.

20. Mohebbi M, Ansarifar E, Hasanpour N, Amiryousefi MR (2012). Suitability of Aloe vera and gum tragacanth as edible coatings for extending the shelf life of button mushroom. Food Bioprocess Technol. 5(8):3193-203.

21. Mohebbi M, Hasanpour N, Ansarifar E, Amiryousefi MR (2014). Physicochemical properties of bell pepper and kinetics of its color change influenced by Aloe vera and gum tragacanth coatings during storage at different temperatures. J Food Process Pres. 38(2):684-93.

22. Monjezi J, Jamaledin R, Ghaemy M, Makvandi P (2019). Antimicrobial

modified-tragacanth gum/acrylic acid hydrogels for the controlled release of quercetin. J Appl Chem Res. 13(1):57-71.

23. Nasar S, Bashir I, Muawiya MA, Khattak MA, Yousaf S, Yousaf A (2023). Effect of bio-preservatives on the shelf life of tomato fruit (Lycopersicon esculentum Mill). J Xi'an Shiyou Uni. 66(05):233-54.

24. Reynolds T, Dweck AC (1999). Aloe vera leaf gel: a review update. J Ethnopharmacol. 68(1-3):3-37.

25. Rico D, Martin-Diana AB, Barat JM, Barry-Ryan C (2007). Extending and measuring the quality of fresh-cut fruit and vegetables: a review. Trends Food Sci Technol. 18(7):373-86.

26. Rong-yu Z, Yao-wen H (2003). Influence of hydroxypropyl methylcellulose edible coating on fresh-keeping and storability of tomato. J Zhejiang Univ Sci A. 4(1):109-13.

27. Singh S, Shalini R (2016). Effect of hurdle technology in food preservation: a review. Crit Rev Food Sci Nutr. 56(4):641-49.

28. Tahmasebi M, Golmohammadi A, Nematollahzadeh A, Davari M, Chamani E (2020). Control of nectarine fruits postharvest fungal rots caused by *Botrytis cinerea* and *Rhizopus stolonifer* via some essential oils. J Food Sci Technol. 57:1647-55.

29. Thiruppathi S, Ramasubramanian V, Sivakumar T, Thirumalaiarasu V (2010). Antimicrobial activity of Aloe vera (L.) Burm. f. against pathogenic microorganisms. J Biosci Res. 1(4):251-58.

30. Tiwari U, Cummins E (2013). Factors influencing levels of phytochemicals in selected fruit and vegetables during pre- and post-harvest food processing operations. Food Res Int. 50(2):497-506.

31. Toğrul H, Arslan N (2004). Extending shelf-life of peach and pear by using CMC from sugar beet pulp cellulose as a hydrophilic polymer in emulsions. Food Hydrocolloids. 18(2):215-26.

32. Yaashikaa P, Kamalesh R, Kumar PS, Saravanan A, Vijayasri K, Rangasamy G (2023). Recent advances in edible coatings and their application in food packaging. Food Res Int. 173:113366.

33. Zapata PJ, Guillén F, Martínez-Romero D, Castillo S, Valero D, Serrano M (2008). Use of alginate or zein as edible coatings to delay postharvest ripening process and to maintain tomato (Solanum lycopersicon Mill) quality. J Sci Food Agric. 88(7):1287-93.

LGU Journal of
LIFE SCIENCES

LGU Society of Life Sciences

DOI: https://doi.org/10.54692/lgujls.2024.0803350

Paper Submission: 4th Oct 2022; Paper Acceptance: 10th July 2024; Paper Publication: 10th Sep 2024

Review Article | LGU J. Life. Sci
Vol 8 Issue 3 July- Sep 2024 | ISSN 2519-9404 eISSN 2521-0130

Evaluating the Environmental Impact of Metal Oxide Nanoparticles: An Ecotoxicological Perspective

Fatima Tu Zahra*[1], Izza Taufiq[2], Ayesha Siddiqa[1]

1. Institute of Microbiology and Molecular Genetics, University of the Punjab, Lahore
2. National Centre of Excellence in Molecular Biology, University of the Punjab, Lahore

Corresponding Author's Email: fatimatuzahra2015@gmail.com

ABSTRACT: *Various nanoparticles (NPs) from the food industry, pharmaceuticals, cosmetics, and drugs significantly impact our daily lives. The association of these nanoparticles with the cellular environment adversely affects the normal functioning of cells and their components. For this review approximately 150 research papers were extensively reviewed, and information gathered from 100 articles were included. This review examines the nanotoxicology of metal oxides and their effects at both in vivo and in vitro levels. It addresses factors related to the synthesis of biogenic metal oxide NPs, including size, concentration, and exposure methodologies. The primary goal is to understand the ecotoxicology of metal oxides, their risk evaluation, and public health implications. Offering a concise overview, this article discusses current understanding and future research avenues in nanoparticle biology. It highlights the complications and risks to public health posed by toxic metal oxides and emphasizes the importance of understanding the synthesis of nanoparticles to determine their physicochemical properties. Biological interactions of these NPs with the environment pose significant hazards to human health. Recent studies have advanced our knowledge of the emerging trends and prospects in nanoparticle ecotoxicology. This review provides a comprehensive outline of the objectives and domains of various toxicological impacts of nanoparticles, emphasizing a balanced approach to managing risks to ecosystems and human health.*

Keywords: *Bioremediation, Cytotoxicity, Drug delivery, Nanotoxicology*

INTRODUCTION

Nanotoxicology is a rapidly expanding research area focusing on the safety concerns of nanoparticles (NPs) and their wide applications across various disciplines. It primarily assesses the ecotoxicity and lethal impacts of NPs on human cells. NPs, ranging from 1 to 100 nm, are aggregates of atomic particles with unique properties due to their quantum-scale dimensions and significant surface area to volume ratio. These particles are often composed of inert elements such as zinc, magnesium, iron, copper, cobalt, tin, and gallium.

Research has shown that metal oxide NPs often consist of multiple metals, including titanium, iron, chromium, nickel, and zinc (Sanderson et al., 2014). NPs can cause severe biological effects, such as DNA damage and apoptosis due to free radical production (Tee et al., 2016). Additionally, exposure to toxic NPs can alter cell proliferation and lead to chronic health issues. The rapid development of new NPs with unique properties poses potential health risks to the environment.

Traditional methods for generating metal oxide NPs rely on physical and biochemical techniques that use expensive and hazardous chemicals, contributing to environmental harm (Seabra and Durán, 2015). Biogenic synthesis involves using capping agents to stabilize nanomaterials, improving biocompatibility and preventing aggregation. Various metal nanoparticles, including cobalt oxide, bismuth trioxide, copper oxide, iron oxide, tin oxide, gold, and silver NPs, have been extensively studied for their adverse effects on living systems and guidelines for safe use (Demir, 2021). The following section will briefly describe the biogenic synthesis of these metal oxide NPs and their environmental applications.

1. Types of NPs

Two major groups of NPs are classified according to their nature and origin. They are either naturally produced or artificially synthesized by a physical or a chemical process. These are generated through mechanisms taking place in nature or by engineered activities.

Nanoparticles (NPs) are naturally found in volcanic eruptions, deep oceans, forest fires, and crushed rocks such as silica (SiO2), titanium dioxide, iron oxides, and manganese oxides. Natural NPs are present in many living organisms, with examples including carbon nanotubes and fullerenes (Guo and Barnard, 2013). These NPs often have reproducible structures and are biocompatible, such as mesoporous silica nanoparticles (MSNs) and protein nanoparticles (Griffin et al., 2017). They can exist intracellularly or

extracellularly, with viruses and liposomes being notable examples (Harish et al., 2022).

1.1. Mechanism of Action of Protein NPs

Protein nanoparticles (NPs) are extensively used in biological processes due to their high stability, making them effective for drug delivery. Besides stability, they also facilitate biodegradation and bioaccumulation (Herrera Estrada and Champion, 2015). Protein NPs are preferred over engineered NPs because they are non-antigenic, have lower immunogenicity and toxicity, and can be easily incorporated into various biopolymers.

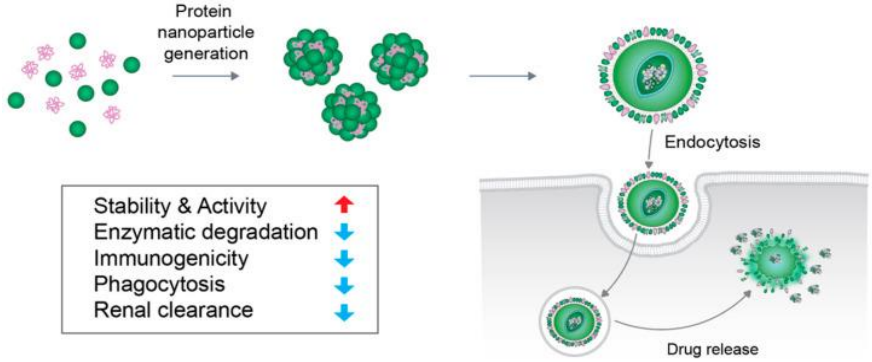

Fig. 1. The endocytosis process used for the delivery of various protein NPs and insoluble drugs in vivo (Hong et al., 2020)

Protein nanoparticles are also utilized for delivering non-soluble drugs within the internal cell region by the mechanism of endocytosis. These NPs show more protection from various processes like toxicity, degradation by enzymes, phagocytic reactions and endocytosis and hence increase the life and stability of the drug being introduced, as shown in Figure 1 (Hong et al., 2020). These protein NPs are prepared through a complex physical and chemical method following a self-assembly method.

1.2. Engineered NPs

Such NPs are specifically manufactured and have a particular morphology and geometry e.g. quantum nano-dots, gold and silver NPs (Montano et al., 2014). Because of their definite shape and structure, they are easily made through chemical process. They are found in composition with other materials like a layer of gold or a central element such as gold covered with a shell made up of any other element like cobalt or silica (Flannery et al., 2015).

2. Metal Oxide NPs

2.1. Cobalt Oxide (Co_3O_4) Nanocrystals

Cobalt oxide nanocrystals have various applications due to their desirable properties, i.e. optical magnetic and electrochemical capabilities. They are used as supercapacitors in different kinds of devices for the purpose of storing energy. (Abdel Maksoud et al., 2021). For the biogenic formation of Co_3O_4 nanocrystals thermal and solvothermal decomposition routes are usually the main classical methods. A marine bacterium *Brevibacterium casei*, plays an important role in the production of NPs (Savi et al., 2021). Biogenic cobalt oxide NPs have proteins coated on their surface to conserve their identity. Furthermore, these proteins also aid in reduction of agglomeration of isolated NPs (Iravani and Varma, 2020).

2.2. Bismuth Trioxide (Bi_2O_3) NPs

Bismuth trioxide (Bi_2O_3) NPs have significant importance in our daily life. They are used as a semiconductor due to their visible photo sensitivity and enhanced photocatalytic activity. This metal oxide plays an effective role in wastewater treatment. Photocatalytic activity, low toxicity, chemical stability, the combination of visible photosensitivity and cost-effectiveness makes bismuth trioxide nanoparticles efficient for the treatment of waste water (Ahamed et al., 2019). They are used as an optoelectronic material e.g. gold, copper, aluminium and silver nanoparticles. They are obtained by adding toxic or organic solvents at an elevated temperature. Besides conventional chemical methods, *Fusarium oxysporum* is used as an alternate for the development of these nanocrystals (Zulkifli et al., 2018). However, the generation of bismuth trioxide NPs by biogenic synthesis is more environment friendly than conventional chemical methods.

2.3. Copper Oxide (CuO, Cu_2O) NPs

Copper oxide nanoparticles have wide array of applications in electric devices and ophthalmic treatments (Magdassi et al., 2010). They can also be used as good antimicrobial agent. At room temperature, Cu_2O nanoparticles with the diameter around 10–20 nanometer was made with the help of Baker's yeast *Saccharomyces cerevisiae*. Copper oxide nanoparticles are effective for reducing several bacterial and fungal strains. For example, *E. coli* and *A. niger*, respectively. These were obtained by the action of reductase enzyme which reduced copper sulfate. Several strains of fungi like *Penicillium aurantiogriseum*, *P. citrinum* and *P. waksmanii*, obtained from soil, are utilized in the biosynthesis of copper oxides.

2.4. Iron Oxide (Fe_2O_3, Fe_3O_4) Magnetic NPs

Iron oxide NPs have important applications in biomedical techniques including hyperthermia nuclear MRI and precise delivery of drugs. Biogenic techniques are mainly applied for obtaining iron oxide NPs rather than classical chemical methods. Iron oxide is reduced to iron by using a bacterium *Shewanella* strain HN-41, where pyruvate acts as an electron donor. The toxic effect of biogenic and commercial Fe_2O_3 nanoparticles was compared by observing hemagglutination and changes in morphology (Khalil et al., 2017). The capping agents of iron oxide present externally promotes structure stability and inhibit them from being aggregated.

2.5. Titanium Dioxide (TiO_2) NPs

Titanium dioxide nanoparticles have a vast variety of applications in biomedicine, environment and modern technology (Sagadevan et al., 2022). *Lactobacillus* sp. has been reported to be the main source of production of titanium dioxide NPs at room temperature. Yeast cells or *Lactobacillus* undergo interaction with $TiO(OH)_2$ and result in the production of these NPs using carbon and nitrogen sources (Khan et al., 2020).

2.6. Gold (Au) NPs

It has been shown by recent research studies that nano-sized gold particles possess antimicrobial activity. These have the ability to generate free oxygen radicals which are toxic to the environment as they result in production of ROS (Rajan et al., 2015). Artists have been utilizing their properties such as colloidal nature and radiant colors. Special properties, i.e. optical and electrical are possessed by these NPs because of their varying physical characteristics like morphology, diameter and surface composition. The significant usage of gold NPs in healthcare and diagnostics is due to their unique physical and chemical characteristics which can be utilized to detect biomolecules at minute concentrations.

2.7. Silver Oxide (Ag_2O) NPs

The medical fields of nanoscience and biomedicine mainly apply silver oxide nanoparticles which are essential for their research experiments (Wang et al., 2016). Several methodologies involving physiochemical and biological processes have been implemented to produce silver NPs. Studies have determined that Ag NPs possess extensive multifunctional properties, for example, as anti-inflammatory, antiviral, anticancer and antimicrobial agents (Gherasim et al., 2020). Biosynthetic silver NPs show high solubility, high stability and maximum yield (Gurunathan et al., 2015). Moreover, they have a well-defined size and morphology and are relatively less toxic and can

therefore be used in green chemistry.

3. Effects of Metal Oxide NPs

Several mechanisms contribute to the toxicity of metal oxide nanoparticles (NPs) as they interact with cellular components, including DNA, proteins, mitochondria, and lysosomes, often generating reactive oxygen species (ROS) that disrupt cell function (Jamuna and Ravishankar, 2014). Co3O4 nanocrystals release cobalt ions, activating NADPH oxidase and producing ROS, leading to oxidative stress on lymphocytes and being lethal to human immune cells (Chattopadhyay et al., 2015; Savi et al., 2021). Bismuth trioxide NPs negatively affect mammalian cells and ecosystems, causing cytotoxic and genotoxic effects such as apoptosis and necrosis (Zulkifli et al., 2018; Mohamed et al., 2021). Copper oxide NPs induce DNA methylation, fragmentation, chromosomal damage, and lipid peroxidation.

Iron oxide NPs (Fe_2O_3, Fe_3O_4) disrupt cell count, coagulation, cause inflammation, and damage various organs after inhalation (Valdiglesias et al., 2015; Chrishtop et al., 2021). Titanium dioxide NPs generate ROS, leading to genotoxicity, inflammation, cellular damage, and tumorigenesis. Gold NPs, in large amounts, reduce red blood cell count and cause anemia, spleen damage, and increased toxicity (Albanese and Chan, 2011). Silver NPs induce DNA damage, oxidative stress, and harmful effects on major organs (Antony et al., 2015; Bamal et al., 2021).

4. Applications of Metal Oxide NPs

Metal oxide NPs are widely used in biotechnology and biomedical sciences for sensing, imaging, gene and drug delivery, and surface functionalization (Falcaro et al., 2016; Savi et al., 2021). Cobalt oxide NPs are used for environmental remediation, including dye degradation and wastewater treatment (Anele et al., 2022). Bismuth trioxide NPs are applied in cosmetics, pharmaceuticals, industrial fields, cancer imaging, and wastewater treatment (Wang et al., 2016; Shahbazi et al., 2020). Copper oxide NPs are used in biomedical research, biosensing, and as fungicides and antibacterial agents (Verma and Kumar, 2019). Iron oxide NPs are utilized in drug delivery, molecular imaging, and wastewater treatment (Sangaiya and Jayaprakash, 2018; Gallo-Cordova et al., 2020).

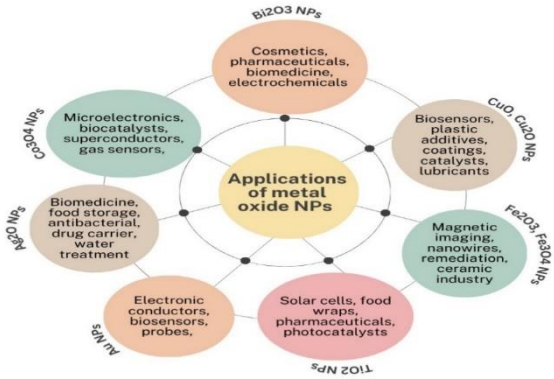

Fig. 2. Applications of metal oxide NPs in different sectors

TiO_2 NPs have vast applications in pharmaceutical products, food industries and cosmetics (Nadeem et al., 2018). These NPs also have immense industrial importance due to their usage as pesticides, for remediation of dyes, antibiotics and photocatalysts (Waghmode et al., 2019). Titanium dioxide is environmentally friendly because it has high chemical stability and non-toxicity. It can be used as an environment sanitizing agent due to its antifogging and self-cleaning properties (Waghmode et al., 2019).

Gold NPs have a broad spectrum applications, which include electronics, conductors, photodynamic therapy, biosensors, probes, diagnostic markers and catalyst for chemical reactions (Sýkora et al., 2010). Gold NPs have been shown to be effective for eradicating localized tumors. The extensive surface area relative to volume ratio enables these NPs to be used in surface coating. Different food items can be checked for their suitable consumption by using a colorimetric sensor made of Au NPs. Gold NPs have broad spectrum applications in the areas of water filtration, photothermal therapy, antimicrobial and the food industry. Gold NPs are known to be biocompatible due to their green synthesis (Küünal et al., 2018).

Several reviews and studies emphasize the widespread benefits in the industries of biomedicine, healthcare, food storage and ecosystem (Bapat et al., 2018). The antimicrobial activity of these NPs was reported against *E. coli*, in their cell walls. Various applications include biosensing, bioimaging, water treatment, textiles and as a drug carrier (Verma and Maheshwari, 2019). Silver NPs are found in containers used for food storage and packaging, purificants used in water and detergents. They are used as

surfactants and oxidizing and bleaching agents.

Table 1. Effects and applications of various metal oxide NPs

Metal	Sources	Toxicological effects	Uses and applications	References
Co_3O_4 NPs	Aqueous extracts of leaves, medicinal plants, biotic compounds	ROS production, oxidative stress on lymphocytes, lethal to immune cells	Microelectronics, biocatalysts, superconductors, gas sensors, electronic ceramics, nanowires	(Mei et al., 2019; Savi et al., 2021)
Bi_2O_3 NPs	Smelting of ores, weathering of rocks, leaf extracts	Cytotoxicity, genotoxicity, apoptosis and necrosis of cells, cellular damage	Cosmetics, pharmaceuticals, biomedicine, electrochemical applications such as solid oxide fuel cells (SOFC), cancer imaging, photoconduction	(Jagdale et al., 2021)
CuO, Cu_2O NPs	Wood preservatives, mineral supplements, weathering of rocks	DNA methylation, DNA fragmentation, lipid peroxidation, chromosomal aberrations, micronucleus formation	Biosensors, electrochemical sensors, plastic additives, coatings, textiles, catalysts, lubricants	(Perreault et al., 2012)
Fe_2O_3, Fe_3O_4 NPs	Sedimentary rocks, iron mineral ores, atmospheric dust, aeolian deposits	Reduced cell viability, cell lysis, inflammation, generation of ROS, lipid peroxidation, DNA damage	Magnetic imaging, nanowires, coatings, resonance imaging, environmental remediation, glass and ceramic industry	(Attarilar et al., 2020)
TiO_2 NPs	Sand, mineral ores, atmospheric dust, soil, volcanic eruption, sea water, fire smoke	Oxidative stress leading to ROS production, pulmonary inflammation, carcinogenesis, tumor formation, genotoxicity, cellular damage	Solar cells, food wraps, medicines, pharmaceuticals, photocatalysts, agriculture, antibacterial coatings, cosmetics	(Waghmode et al., 2019; Banerjee and Thiagarajan, 2014)
Au NPs	Quartz, gold bearing mineral, gold mining, sedimentary rocks	Decrease in RBCs, decrease in body weight, lower spleen index, increased cytotoxicity, apoptosis, inflammatory immune responses	Electronic conductors, biosensors, diagnostic markers, probes, catalysts	(Daraee et al., 2016; Li et al., 2014)
Ag_2O NPs	Industrial effluents, leaching of metal tailings, sewage, ore processing, atmospheric deposition	DNA damage, cytokine induction, oxidative stress, organ damage, edema, epidermal hyperplasia, focal inflammation	Biomedicine, healthcare products, food storage, antibacterial agents, bioimaging, drug carrier, water treatment	(Prabhu and Poulose, 2012)

5. Sources of Metal Oxide NPs

Metal oxide NPs are formed through various biotic and abiotic methods. Major sources of metal oxide NPs include biogenic synthesis through biomineralization and other electrochemical methods. The details are as follows:

5.1. Natural Sources

For cobalt oxide, medicinal plants, aqueous extracts of leaves and biotic compounds are used for their synthesis (Shafey, 2020). Furthermore, smelting of mineral ores like bismite, bismuthinite are the major sources for the extraction of bismuth trioxide (Motakef-Kazemi and Yaqoubi, 2020). For copper oxide NPs, wood preservatives, inorganic compounds, vitamin and mineral supplements and weathering of rocks are the main sources for metal oxide NPs production (Alavi and Karimi, 2018). Iron oxide NPs are extracted from sedimentary rocks, iron mineral ores and aeolian deposits found in atmospheric dust. Titanium oxide NPs are obtained from sand, mineral ores, atmospheric dust, soil, volcanic eruptions, sea water and fire smoke.

5.2. Anthropogenic Sources

Anthropogenic NPs are made through human activities which are divided into two categories, i.e. the first category includes NPs without predetermined size and shows undefined chemistry (Strambeanu et al., 2014). For example, diesel exhaust, coal fly ash, welding fumes and combustion particulates. The second type of anthropogenic NPs is also known as engineered nanoparticles which have a particular size range of 1–100 nm. They are made up of pure materials with controlled surfaces (Chavali and Nikolova, 2019). For example, nanotubes made up of carbon, dendrimers, quantum dots, silver and gold nanocrystals as shown in Fig. 3 (Sadik, 2013).

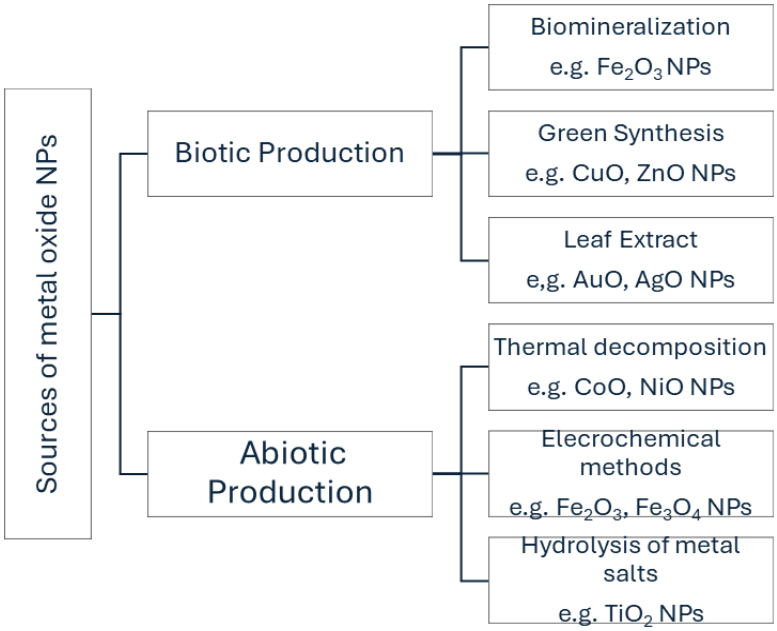

Fig. 3. Sources of metal oxide NPs

5.3. Types of Toxicity

Metal oxide nanoparticles (NPs) exhibit both aquatic and terrestrial toxicity by disrupting aquatic ecosystems, affecting organisms' morphology, reproduction, and survival and soil toxicity, altering plant growth and fauna behavior through prolonged exposure respectively.

5.3.1. Aquatic Toxicity

Metal oxide NPs pose serious threats to aquatic organisms. For instance, nano TiO2 is toxic to Daphnia magna at levels greater than 100 mg/L. Photo-induced toxicity of nano TiO2 under UV exposure can cause fatal damage to marine plankton.

5.3.2. Terrestrial Toxicity

Nano TiO2 and other metal oxide NPs also impact terrestrial organisms. Studies show that nano TiO2 exposure causes DNA and mitochondrial damage in soil invertebrates like earthworms and nematodes, inhibiting reproduction (Samarasinghe et al., 2023). Nano CuO and nano NiO affect seed germination in cucumber, radish, and lettuce, while nano Co3O4 impacts root elongation of radish (Ahmad et al., 2023).

5.4. Relative Toxicity of Metal Oxide NPs

Research comparing the toxicity of various metal oxide NPs ranks CuO as the most toxic and TiO2 as the least toxic. The toxicity is assessed based on ROS production, lipid peroxidation, oxidative stress, and metal ion release (Sengul and Asmatulu, 2020). Experiments on Lactuca seeds and bacteria like S. aureus and E. coli confirm copper

oxide's high toxicity (Sajjad et al., 2023).

5.5.Nanobioremediation

Nanoparticles play a crucial role in environmental remediation, effectively cleaning air, water, and soil. For example, iron oxide NPs are used to remove contaminants due to their high reactivity (Latif et al., 2020). Various NPs are employed in wastewater treatment through adsorption, degradation, and filtration (Naseem and Durrani, 2021).

5.6. Wastewater Treatment

Metal oxide NPs like iron oxide and cobalt are used to remove toxic elements from water, improving the hydrosphere (Abuhatab et al., 2020; Gautam et al., 2022).

5.7. Metal Oxide NPs and Microbes

Microorganisms can synthesize metal oxide NPs for environmental cleanup. Copper oxide NPs from Escherichia sp. degrade dyes, while iron oxide NPs from Aspergillus tubingensis remove heavy metals from contaminated water (Mandeep and Shukla, 2020; Yamini and Rajeswari, 2023).

5.8. Implications for Environmental Management

Understanding the ecotoxicological impact of metal oxide NPs is crucial for environmental conservation and decision-making. Establishing safe exposure limits, incorporating nanomaterial-specific regulations, and effective risk communication are essential. Promoting interdisciplinary research and international cooperation can lead to innovative solutions for managing nanoparticle pollution (Navarro et al., 2008).

CONCLUSION

It was concluded metal oxide nanoparticles offer significant benefits in various applications such as bioremediation, drug delivery, and biomedicine, their potential toxicity cannot be overlooked. These nanoparticles pose risks including cellular and DNA damage, ROS formation, and inflammation, necessitating thorough toxicity evaluations before their use in diagnostics and therapies. Understanding and mitigating these risks is essential to harness their full potential while ensuring safety for humans and the environment.

ACKNOWLEDGEMENT

N/A

CONFLICT OF INTEREST

Authors declare no conflict of interest.

REFERENCES

1. Abdel Maksoud M, Fahim RA, Shalan AE, Abd Elkodous M, Olojede S, Osman AI, Farrell C, Al-Muhtaseb AAH, Awed A, Ashour A (2021). Advanced materials and technologies for supercapacitors used in energy conversion and storage: a review. Environ. Chem. Lett. 19: 375-439.
2. Abuhatab S, El-Qanni A, Al-Qalaq H, Hmoudah M, Al-Zerei

W (2020). Effective adsorptive removal of Zn2+, Cu2+, and Cr3+ heavy metals from aqueous solutions using silica-based embedded with NiO and MgO nanoparticles. J. Environ. Manage. 268: 110713.

3. Adachi K, Buseck PR (2010). Hosted and free-floating metal-bearing atmospheric nanoparticles in Mexico City. Environ. Sci. Technol. 44(7): 2299-2304.

4. Ahamed M, Akhtar MJ, Khan MM, Alrokayan SA, Alhadlaq HA (2019). Oxidative stress mediated cytotoxicity and apoptosis response of bismuth oxide (Bi2O3) nanoparticles in human breast cancer (MCF-7) cells. Chemosphere 216: 823-831.

5. Ahmad S, Pathak AK, Minj RP, Chaudhary S, Kumar A, Chalotra T, Raina N (2023). A Comprehensive Review of Nanoparticles Induced Stress and Toxicity in Plants. Univ. J. Green Chem. 11: 18-43.

6. Alavi M, Karimi N (2018). Characterization, antibacterial, total antioxidant, scavenging, reducing power and ion chelating activities of green synthesized silver, copper and titanium dioxide nanoparticles using Artemisia haussknechtii leaf extract. Artif. Cells Nanomed. Biotechnol. 46: 2066-2081.

7. Anele A, Obare S, Wei J (2022). Recent trends and advances of Co3O4 nanoparticles in environmental remediation of bacteria in wastewater. Nanomaterials 12: 1129.

8. Antony JJ, Sivalingam P, Chen B (2015). Toxicological effects of silver nanoparticles. Environ. Toxicol. Pharmacol. 40: 729-732.

9. Attarilar S, Yang J, Ebrahimi M, Wang Q, Liu J, Tang Y, Yang J (2020). The toxicity phenomenon and the related occurrence in metal and metal oxide nanoparticles: a brief review from the biomedical perspective. Front. Bioeng. Biotechnol. 8: 822.

10. Bamal D, Singh A, Chaudhary G, Kumar M, Singh M, Rani N, Mundlia P, Sehrawat AR (2021). Silver nanoparticles biosynthesis, characterization, antimicrobial activities, applications, cytotoxicity and safety issues: An updated review. J. Nanomater. 11: 2086.

11. Banerjee K, Thiagarajan P (2014). A review of titanium Di oxide nanoparticles-synthesis, applications and toxicity concerns. Nanoscience Nanotechnol. Asia 4: 132-143.

12. Bapat RA, Chaubal TV, Joshi CP, Bapat PR, Choudhury H, Pandey M, Gorain B, Kesharwani P (2018). An overview of application of silver nanoparticles for biomaterials in dentistry. Mater. Sci. Eng. C 91: 881-898.

13. Baranowska-Wójcik E, Szwajgier D, Oleszczuk P, Winiarska-Mieczan A (2020). Effects of titanium dioxide

nanoparticles exposure on human health—a review. Biol. Trace Elem. Res. 193: 118-129.

14. Braunschweig J, Bosch J, Meckenstock RU (2013). Iron oxide nanoparticles in geomicrobiology: from biogeochemistry to bioremediation. New Biotechnol. 30: 793-802.

15. Bzdek BR, Pennington MR, Johnston MV (2012). Single particle chemical analysis of ambient ultrafine aerosol: A review. J. Aerosol Sci. 52: 109-120.

16. Chae H, Song D, Lee YG, Son T, Cho W, Pyun YB, Kim TY, Lee JH, Fabregat-Santiago F, Bisquert J (2014). Chemical effects of tin oxide nanoparticles in polymer electrolytes-based dye-sensitized solar cells. J. Phys. Chem. C 118: 16510-16517.

17. Chattopadhyay S, Dash SK, Tripathy S, Das B, Mandal D, Pramanik P, Roy S (2015). Toxicity of cobalt oxide nanoparticles to normal cells; an in vitro and in vivo study. Chem. Biol. Interact. 226: 58-71.

18. Chavali MS, Nikolova MP (2019). Metal oxide nanoparticles and their applications in nanotechnology. SN Appl. Sci. 1: 607.

19. Chrishtop VV, Mironov VA, Prilepskii AY, Nikonorova VG, Vinogradov VV (2021). Organ-specific toxicity of magnetic iron oxide-based nanoparticles. Nanotoxicology 15: 167-204.

20. Daraee H, Eatemadi A, Abbasi E, Fekri Aval S, Kouhi M, Akbarzadeh A (2016). Application of gold nanoparticles in biomedical and drug delivery. Artif. Cells Nanomed. Biotechnol. 44: 410-422.

21. Dasari TP, Pathakoti K, Hwang HM (2013). Determination of the mechanism of photoinduced toxicity of selected metal oxide nanoparticles (ZnO, CuO, Co3O4 and TiO2) to E. coli bacteria. J. Environ. Sci. 25: 882-888.

22. Demir E (2021). A review on nanotoxicity and nanogenotoxicity of different shapes of nanomaterials. J. Appl. Toxicol. 41: 118-147.

23. Donovan AR, Adams CD, Ma Y, Stephan C, Eichholz T, Shi H (2016). Single particle ICP-MS characterization of titanium dioxide, silver, and gold nanoparticles during drinking water treatment. Chemosphere 144: 148-153.

24. Ejileugha C, Ezejiofor AN, Ezealisiji KM, Orisakwe OE (2022). Metal oxide nanoparticles in oil drilling: Aquatic toxicological concerns. J. Hazard. Mater. Adv. 7: 100116.

25. Falcaro P, Ricco R, Yazdi A, Imaz I, Furukawa S, Maspoch D, Ameloot R, Evans JD, Doonan CJ (2016). Application of metal and metal oxide nanoparticles@ MOFs. Coord. Chem. Rev. 307: 237-254.

26. Flannery M, Desai TG, Matsoukas T, Lotfizadeh S, Oehlschlaeger MA (2015). Passivation and Stabilization of Aluminum Nanoparticles for Energetic Materials. J. Nanomater. 2015: 682153.
27. Gallo-Cordova Á, Espinosa A, Serrano A, Gutiérrez L, Menéndez N, del Puerto Morales M, Mazarío E (2020). New insights into the structural analysis of maghemite and (MFe2O4, M= Co, Zn) ferrite nanoparticles synthesized by a microwave-assisted polyol process. Mater. Chem. Front. 4: 3063-3073.
28. Gautam PK, Banerjee S, Samanta SK (2022). Chapter 7 - Sustainable approaches for synthesis of biogenic magnetic nanoparticles and their water remediation applications. In J. R. Koduru, et al. (Eds.), Sustainable Nanotechnology for Environmental Remediation. Elsevier: 157-178.
29. Gherasim O, Puiu RA, Bîrcă AC, Burdușel AC, Grumezescu AM (2020). An updated review on silver nanoparticles in biomedicine. Nanomaterials 10: 2318.
30. Ghosh N, Ghosh R, Babu SP (2021). Nanotechnology in microalgae for biofuel production and CO2 sequestration: A review. Environ. Chem. Lett. 19: 2777-2796.
31. Griffin S, Masood MI, Nasim MJ, Sarfraz M, Ebokaiwe AP, Schäfer KH, Keck CM, Jacob C (2017). Natural nanoparticles: a particular matter inspired by nature. Antioxidants 7: 3.
32. Guo H, Barnard AS (2013). Naturally occurring iron oxide nanoparticles: morphology, surface chemistry and environmental stability. J. Mater. Chem. A 1: 27-42.
33. Gurunathan S, Han JW, Kim ES, Park JH, Kim JH (2015). Reduction of graphene oxide by resveratrol: a novel and simple biological method for the synthesis of an effective anticancer nanotherapeutic molecule. Int. J. Nanomed. 4: 2951-2969.
34. Handy RD, Owen R, Valsami-Jones E (2008). The ecotoxicology of nanoparticles and nanomaterials: current status, knowledge gaps, challenges, and future needs. Ecotoxicology 17: 315-325.
35. Harish V, Tewari D, Gaur M, Yadav AB, Swaroop S, Bechelany M, Barhoum A (2022). Review on nanoparticles and nanostructured materials: bioimaging, biosensing, drug delivery, tissue engineering, antimicrobial, and agro-food applications. Nanomaterials 12: 457.
36. Herrera Estrada LP, Champion JA (2015). Protein nanoparticles for therapeutic protein delivery. Biomater. Sci. 3: 787-799.
37. Hong S, Choi DW, Kim HN, Park CG, Lee W, Park HH (2020). Protein-based

nanoparticles as drug delivery systems. Pharmaceutics 12: 604.
38. Hu C, Hou J, Zhu Y, Lin D (2020). Multigenerational exposure to TiO2 nanoparticles in soil stimulates stress resistance and longevity of survived C. elegans via activating insulin/IGF-like signaling. Environ. Pollut. 263: 114376.
39. Hussain I, Singh N, Singh A, Singh H, Singh S (2016). Green synthesis of nanoparticles and its potential application. Biotechnol. Lett. 38: 545-560.
40. Hwang GH, Han WK, Kim SJ, Hong SJ, Park JS, Park HJ, Kang SG (2009). An electrochemical preparation of bismuth nanoparticles by reduction of bismuth oxide nanoparticles and their application as an environmental sensor. J. Ceram. Process. Res. 10: 190-194.
41. Iravani S, Varma RS (2020). Sustainable synthesis of cobalt and cobalt oxide nanoparticles and their catalytic and biomedical applications. Green Chem. 22: 2643-2661.
42. Jagdale P, Serino G, Oza G, Audenino AL, Bignardi C, Tagliaferro A, Alvarez-Gayosso C (2021). Physical characterization of bismuth oxide nanoparticle based ceramic composite for future biomedical application. J. Mater. 14: 1626.
43. Jamuna BA, Ravishankar RV (2014). Environmental risk, human health, and toxic effects of nanoparticles. Nanomater. Environ. Prot. 1: 523-535.
44. Jeng HA, Swanson J (2006). Toxicity of metal oxide nanoparticles in mammalian cells. J. Environ. Sci. Health A 41: 2699-2711.
45. Jiang Z, Shan K, Song J, Liu J, Rajendran S, Pugazhendhi A, Jacob JA, Chen B (2019). Toxic effects of magnetic nanoparticles on normal cells and organs. Life Sci. 220: 156-161.
46. Jung H, Park H, Kim J, Lee JH, Hur HG, Myung NV, Choi H (2007). Preparation of biotic and abiotic iron oxide nanoparticles (IOnPs) and their properties and applications in heterogeneous catalytic oxidation. Environ. Sci. Technol. 41: 4741-4747.
47. Khalil AT, Ovais M, Ullah I, Ali M, Shinwari ZK, Maaza M (2017). Biosynthesis of iron oxide (Fe2O3) nanoparticles via aqueous extracts of Sageretia thea (Osbeck.) and their pharmacognostic properties. Green Chem. Lett. Rev. 10: 186-201.
48. Khan MR, Fromm KM, Rizvi TF, Giese B, Ahamad F, Turner RJ, Füeg M, Marsili E (2020). Metal nanoparticle–microbe interactions: synthesis and antimicrobial effects. Part. Part. Syst. Charact. 37: 1900419.
49. Kiser M, Westerhoff P, Benn T, Wang Y, Perez-Rivera J, Hristovski K (2009). Titanium nanomaterial removal and release from wastewater treatment plants.

Environ. Sci. Technol. 43: 6757-6763.
50. Ko KS, Kong IC (2014). Toxic effects of nanoparticles on bioluminescence activity, seed germination, and gene mutation. Appl. Microbiol. Biotechnol. 98: 3295-3303.
51. Kushwaha M, Mishra A, Goel D, Shankar S (2023). Nanotechnological approach for the abatement of environmental pollution: a way forward toward a clean environment. Biotechnol. Environ. Remediation 2: 221-247.
52. Küünal S, Rauwel P, Rauwel E (2018). Plant extract mediated synthesis of nanoparticles. In: Emerging applications of nanoparticles and architecture nanostructures. Elsevier: 411-446.
53. Latif A, Sheng D, Sun K, Si Y, Azeem M, Abbas A, Bilal M (2020). Remediation of heavy metals polluted environment using Fe-based nanoparticles: mechanisms, influencing factors, and environmental implications. Environ. Pollut. 264: 114728.
54. Li C, Zhang Y, Wang M, Zhang Y, Chen G, Li L, Wu D, Wang Q (2014). In vivo real-time visualization of tissue blood flow and angiogenesis using Ag2S quantum dots in the NIR-II window. Biomater. Res. 35: 393-400.
55. Magdassi S, Grouchko M, and Kamyshny A (2010). Copper nanoparticles for printed electronics: Routes towards achieving oxidation stability. Materials. 3(9): 4626-4638.
56. Mandeep and Shukla P (2020). Microbial nanotechnology for bioremediation of industrial wastewater [Mini Review]. Front. Microbiol. 1: 11.
57. Mei J, Liao T, Ayoko GA, Bell J, and Sun Z (2019). Cobalt oxide-based nanoarchitectures for electrochemical energy applications. Prog. Mater. Sci. 103: 596-677.
58. Mohamed AE, Celik A, Yetkin D, and Guler G (2021). Bismuth oxide nanoparticle: The potential of apoptotic and genetic damage on MDBK cell line. Nanomed. Nanotechnol. 1(1): 1-5.
59. Montano MD, Lowry GV, von der Kammer F, Blue J, and Ranville JF (2014). Current status and future direction for examining engineered nanoparticles in natural systems. Environ. Chem. 11(4): 351-366.
60. Moore T, Hennessy EM, Myles J, Johnson SJ, Draper ES, Costeloe KL, and Marlow N (2012). Neurological and developmental outcome in extremely preterm children born in England in 1995 and 2006: the EPICure studies. BMJ: 345.
61. Motakef-Kazemi N, and Yaqoubi M (2020). Green synthesis and characterization of bismuth oxide nanoparticle using Mentha pulegium extract. Iran. J. Pharm. Res. IJPR. 19(2): 70.
62. Nadeem M, Tungmunnithum D, Hano C,

Abbasi BH , Hashmi SS, Ahmad W, and Zahir A. (2018). The current trends in the green syntheses of titanium oxide nanoparticles and their applications. Green Chem. Lett. Rev. 11(4): 492-502.

63. Naseem T, and Durrani T (2021). The role of some important metal oxide nanoparticles for wastewater and antibacterial applications: A review. Environ. Chem. Ecotoxicol. 3: 59-75.

64. Navarro E, Piccapietra F, Wagner B, Marconi F, Kaegi R, Odzak N, Behra R. (2008). Toxicity of silver nanoparticles to Chlamydomonas reinhardtii. Environ. Sci. Technol. 42(23): 8959-8964.

65. Nizamuddin S, Siddiqui M, Mubarak N, Baloch HA, Abdullah E, Mazari SA, Tanksale A (2019). Iron oxide nanomaterials for the removal of heavy metals and dyes from wastewater. Nanoscale Mater. Water Purif: 447-472.

66. Nowack B, and Bucheli TD (2007). Occurrence, behavior and effects of nanoparticles in the environment. Environ. Pollut. 150(1): 5-22.

67. Oukarroum A, Bras S, Perreaul F, and Popovic R (2012). Inhibitory effects of silver nanoparticles in two green algae, Chlorella vulgaris and Dunaliella tertiolecta. Ecotoxicol. Environ. Saf. 78: 80-85.

68. Perreault F, Melegari SP, da Costa CH, Rossetto AL, Popovic R, and Matias WG (2012). Genotoxic effects of copper oxide nanoparticles in Neuro 2A cell cultures. Sci. Total Environ. 441: 117-124.

69. Prabhu S, and Poulose EK (2012). Silver nanoparticles: mechanism of antimicrobial action, synthesis, medical applications, and toxicity effects. Int. Nano Lett. 2: 1-10.

70. Rahman MM, Uddin J, Asiri AM, and Rahman MR (2024). Toxicity of nanoparticles: Recent advances and new perspectives.

71. Rajan, A., Vilas, V., and Philip, D. (2015). Studies on catalytic, antioxidant, antibacterial and anticancer activities of biogenic gold nanoparticles. J. Mol. Liq., 212, 331-339.

72. Rajput VD, Minkina T, Sushkova S, Chokheli V, and Soldatov M (2019). Toxicity assessment of metal oxide nanoparticles on terrestrial plants. Compr. Anal. Chem. Elsevier 87: 189-207.

73. Revell P (2006). The biological effects of nanoparticles. Nanotechnol. Percept. 2(3): 283-298.

74. Sadik OA (2013). Anthropogenic nanoparticles in the environment. Environ. Sci. Processes Impacts. 15(1): 19-20.

75. Sagadevan S, Imteyaz S, Murugan B, Anita L, Sridewi N, Weldegebrieal GK (2022). A comprehensive review on green synthesis, characterization, and applications of biogenic bismuth

nanoparticles. Int. J. Energy Res. 46(4): 4909-4932.

76. Saleh TA, Wahab MA, and Mahtab A (2020). Environmental applications of nanoparticles and their mechanisms of action and factors influencing their toxicology. Comp. Biochem. Physiol. Part C Toxicol. Pharmacol: 109682.
77. Sajjad H, Sajjad A, Haya RT, Khan MM, Zia M (2023). Copper oxide nanoparticles: In vitro and in vivo toxicity, mechanisms of action and factors influencing their toxicology. Comp. Biochem. Physiol. C Toxicol. Pharmacol. 109682.
78. Samarasinghe SV, Krishnan K, Aitken R J, Naidu R, and Megharaj M (2023). Chronic effects of TiO2 and ZnO nanoparticles to earthworm Eisenia fetida. Environ. Chem. Ecotoxicol. 5: 129-134.
79. Sanderson P, Delgado-Saborit JM, and Harrison RM (2014). A review of chemical and physical characterisation of atmospheric metallic nanoparticles. Atmos. Environ. 94: 353-365.
80. Sangaiya P, and Jayaprakash R (2018). A review on iron oxide nanoparticles and their biomedical applications. J. Supercond. Nov. Magn. 31(11): 3397-3413.
81. Savi M, Bocchi L, Cacciani F, Vilella R, Buschini A, Perotti A, Frati C (2021). Cobalt oxide nanoparticles induce oxidative stress and alter electromechanical function in rat ventricular myocytes. Part. Fibre Toxicol. 18:1-17.
82. Seabra AB, and Durán N (2015). Nanotoxicology of metal oxide nanoparticles. Metals 5(2): 934-975.
83. Sengul Ab, and Asmatulu E (2020). Toxicity of metal and metal oxide nanoparticles: A review. Environ. Chem. Lett. 18(5): 1659-1683.
84. Shafey A (2020). Green synthesis of metal and metal oxide nanoparticles from plant leaf extracts and their applications: A review. Green Process. Synth. 9(1): 304-339.
85. Shahbazi MA, Faghfouri L, Ferreira MP, Figueiredo P, Maleki H, Sefat F, Santos HA (2020). The versatile biomedical applications of bismuth-based nanoparticles and composites: Therapeutic, diagnostic, biosensing, and regenerative properties. Chem. Soc. Rev. 49(4): 1253-1321.
86. Siddiqi KS, and Husen A (2017). Plant response to engineered metal oxide nanoparticles. Nanoscale Res. Lett. 12: 1-18.
87. Stark WJ (2011) Nanoparticles in biological systems. Angew. Chem. Int. Ed. 50(6): 1242-1258.
88. Strambeanu N, Demetrovici L, Dragos D (2014). Anthropogenic sources of nanoparticles. In: Nanoparticles'

Promises and Risks: Characterization, Manipulation, and Potential Hazards to Humanity and the Environment. Springer: 21-54.

89. Stuchinskaya T, Moreno M, Cook MJ, Edwards DR, and Russell DA (2011). Targeted photodynamic therapy of breast cancer cells using antibody-phthalocyanine-gold nanoparticle conjugates. Photochem. Photobiol. Sci. 10(5): 822-831.

90. Sýkora D, Kašička V, Mikšík I, Řezanka P, Záruba K, Matějka P, and Král V (2010). Application of gold nanoparticles in separation sciences. J. Sep. Sci. 33(3): 372-387.

91. Tee JK, Ong CN, Bay BH, Ho HK, and Leong DT (2016). Oxidative stress by inorganic nanoparticles. Wiley Interdiscip. Rev. Nanomed. Nanobiotechnol. 8(3): 414-438.

92. Tolocka MP, Lake DA, Johnston MV, and Wexler AS (2004). Number concentrations of fine and ultrafine particles containing metals. Atmos. Environ. 38(20): 3263-3273.

93. Valdiglesias V, Kiliç G, Costa C, Fernández-Bertólez N, Pásaro E, Teixeira J P, and Laffon B (2015). Effects of iron oxide nanoparticles: cytotoxicity, genotoxicity, developmental toxicity, and neurotoxicity. Environ. Mol. Mutagen. 56(2): 125-148.

94. Verma N, and Kumar N (2019). Synthesis and Biomedical Applications of Copper Oxide Nanoparticles: An Expanding Horizon. ACS Biomater. Sci. Eng. 5(3): 1170-1188.

95. Verma P, and Maheshwari SK (2019). Applications of Silver nanoparticles in diverse sectors. Int. J. Nano Dimens.10(1): 18-36.

96. Waghmod MS, Gunjal AB, Mulla JA, Patil NN, and Nawani NN (2019). Studies on the titanium dioxide nanoparticles: Biosynthesis, applications and remediation. SN Appl. Sci. 1(4): 310.

97. Wan R, Mo Y, Feng L, Chien S, Tollerud DJ, and Zhang Q (2012). DNA damage caused by metal nanoparticles: involvement of oxidative stress and activation of ATM. Chem. Res. Toxicol. 25(7): 1402-1411.

98. Wang T, Huang D, Yang Z, Xu S, He G, Li X, Zhang L (2016). A review on graphene-based gas/vapor sensors with unique properties and potential applications. Nano-Micro Lett. 8: 95-119.

99. Yamini V, and Rajeswari VD (2023). Effective bio-mediated nanoparticles for bioremediation of toxic metal ions from wastewater–A review. J. Environ. Nanotechnol. 12(2): 12-33.

100. Zhang XD, Wu HY, Wu D, Wang YY, Chang JH, Zhai ZB, Fan FY (2010). Toxicologic effects of gold nanoparticles in vivo by different administration routes. Int. J. Nanomed: 771-781.

LGU Journal of

LIFE SCIENCES

LGU Society of Life Sciences

DOI: https://doi.org/10.54692/lgujls.2024.0803351

Paper Submission: 3rd April 2024; Paper Acceptance: 8th Sep 2024; Paper Publication: 10th Sep 2024

Research Article | LGU J. Life. Sci

Vol 8 Issue 3 July- Sep 2024 | ISSN 2519-9404

eISSN 2521-0130

Ganoderma curtisii, Firstly Reported from Districts Lahore and Gujranwala of Punjab Province, Pakistan

Sadaf Saeedullah[1], Maryam Nawaz[1], Nousheen Yousaf*[1], Saliha Rukhsar[1], Khadija Malhi[1], Muhammad Hanif[1]

1. Department of Botany, Government College University Lahore, Katchery Road, 54000, Lahore, Pakistan

Corresponding Author's Email: dr.nousheenyousaf@gcu.edu.pk

ABSTRACT: *The current study presents a Ganoderma sp., as a new record from three different localities of districts Lahore and Gujranwala of Punjab province, Pakistan. Based on morpho-anatomical characteristics, collected specimens were identified as Ganoderma curtisii. The macroscopic and microscopic features of G. curtisii include; semicircular to kidney shaped laccate pileus that is beautifully lacquered, duplex context, resinous bands, no concentric growth zones, pore surface white to cream brown and sub circular to circular pores, stipe lateral making an angle with the pileus (45-90 degrees), basidiospores 11.4 × 5.7 µm, ellipsoidal with the hyaline vesicular appendix double walled, trimitic hyphal system and club shaped cutis. The detailed study of different Ganoderma species from the published literature and comparisons with those species confirmed the identity of our specimen as G. curtisii. In this article, taxonomic descriptions, micrographs and illustrations elaborate the morphological and anatomical characters of Ganoderma curtisii, a distribution map of this species across Pakistan and a comparison table of morphoanatomical characteristics of Ganoderma curtisii reported from neighbouring countries is given. Conduction of molecular studies, investigation of ecological roles, development of conservational strategies, and exploration of biotechnological exploration are future perspectives for this taxon.*

Keywords: Canal-bank Road Lahore, *Ganoderma curtisii*, Macrofungi, Polyporaceae

INTRODUCTION

Ganoderma genus was founded by Karsten (1881) as a member of laccate pileated group of species, with *G. lucidum* as a type specimen. Genus *Ganoderma* has following subgenera, *Ganoderma* (which is classified in further sections *Ganoderma* and *Phaenema*), *Elfvingia*, and *Trachyderma* (Thawthong et al., 2017; Zhao and Zhang, 2000; Galappaththi et al., 2024). There are about 219 species assigned to genus *Ganoderma* (Moncalvo, 2000; Wachtel-Galor et al., 2012). This genus has distinguishing characters of laccate (shiny) surface with thick-walled pilocystidia that are present in an extracellular melanin matrix (Moncalvo, 2000), sessile to stipitate basidiomata and bilayed basidiospores with inter-wall pillars (Karsten, 1881; Moncalvo and Ryvarden, 1997; Luangharn et al., 2021). Due to extreme phenotypic plasticity, the identification of *Ganoderma* species is difficult (Ryvarden, 1994; Zhao and Zhang, 1994; Wachtel-Galor et al., 2012; Chen et al., 2024). More reliable criteria to identify and distinguish *Ganoderma* species includes context color and consistency, shape and size of spore and micro-anatomy of the pileal crust. *Ganoderma* is a cosmopolitan genus with global distribution in tropical and sub-tropical forests. Specimens flourish in hot and humid conditions (Pilotti et al., 2004; Singh et al., 2014; Thawthong et al., 2017).

Basidiomes are commonly found in bracket form (Pilotti et al., 2004), with most *Ganoderma* species are pathogenic and grow as facultative parasites of trees and cause various diseases in plants such as stem rot, wood decay and white rot (Ryvarden, 2004; Pilotti, 2005; Dai et al., 2007; Cao and Yuan, 2013; Coetzee et al., 2015). Some *Ganoderma* species are saprobes on rotting stumps and roots (Turner, 1981; Pilotti, 2005). This genus has a great pharmaceutical importance due to the presence of natural bioactive compounds, e.g., high and low molecular weight sterols, triterpenoids polysaccharides, and proteins (Ahmadi and Riazipour, 2007; Chan et al., 2007; Chen and Seleen, 2007; Luangharn et al., 2021). The bioactive constituents present in the genus *Ganoderma* are known to have broad therapeutic properties, such as antiviral, anticancer, anti-tumor, anti-inflammatory, anti-oxidant, anti-hypotensive, immunomodulatory, anti-diabetic, anti-viral, anti-bacterial, anti-fungal potentials (Liu et al., 2002; Paterson, 2006; Teng et al., 2011; De Silva et al., 2012a, b; Kao et al., 2013; Singh et al., 2014; Richter et al., 2015; Hyde et al., 2019; Luangharn et al., 2021).

Fruiting bodies of some *Ganoderma* species have been used as traditional medicine for more than 2,000 years in some countries for promoting longevity and health, boosting the immune system, lowering the risk of cancer, treatment of diabetes, insomnia, debility and weakness etc (Galor et al., 2004; Singh et al., 2014). The cultivated yield for *Ganoderma* has exceeded 10,000 tons per annum due to its unique pharmacological activity (El Sheikha, 2022; Khadbaatar et al., 2024), this is due to the presences of highly active compounds including polyphenols, polysaccharides, quinones, sterols, triterpenes (Seweryn et al., 2021; Fang et al., 2023; Khadbaatar et al., 2024).

In Pakistan, previously, about 18 species of this genus have been reported so far and these are *Ganoderma applanatum* (Pers.) Pat., *Ganoderma australe* (Fr.) Pat., *Ganoderma ahmadii* Steyaert, *Ganoderma boninense* Pat., *Ganoderma curtisii* (Berk.) Murrill, *Ganoderma colossus* (Fr.) C.F. Baker, *Ganoderma chalceum* (Cooke) Steyaert, *Ganoderma flexipes* Pat., *Ganoderma. gibbosum* (Blume & T. Nees) Pat., *Ganoderma lucidum* (Curtis) P. Karst., *Ganoderma leucocontextum* T.H. Li, W.Q. Deng, Sheng H. Wu, Dong M. Wang & H.P. Hu, *Ganoderma multipileum* Ding Hou, *Ganoderma multistipitatum* S. Ahmed, M. Awais, M.M. Sadiq, A. Umar, L. Dufosse, M.T. Khan, J. Alkahtani& R.M. Mahmoud, *Ganoderma multicornum* Ryvarden, *Ganoderma multiplicatum* (Mont.) Pat., *Ganoderma pakistanicum* Umar, A., Ahmed, S., & Gafforov, Y., *Ganoderma resinaceum* Boud., and *Ganoderma tornatum* (Pers.) Bres.

In this study, we are dealing with three specimens of *G. curtisii* species collected from three different localities of Lahore and Gujranwala districts. Previously this taxon has already been reported only from Murree Hills of Pakistan. The morphological and anatomical descriptions, macrographs of fruiting bodies, micrographs of anatomical features, comparison morpho-anatomical features of *Ganoderma curtisii* described from neighboring countries of Pakistan along with a map showing geographical locations of *G. curtisii* from Pakistan are given in this article.

MATERIALS AND METHODS

Three of *G. curtisii* specimens were collected during the during rainy seasons of 2021 from Canal-bank Road (Lahore) Wazirabad tehsil and Uggo Chak, along Hafizabad road (Gujranwala). Each specimen was photographed, tagged with a specific code and documented with location, date

and host tree details. In laboratory, the specimens were dried using a fan heater and preserved in zip locked bags with their tags.

Macroscopic Analysis

Macroscopic characteristics of fruiting body were analyzed including length and width, color and size of pileus, resinous bands, laccate surfaces, texture, margins of stipe and pileus, presence or absence of stipe, hymenial surface, discoloration, taste and odor.

Slide Preparation and Micrometry

For the slide preparations, small pieces of the dried specimens were soaked in alcohol for 5 minutes then thin sections were placed on glass slides. Two drops of 5% KOH were used as mounting medium and 1% aqueous Congo red solution (w/v) was applied for hyaline structures. The fine sections of fruiting bodies were sharply cut and covered with cover slip for observation. Microscopic characteristics were measured and recorded under a light microscope at 40X magnification.

For anatomical analysis, at least 20 readings were taken, focusing on the length and width, shape, and quotient value and range of basidiospores, basidiole, cutis elements. The width range of generative hyphae, skeletal hyphae, binding hyphae and stipe hyphae were also measured. Additionally, extreme spore length and width values were also noted. Total number of spores determined for each collection was n and Qavg was the average of the Q coefficient (length/width ratio). Manual illustrations were created observing hymenial section. Identification of the species was conducted based on morpho-anatomical features.

RESULTS

The morpho-anatomical explanation species *Ganoderma curtisii* (Berk.) Murrill, with voucher codes (KM-09; GM-95; GM-15) is given in the form of description, micrographs, and illustrations. This species was collected at young and mature stages and reported here as two new locality records from districts Lahore and Gujranwala of Punjab province, Pakistan.

Taxonomy

Ganoderma curtisii (Berk.) Murrill, N. Amer. Fl. (New York) 9(2): 120 (1908)

(Fig. 1-4)

Macroscopic Analysis

Basidiocarp 4-10 cm, annual, stalked or finger-like structure, aplanate, coriaceous to woody hard. **Pileus** 1.3-1.5 × 1-1.2 cm (when young), 3.5-12 × 9-10 cm, 2-6 cm deep (when mature) medium sized to large, upper surface smooth, flabellate to subflabellate, glabrous, semicircular to kidney shaped when mature, laccate, creamy

white to light brown when young and brownish red to reddish brown when mature with purple hues, reddish brown to orange-yellow and ultimately white from center to margins, uneven and bald surface, lacquered. Texture tough and hard but not woody. **Margins** slippery when wet, thin and sharp, unlike to the center softer and thinner, varies in color from orange red to brown from young to mature, have active developing hyphae, clearly laccate, thinner than center. **Hymenial surface** of the basidiocarp is fertile and porous, light brown and not even. Duplex context 0.35 cm thick, resinous bands (melanoid zone) present, no concentric growth zones as present in G. sessile, corky-woody, has club-shaped cuticle cells, thick at the base, clamped, and subsolid hyphae. **Pore surface** whitish to light brown color when young stage and medium dark brown when maturity, sub circular to circular in shape and 4-6 per mm, thin dissepiments. Tubes 0.5-2 cm deep, unstratified, have variations in thickness, scretched when dried, light brown, with a typical melanoid zone. **Stipe** (usually present) 6.8- 7.8 × 1.5- 2.2 cm, bald, reddish-brown color, glabrous lacquered, rough and solid texture, lateral making an angle with the pileus (45-90 degrees). **Taste and odor** not distinctive. **Habit and habitat** grow in solitary or group, present at the base of *Eucalyptus camaldulensis* Dehnh in terrestrial area.

Microscopic Analysis

Basidiospores 11.4 × 5.7 µm, with hyaline vesicular appendum; avgL 11.4 µm, avgW 5.7 µm, avgQ 2 µm, broadly ellipsoid with truncate apex, brown in KOH double walled, inamyloid, contains oil droplet, sharply spotted, utriculate, brown color overlaid by hyaline apex and the wall have a range of "pillars" that are intermediately thick (0.3-0.7 µm). **Hyphal system** trimitic; consist of generative hyphae that were difficult to observe, hyaline to yellowish, branched, clamped. Skeletal hyphae W_{range} 2.85-5.7 µm, avgW 4.27 µm, from pileus width ranges from 2.85-8.55 µm, avgW 5.13 µm, grouped, thick walled, apically branched, aseptate, golden brown, broader in the context and thinner crustohymeniderm, Binding hyphae hyaline to yellow in color and narrower than skeletal hyphae. **Basidia** 28-40 × 7-8.5 µm, double walled, light yellowish in color, bisporic, clavate to cylindrical, clamped at base, thin, without oil droplets. Cutis element 22.8-28.5 × 5.7-8.55 µm, avgL 25.65 µm, avgW 7.125 µm, Qrange 2.66-5 µm, avgQ 3.83 µm, clavate to sub-clavate shape, clustered, apedicellate, smooth, and golden brown-yellow, thin or thick laccate lines of melanoid

substance present that start off from the stipe and run to the upper surface correspondingly. **Stipe hyphae**; 3-7 µm, branched, aseptate, thin walled, light golden yellowish color, narrow.

Collection Sites

PAKISTAN: Punjab, Lahore, Canal Bank Road, Green belt near H-3 block, 217 m above sea level, growing singly or groups, on the bottom of *Eucalyptus camaldulensis* Dehnh trunk, Khadija Malhi, KM-09, 14th October 2021; District Gujranwala, Wazirabad Tehsil, Neevan Ojla, Wazirabad, attached with wood, solitary, 226 meters (744 ft.) above sea level, S.

Rukhsar (GM-15) 30th August 2021; Gujranwala Tehsil, Uggo Chak, Hafizabad Road, attached with base of tree trunk, solitary, 226 meters (744 ft.) above sea level, S. Rukhsar (GM-95) 25th September 2021.

Literature Reviewed for Species Identification:

The description of morphological and anatomical characters of the reported species was confirmed from published literature of Steyaert (1980), Torres-Torres and Guzman-Davalos (2012), Torres-Torres et al. (2015), Loyd et al. (2018), Mardones et al. (2023), and Chouhan & Kaur (2023).

Fig. 1: Morphology of *Ganoderma curtisii* **(**KM-09**). A & B.** Basidiocarp in its natural habitat. **C & D.** Basidiocarp showing both white cap and stipe. **Scale bars: A.** 0.8 cm. **B.** 0.5 cm. **C.** 1.95 cm. **D.** 1.5 cm.

Fig. 2: Morphology of basidiomata of *Ganoderma curtisii* (GM-15; GM-95). **A–C.** Basidioma. **D–F.** Pore surface. **Scale bars: A, D & E.** 2 cm, **B & C.** 1.5 cm, **F.** 1 cm.

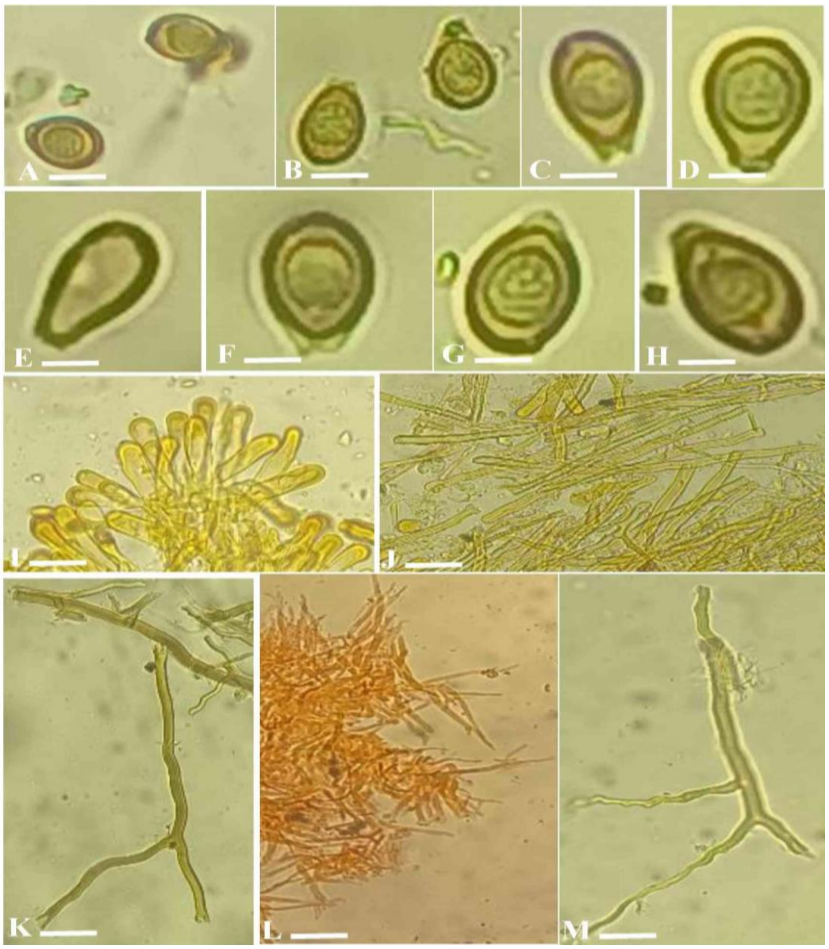

Fig. 3: Light micrographs of microscopic features of *Ganoderma curtisii* (GM-95)**. A–H.** Basidiospores. **I.** Cutis elements. **J & K.** Generative hyphae. **L.** Skeletal hyphae. **M.** Stipe hyphae. **Scale bars: A.** 8 µm, **B.** 7 µm, **C.** 4.5 µm, **D–F.** 4 µm, **G & H.** 3.5 µm, **I.** 17 µm, **J & K.** 25 µm, **L.** 30 µm, **M.** 12.5 µm.

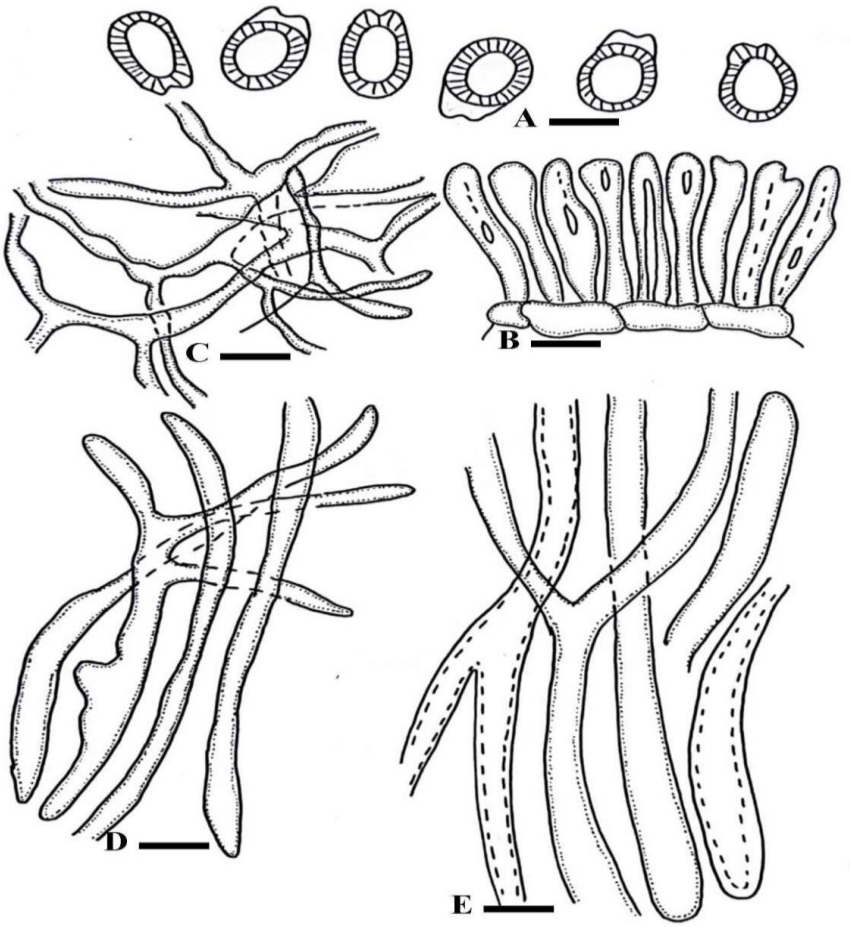

Fig. 4: Illustrations of microscopic features of *Ganoderma curtisii* (GM-95). **A.** Basidiospores. **B.** Cutis elements. **C.** Skeletal hyphae. **D.** Stipe hyphae. **E.** Generative hyphae. **Scale bars: A.** 6.5 µm, **B.** 14 µm, **C.** 8 µm, **D.** 8.5 µm, **E.** 10 µm.

Table 1: Comparison of Characteristic Features of *Ganoderma curtisii* reported from Neighbouring Countries of Pakistan

Species Name with country	Macroscopic characters							Microscopic Characterization							Source
	Pileus						Stipe Length (cm)	Basidiospores		Type of Hyphal system	Hyphal system			Basidia size (µm)	
	Size (cm)	Shape	Colour (at maturity)	Resinous Bands/ Non-Resinous Bands	Lactate/ Non Laccate	Concentric Zones (on the upper surface of the pileus)		Size (µm)	Shape		Generative Hyphae (Diameter in µm)	Skeletal Hyphae (Diameter in µm)	Binding Hyphae (Diameter in µm		
G. curtisii (Pakistan)	1.3-1.5 × 1-1.2	semicircular to kidney shaped	brownish red to reddish brown with purple hues	resinous bands	laccate	concentrically zonate	6.8-7.8	9.5-11.2 ×4.8-6.3	broadly Ellipsoidal	trimitic	2.4-4	2.85-5.7	2-3.1	12-27×5.6-11	Mukhtar, 2019
G. curtisii (India)	14× 2.5	circular	creamish white, r	resinous bands	laccate	concentrically zonate	8.0 × 3.0	14.0-16.5 × 9.0-10.5	ellipsoid	trimitic	5.9	4-5.5	3	21.8 × 3.12	Nagadesi & Arya, 2012; Chouhan & Kaur, 2023
G. curtisii (China)	10.5 ×4.4	reniform	yellowish-brown to reddish-brown with purple hues	resinous bands	laccate	concentrically zonate	9.0 × 4.0	(9-)11-17 × (7-)8-10	ellipsoid to oblong	trimitic	3.5	1.5-6	3-5	not observed	Cao et al., 2012; Zhou et al., 2015; He et al., 2021

DISCUSSION

Ganoderma was named due to its shiny or lustrous surfaces and *curtisii* represented the species name in the honor of Moses Ashley Curtis (1808-1872), an American Epicopal priest, botanist, mycologist and teacher. *Ganoderma curtisii* (Berk.) Murrill belongs to the laccate group of *Ganoderma* occurred in both temperate and sub-tropical forests. Initially, *Ganoderma curtisii*, was defined from North America (Moncalvo and Ryvarden, 1997; Thawthong et al., 2017). This species is saprobic and parasitic may be growing alone or in groups, found on the dead or decaying hardwood logs tree trunks or on the roots. From Pakistan this species was collected and reported from Murree Hills. In this study, *G. curtisii* was reported as new locality records from the base of *Eucalyptus camaldulensis*, and from base of an unknown tree trunk in terrestrial areas from Lahore and Gujranwala districts.

G. curtisii is a white root decay fungus, that causes the greater mass loss from the substrate where they are present, and this activity is comparable to the *F. ambrosius* as reported by (Kasson et al., 2016; Skelton et al., 2020).

G. curtisii, the mushroom of immortality or Ling-Chi, was characterized by semicircular to kidney shaped pileus beautifully lacquered with brilliant yellow new growth and white tips, duplex context, resinous bands, no concentric growth zones (Cao et al., 2012) as present in *G. sessile*, corky- woody, club-shaped cuticle cells present (Haddow and Haddow, 1931; Steyaert, 1980; Ojeda-Lopez et al., 1986; Torres-Torres et al., 2015), Pore surface white to crème brown and sub circular to circular pores (Steyaert, 1980), stipe lateral at the angle of (45-90 degrees) with the pileus, basidiospores 11.4 × 5.7 µm, ellipsoidal (Steyaert, 1980; Torres-Torres and Guzman-Davalos, 2012) with the hyaline vesicular appendix double walled, trimitic hyphal system and club shaped cutis (Torres-Torres et al., 2015; Gurpreet et al., 2017).

G. curtisii by some adjustments has been used to determine antioxidant activity and in the food industries other nutritional manufacturing because of its effective natural antioxidants (Huang et al., 2002; Ivone et al., 2016; Rosales-Lopez et al., 2022).

G. curtisii has been used to make composites due to its ability to form resistant mycelial matrix (Cesar et al., 2023). By this species about 29 lanostane triterpenoids have been obtained, that are the lipopolysaccharides, inhabit the nitric oxide (NO) production in the activated BV-2 microglia cells (Jiao et al., 2016).

G. curtisii exhibits antibacterial activity, in addition to ganoderic acids, phenolic compounds are also involved in this activity (Li et al., 2012; Rempe et al., 2017). The compounds extracted from this species responsible for this antibacterial activity are phenols, terpenes, and fatty acids. (Desbois and Smith, 2010; Rempe et al., 2017). This inedible fungus can be used to lower the blood pressure and to reduce the blood clot. It can also be used in cancer treatments.

G. curtisii was morphologically related to the *G. sessile* as both were annual, perennial (*G. curtisii* is sub-stipitate to stipitate or sessile while *G. sessile* is sessile), pileus surface laccate, flabelliform, dimidiate, lacquered (Steyaert, 1980; Torres-Torres et al., 2015; Nagadesi and Arya, 2016). The duplex context (Torres-Torres and Guzman-Davalos, 2012) have resinous bands (melanoid zone). There were no concentric growth zones in *G. curtisii* (Cao et al., 2012; Luangharn et al., 2021) but were present in *G. sessile*. Basidiospores ellipsoidal (Steyaert, 1980; Torres-Torres and Guzman-Davalos, 2012), the size of basidiospres in *G. sessile* were slightly larger as compared to *G. curtisii* (Luangharn et al., 2021), hyphal system is trimitic (Steyaert, 1980).

G. curtisii closely resembled *G. lingzhi* (*G. lucidum*) in phylogeny. The basidiomata of both resembles each other in juvenile stage, pileal surface is yellow with white pore surface. When mature, *G. lucidum* has pilleus reddish brown in color with a hard crust, however, *G. curtisii* still has yellowish brown to brick red pileus with a thin and soft crust. In *G. curtisii* the pore surface was white with thin dissepiments when mature, while in *G. lucidum* pore surface is yellow when mature with dissepiments thick. The cuticle cells in the *G. lucidum* are, closely packed, slender with narrower apical parts as compared to loosely arranged cutis cells inflated with wider apical parts in *G. curtisii* (Steyaert, 1980; Cao et al., 2012; Torres-Torres et al., 2015).

According to (Torres-Torres et al., 2015) *G. meredithiae* and *G. ravenelii* had identical morphology as that of *G. curtisii* in the basidiomata, pileus shape, color and texture, margins, context features, pore arrangments, stipe color and texture, and in microscopic characterizations. *G. meredithiae* (Adaskaveg and Gilbertson, 1988) had more diverticulated and differentiated cuticle cells. But in case of *G. ravenelii* there was a difference in terms of shape and size of basidiospores, as compared to *G. curtisii* they were more oblong to cylindrical (Steyaert, 1980) and in the context there were no resinous bands.

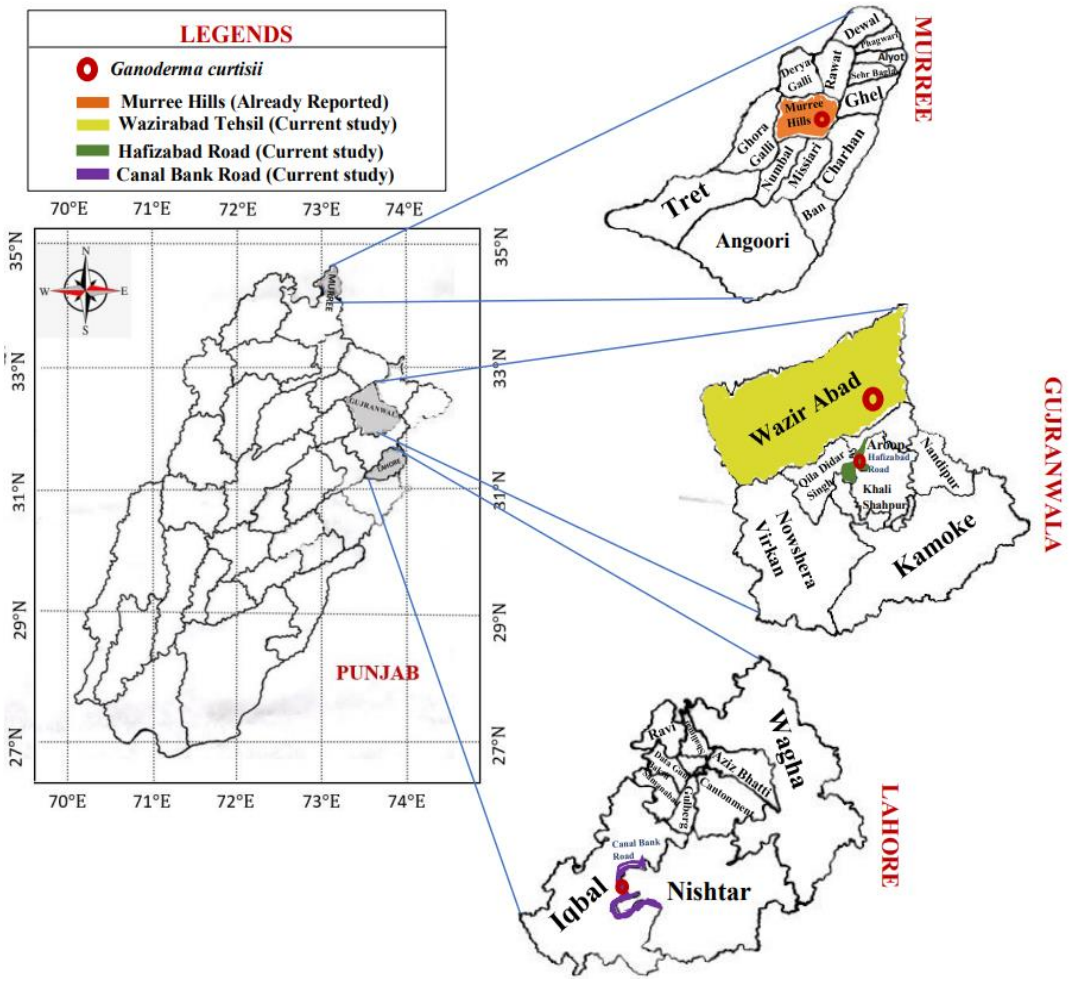

Figure 5: Distribution of *Ganoderma curtisii* in Pakistan

CONCLUSION

In conclusion, new locality reports of *Ganoderma curtisii* from three different sites (one from District Lahore and two from District Gujranwala) signified the notable expansion of its geographical range. This finding suggested that Punjab supports the growth of these macro-mycetes and there are many more that need to be explored. The morphological and anatomical features of *Ganoderma curtisii* was described by the illustrations, micro-plates and colored photographs of micro-plates, a distribution map of this speciesxat Murree (already reported), Lahore and Gujranwala (current study) reported from

Punjab, and a comparison table of characteristic attributes of *Ganoderma curtisii* recorded from neighboring countries of Pakistan were presented in this article.

ACKNOWLEDGEMENT

N/A

CONFLICT OF INTERESTS

The authors declare no conflict of interest.

REFERENCES

1. Adaskaveg JE, Gilbertson RL (1988). Basidiospores, pilocystidia, and other basidiocarp characters in several species of the Ganoderma lucidum complex. Mycologia 80(4): 493-507.
2. Ahmadi K, Riazipour M (2007). Effect of Ganoderma lucidum on cytokine release by peritoneal macrophages. Iran. J. Immunol. 4: 220-226.
3. Cao Y, Wu SH, Dai YC (2012). Species clarification of the prize medicinal Ganoderma mushroom “Lingzhi.” Fungal Divers. 56: 49-62.
4. Cao Y, Yuan HS (2013). Ganoderma mutabile sp. nov. from southwestern China based on morphological and molecular data. Mycol. Prog. 12: 121-126.
5. Cesar E, Castillo-Campohermoso MA, Ledezma-Perez AS, Villarreal-Cardenas LA, Montoya L, Bandala VM, Rodriguez-Hernandez AM (2023). Guayule bagasse to make mycelium composites: An alternative to enhance the profitability of a sustainable guayule crop. Biocatal. Agric. Biotechnol. 47: 102602.
6. Chan WK, Law HK, Lin ZB, Lau YL, Chan GC (2007). Response of human dendritic cells to different immunomodulatory polysaccharides derived from mushroom and barley. Int. Immuno pharmacol. 19: 891-899.
7. Chen AW, Seleen J (2007). Potential benefits of Ling-Zhi or Reishi mushroom Ganoderma lucidum (W. curt. Fr.) P. Karst. (Aphyllophoromycetideae) to breast cancer patients. Int. J. Med. Mushrooms 9: 29-38.
8. Chen TQ, Xu XL, Yang C, Yang L, Ying ZH, Shi XK, Ding MG (2024). Comparative genomics reveals ample evidence to Ganoderma sinense cultivars for molecular identification and new FIP exploration. Genomics 116: 110924.
9. Chouhan R, & Kaur S (2023). Diversity of the

Ganoderma species from Rajasthan, India. J. Mycol. Pl. Pathol. 53: 3.
10. Coetzee MP, Marincowitz S, Muthelo VG, Wingfield MJ (2015). Ganoderma species, including new taxa associated with root rot of the iconic Jacaranda mimosifolia in Pretoria, South Africa. IMA fungus 6: 249-25.
11. Dai YC, Cui BK, Yuan HS, Li BD (2007). Pathogenic wood-decaying fungi in China. For. Pathol. 37: 105-120.
12. De Silva DD, Rapior S, Fons F, Bahkali AH, Hyde KD (2012b). Medicinal mushrooms in supportive cancer therapies: An approach to anti-cancer effects and putative mechanisms of action. Fungal Divers. 55: 1-35.
13. De Silva DD, Rapior S, Hyde KD, Bahkali AH (2012a). Medicinal mushrooms in prevention and control of diabetes mellitus. Fungal Divers. 56: 1-29.
14. Desbois AP, Smith VJ (2010). Antibacterial free fatty acids: activities, mechanisms of action and biotechnological potential.Appl. Microbiol. Biotechnol. 85: 1629-1642.
15. El Sheikha AF (2022). Nutritional profile and health benefits of Ganoderma lucidum "lingzhi, reishi, or mannentake" as functional foods: Current scenario and future perspectives. Foods 11: 1030.
16. Fang H, Li X, Lin D, Wang L, Yang T, Yang B (2023). Inhibition of intrarenal PRR-RAS pathway by Ganoderma lucidum polysaccharide peptides in proteinuric nephropathy. Int. J. Biol. Macromol. 253: 127336.
17. Galappaththi MCA, Priyashantha AKH, Patabendige NM, Stephenson SL, Hapuarachchi KK, Karunarathna SC (2024). Taxonomy, Phylogeny, and Beneficial Uses of Ganoderma (Ganodermataceae, Polyporales). CRC Press. In Ganoderma Pp. 1-18.
18. Galor SW, Tomlinson B, Benzie IFF (2004): Ganoderma lucidum ('Lingzhi'), a Chinese medicinal mushroom: biomarker responses in a controlled human supplementation study. Brit. J. Nutr. 91: 263-269.
19. Gurpreet K, Singh AP, Dhingra GS (2017). Diversity of the genus Ganoderma in Punjab (India). Mycobiota 7: 25-49.
20. Haddow WR, Haddow WH (1931). Studies in

Ganoderma. J. Arnold Arbor. 12(1): 25-46.
21. He J, Luo ZL, Tang SM, Li YJ, Li SH, Su HY (2021). Phylogenetic analyses and morphological characters reveal two new species of Ganoderma from Yunnan province, China. MycoKeys 84: 141.
22. Huang D, Ou B, Hampsch-Woodill M, Flanagan J, Prior R (2002). High-throughput Assay of Oxigen Radical Absorbance Capcity (ORAC), using a Multichannel Liquid Handling System Coupled with a Microplate Fluorescence Reader in 96-well format. J. Agric. Food Chem.50: 4437-4444.
23. Hyde KD, Xu J, Rapior S, Jeewon R, Lumyong S, Niego AGT, ..., Stadler M (2019). The amazing potential of fungi: 50 ways we can exploit fungi industrially. Fungal Divers. 97: 1-136.
24. Ivone HA, Jorge MT, Guadalupe GRM, Berenice YJ (2016). Total polyphenols and antioxidant activity of Ganoderma curtisii extracts. J. of Med. Plants Studies 4(4): 136-141.
25. Jiao Y, Xie T, Zou LH, Wei Q, Qiu L, Chen LX (2016). Lanostane triterpenoids from Ganoderma curtisiiand their NO production inhibitory activities of LPS-induced microglia. Bioorg. Med. Chem. Lett. 26(15): 3556-3561.
26. Kao C, Jesuthasan AC, Bishop KS, Glucina MP, Ferguson LR (2013). Anti-cancer activities of Ganoderma lucidum: active ingredients and pathways. Funct. Foods Health Dis. 3(2): 48-65.
27. Karsten P (1881). Enumeratio Boletinearumet Polyporearum Fennicarum, systemate novo dispositarum. Rev. Mycol. 3: 16-19.
28. Kasson MT, Wickert KL, Stauder CM, Macias AM, Berger MC, Simmons DR, ..., Hulcr J (2016). Mutualism with aggressive wood-degrading Flavodonambrosius (Polyporales) facilitates niche expansion and communal social structure in Ambrosiophilus ambrosia beetles. Fungal Ecol. 23: 86-96.
29. Khadbaatar S, Bao H, Gao X, Huo H (2024). Study on Differences of Metabolites among Different Ganoderma Species with Comprehensive Metabolomics. J. Fungi 10(8): 524.
30. Li WJ, Nie SP, Liu XZ, Zhang H, Yang Y, Yu Q, Xie MY (2012). Antimicrobial properties,

antioxidant activity and cytotoxicity of ethanol-soluble acidic components from Ganoderma atrum. Food Chem. Toxicol. 50: 689-694.
31. Liu X, Yuan JP, Chung CK, Chen XJ (2002). Antitumor activity of the sporoderm broken germinating spores of Ganoderma lucidum. Cancer Lett. 182: 155-161.
32. Loyd AL, Held BW, Barnes CW, Schink MJ, Smith ME, Smith JA, Blanchette RA (2018). Elucidating 'lucidum': Distinguishing the diverse laccate Ganoderma species of the United States. PLoS ONE 13(7): e0199738.
33. Luangharn T, Karunarathna SC, Dutta AK, Paloi S, Promputtha I, Hyde KD, ..., Mortimer PE (2021). Ganoderma (Ganodermataceae, basidiomycota) species from the greater mekongsubregion. J. Fungi 7(10): 819.
34. Mardones M, Carranza-Velazquez J, Mata-Hidalgo M, Amador-Fernandez X, Urbina H (2023). Taxonomy and phylogeny of the genus Ganoderma (Polyporales, Basidiomycota) in Costa Rica. MycoKeys 100: 5.
35. Moncalvo JM (2000). Systematics of Ganoderma. In: Ganoderma Diseases of Perennial Crops. CAB International, Wallingford, UK. Pp. 23-45.
36. Moncalvo JM, Ryvarden L (1997). A nomenclatural study of the Ganodermataceae Donk. Fungi flora 10: 1-114.
37. Mukhtar T (2019). Morphological characterization of Ganoderma species from Murree hills of Pakistan. Plant Prot. 3(2): 73-84.
38. Nagadesi PK, Arya A (2012). New records of lignicolous fungi deteriorating wood in India. Mycosphere 3(6): 997-1004.
39. Nagadesi PK, Arya A (2016). Lignicolous macro fungi from Gujarat, India. World Sci. News 2(45): 307-330.
40. Ojeda-Lopez S, Sandoval MDLL, Valenzuela R (1986). The polypores of Mexico I. descriptions of some species from the northeastern of the guanajuato state. Rev. Mex. Mic. 2: 367-436.
41. Paterson RR (2006). Ganoderma- A therapeutic fungal biofactory. Phytochemistry 67: 1985-2001.
42. Pilotti CA (2005). Stem rots of oil palm caused by Ganoderm aboninense: Pathogen biology and epidemiology.

Mycopathologia 159: 129-137.
43. Pilotti CA, Sanderson FR, Aitken AB, Armstrong W (2004) Morphological variation and host range of two Ganoderma species from Papua New Guinea. Mycopathologia 158(2): 251-265.
44. Rempe CS, Burris KP, Lenaghan SC, Stewart Jr CN (2017). The potential of systems biology to discover antibacterial mechanisms of plant phenolics. Front. Microbial. 8: 422.
45. Richter C, Wittstein K, Kirk PM, Stadler M (2015). An assessment of the taxonomy and chemotaxonomy of Ganoderma. Fungal Divers. 71: 1-15.
46. Rosales-Lopez C, Arce-Torres F, Monge-Artavia M, Rojas-Chaves M (2022). Evaluation of the Use of Elicitors for the Production of Antioxidant Compounds in Liquid Cultures of Ganoderma curtisii from Costa Rica. Molecules 27(13): 4265.
47. Ryvarden L (1994). Can we trust morphology in Ganoderma? In: Buchanan PK, Hseu RS, Moncalvo JM (eds) Ganoderma: systematics, phytopathology and pharmacology. Proceedings of contributed symposium 59A, B, 5th International Mycological Congress, Vancouver 1994: Pp. 19-24.
48. Ryvarden L (2004). Neotropical Polypores Part 1. Fungi Flora, Oslo. Pp. 1-227.
49. Seweryn E, Ziała A, Gamian A (2021). Health-promoting of polysaccharides extracted from Ganoderma lucidum. Nutrients 13: 2725.
50. Singh R, Singh AP, Dhingra GS, Shri R (2014). Taxonomy, physicochemical evaluation and chemical investigation of Ganoderma applanatum and G. brownie. Int. J. Adv. Res. 2(5): 702-711.
51. Skelton J, Loyd A, Smith JA, Blanchette RA, Held BW, Hulcr J (2020). Fungal symbionts of bark and ambrosia beetles can suppress decomposition of pine sapwood by competing with wood-decay fungi. Fungal Ecol. 45: 100926.
52. Steyaert RL (1980). Study of some Ganoderma species. Bulletin du Jardin botanique national de Belgique/Bulletin van de Nationale Plantentuin van België, 50: 135-186.
53. Teng BS, Wang CD, Yang HJ, Wu JS, Zhang D, Zheng M, Fan ZH, Pan D, Zhou PA (2011). protein tyrosine

phosphatase 1B activity inhibitor from the fruiting bodies of Ganoderma lucidum (Fr.) Karst and its hypoglycemic potency on streptozotocininduced type 2 diabetic mice. J. Agric. Food Chem. 59: 6492-6500.

54. Thawthong A, Hapuarachchi KK, Wen TC, Raspe O, Thongklang N, Kang JC, Hyde KD (2017). Ganoderma sichuanense (Ganodermataceae, Polyporales) new to Thailand. MycoKeys 22: 27-43.
55. Torres-Torres MG, Guzman-Davalos L (2012). The morphology of Ganoderma species with a laccate surface. Mycotaxon 119(1): 201-216.
56. Torres-Torres MG, Ryvarde L, Guzman-Davalos L (2015). Ganoderma subgenus Ganoderma in Mexico. Rev. Mex. Mic. 41: 27-45.
57. Turner PD (1981). Oil Palm Diseases and Disorders. Oxford University Press, Oxford. Pp. 88-110.
58. Upton R (2000). American herbal pharmacopeia and therapeutic compendium: reishi mushroom, Ganoderma lucidum. Standards of Analysis, Quality Control, and Therapeutics. USA Canada: Santa Cruz. Pp. 405-407.
59. Wachtel-Galor S, Yuen J, Buswell JA, Benzie IF (2012). Ganoderma lucidum (Lingzhi or Reishi): a medicinal mushroom. CRC Press, Boca Raton, Florida, USA.
60. Woo YA, Kim HJ, Cho JH, Chung H (1999). Discrimination of herbal medicines according to geographical origin with near infrared reflectance spectroscopy and pattern recognition techniques. J. Pharm. Biomed. Anal. 21: 407-13.
61. Zhao JD, Zhang XQ (1994). Importance, distribution and taxonomy of Ganodermataceae in China. In Proceedings of Contributed Symposium, B 5th International Mycological Congress, Vancouver 1994: Pp. 14-21.
62. Zhao JD, Zhang XQ (2000). Ganodermataceae. Flora Fungorum Sinicorum Science Press, Beijing 18: 1-178.
63. Zhou LW, Cao Y, Wu SH, Vlasák J, Li DW, Li MJ, Dai YC (2015). Global diversity of the Ganoderma lucidum complex (Ganodermataceae, Polyporales) inferred from morphology and multilocus phylogeny. Phytochemistry 114: 7-15.

LGU Journal of

LIFE SCIENCES

LGU Society of Life Sciences

DOI: https://doi.org/10.54692/lgujls.2024.0803352

Paper Submission: 3rd July 2024; Paper Acceptance: 4th Sep 2024; Paper Publication: 10th Sep 2024

Research Article | LGU J. Life. Sci

Vol 8 Issue 3 July- Sep 2024 | ISSN 2519-9404

eISSN 2521-0130

Bioactivity of Ethanolic Leaf Extracts of *Acacia nilotica* and *Eucalyptus camaldulensis*, against *Coptotermes heimi*

Qurat-ul-Ain, Ayesha Aihetasham*

1. Institute of Zoology, University of the Punjab, Quaid-e-Azam Campus, Lahore, Pakistan Postal Code 54590

Corresponding Author's Email: ayesha.zool@pu.edu.pk

ABSTRACT: *Termite infestation poses a significant threat to structural integrity and agricultural productivity worldwide. This study was conducted to investigate the efficacy of ethanolic extracts of Acacia nilotica and Eucalyptus camaldulensis against Coptotermes heimi, focusing on mortality and repellency. The ethanoloic leaf extract of E. camaldulensis showed mortality of 79.33% at 30% concentration while A. nilotica at 30% of concentration revealed a mortality of 74.66%. The LC_{50} value of E. camaldulensis was 7.70% while that of A. nilotica was 13.03%. Both plants were found repellent against C. heimi, but A. nilotica was non-repellent at 10% concentration. Additionally, an analysis of Gas-Chromatography-Mass Spectrometry (GC/MS) was performed to identify and quantify the chemical constituents present in the plant extracts. The GC/MS analysis of E. camaldulensis revealed an important compound Eucalyptol, which has the highest percentage composition of 57.81 % while GC/MS of A. nilotica contains a high concentration of γ-Sitosterol along with Vitamin E and Behenic-alcohol. This study underscores the potential of A. nilotica and E. camaldulensis leaf extracts as ecofriendly alternatives for termite control.*

Keywords: *C. heimi*, GC/MS, Termite control, *A. nilotica, E. camaldulensis*

INTRODUCTION

One of the most common eusocial Isoptera insects are termites, which have intricate work divisions within each colony (Padwal et al 2023). Globally, there are currently 282 genera and nearly 3000 termite species, nearly 1000 reported from Africa (Van Huis, 2017; Ajayi et al., 2020). In Pakistan, there exist 53 distinct termite species, with 13 of them recognized as pests damaging forestry, buildings, and agriculture (Hassan et al., 2018; Ahmed et al., 2020). Termites exhibit diverse feeding patterns, falling into categories such as wood feeders, soil feeders, grass feeders, or fungus growers (Brauman et al., 2015; Ahmad et al., 2021).

An enormous amount of money, estimated to be several hundred million rupees annually, is lost because of termites, as their entire yield loss affects between 10 and 25 percent of the nation's crops (Ranjith et al., 2021; Padwal et al., 2023). Termite creates a major problem in both localities (urban and rural) across the world because they cause significant damage to wood structures, plants, and crops in addition to causing financial losses (Uzunovic et al., 2008; Khanum and Javed, 2020).

Globally, they indiscriminately target wood, with their attacks most prevalent in warmer climates (Aihetasham et al., 2017). Depending on the invasion species, managing termite colonies successfully requires a variety of specialized abilities. Identifying damage and finding management measures can be made easier with an understanding of termite ecology (Khan et al., 2016; Khanum and Javed, 2020).

Historically, the primary method for combating termites was the use of synthetic insecticides (Hertel, 2000; Venkateswara et al., 2005; Sattar et al., 2014; Aihetasham et al., 2015). Unfortunately, the risk is not only posed to mammals but also to birds, were carcinogenic, and contributed to environmental pollution. With the increasing prevalence of termite infestations, the need of finding treatments that are both safe for humans and the environment has become more pronounced (Meepagala et al., 2006; Aihetasham et al., 2015).

The development of botanical pesticides to manage various insect pests is being influenced by the negative consequences of synthetic pesticides. Powders and extracts derived from several bioactive plants that have insecticidal, repulsive, and anti-feeding qualities (Isman, 2006; Kassie, 2019). Since of their inherent biodegradability, plant-based pesticides are favored for the management of insect pests since they are less hazardous to non-target organisms (Prabakar & Jebanesan, 2004; Kassie, 2019). In addition to being toxic to a wide

range of insect pests, many plant extracts also modify the behavior of the pests they are intended to harm (Abbas et al., 2013; Aihetasham et al., 2017). When it comes to controlling termites, plants with both insecticidal and repellent qualities are thought to work best. It is safe to utilize plant bioactive components (Aihetasham et al., 2017).

The goal of the current research was to assess the potential toxicity of *E. camaldulensis* (sufaida) and *A. nilotica* (kikar) against *C. heimi*. Our objectives were to prepare Ethanolic extracts of selected plants by using the Soxhlet extractor, to evaluate the toxicity of these extracts against *C. heimi* by calculating LC_{50} along with Repellency test, and the structural characterization of the leaves extract by GC/MS.

MATERIALS AND METHODS

Termite Collection

Workers and soldiers of *C. heimi* were taken from the old trees of *Populus euramericana* from Canal Bank, University of the Punjab, Quaid-e-Azam campus, Lahore. Termites were maintained in the laboratory at 26±2 ºC for few days, on filter paper soaked with water along with five grams dried soil into the Petri-Plates.

Collection of Leaves

Leaves of the locally available medicinal plant *E. camaldulensis* (sufaida) and *A. nilotica* (kikar) were taken from the botanical garden at the University of the Punjab.

Preparation of Extracts

The leaves were air dried at ambient temperature for two weeks and then grinded into fine powder. Extracts were prepared by using 200 ml of ethanol in 20 grams of powder (leaves) in the Soxhlet extractor (Aihetasham et al., 2017). Rotary evaporator was used to obtain dried residues and stored in refrigerator for making stock solution. Further dilutions of 30%, 20% and 10% were prepared.

Gas chromatography/ GC/MS analysis

The samples of both the plants were analysed by gas chromatography (Trace GC-TSQ Evo 9000 mass spectrometer (Thermo Scientific, Austin, TX, USA) with a TC-SMS direct capillary column). The temperature of the protocol ranged from 80 to 280℃, increasing at a rate of 10℃/min, and remained constant for 10 minutes at 280℃. The injector maintained a temperature of 280℃ throughout the analysis. The carrier gas (helium) was used with a flow of 0.8 ml per minute. The compounds present in extracts were identified based on their retention time and structural formulas. Cross-referencing of mass spectral data with known authentic compounds, information obtained from relevant literature sources, were followed for verification of each compound.

Anti-termitic Assay

Anti-termitic assay was performed by following the methodology of Smith (1979). The base of each sterilized Petri-plate was surfaced with filter paper and 0.5ml of each extract of the desired concentration (30%, 20% and 10%) was applied. Petri plates along with filter paper were then dried at ambient temperature. A Hundred workers and 5 soldiers were placed in each Petri-plate and findings were made after 24 hours.

$$\text{Mortality \%} = \frac{\text{Number of dead insects after treatment}}{\text{Number of initial insects taken for treatment}} \text{ x } 100$$

Test for Repellency

Repellency test was conducted by cutting filter paper of 9cm diameter into 2 equal parts. One half of each filter paper was treated with 30%, 20% and 10% concentration of extracts and the other half with distilled water. Then the two halves of filter paper were placed in the Petri plate with a cut place between them. A total of 10 termites were released in the middle space. Repellency was assessed by counting number of termites after every 15 min on treated (T) and untreated (UT) filter paper and test was performed for a period of 2 hours. For each concentration of plant extracts three replicates were made. A treatment concentration was considered repellent when 21 (sum of three replicates) of 30 termites were present on untreated filter paper for five consecutive readings (Aihetasham, et al., 2017)

Statistical Analysis

A two-way ANOVA was used to compute and assess the termite mortality percentage; statistical significance was defined as $p<0.05$. LC_{50} was determined by Probit analysis.

RESULTS

The ethanolic leaf extracts of *A. nilotica* and *E. camaldulensis* were used to determine their efficacy against *C. heimi.* Greater mortality was observed at 30% concentration of both plant extracts while decreased at 20% and low in 10% concentration (Fig. 1, Table 3) The LC_{50} values of *A. nilotica* and *E.camaldulensis ethanolic leaf extracts against C. hemi were* 13.029 and 7.70, respectively (Table 4).

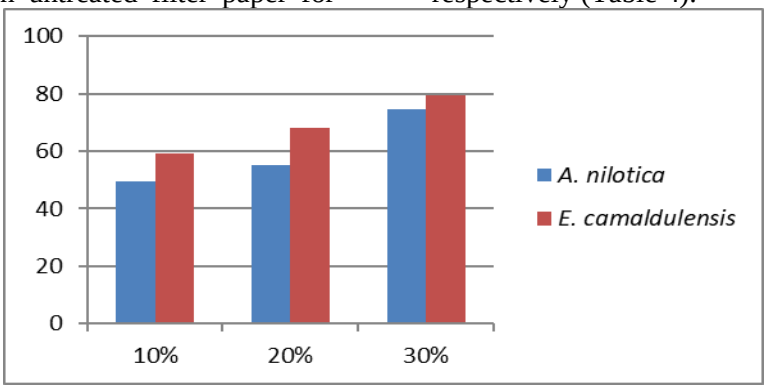

Fig. 1. Percentage mortality of *C. heimi* at different ethanolic leaf extract concentrations (10%, 20%, 30%) of *A. nilotica* and *E. camaldulensis*

Table I. Phytocompounds analysed in *A. nilotica* (ethanolic extract)

Sr #	Phytocompounds	Retention time (RT)	Relative % composition	Structural formulas
1	Bisphenol C	17.283	3.373%	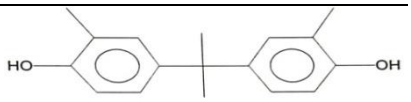
2	Neophytadiene	23.782	9.274%	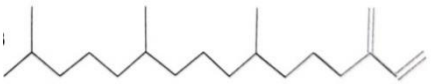
3	Phytol	26.702	2.848%	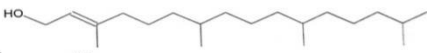
4	17-Pentatriacontene	28.690	1.836%	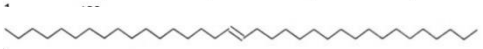
5	γ -Sitosterol	30.030	28.262%	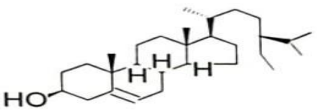
6	α – Amyrin	32.000	4.733%	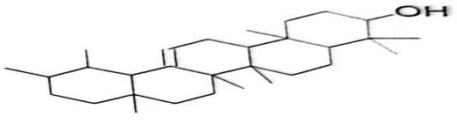
7	5,9,13,17-Tetramethyl 4,8,12,16-octadecatetraec acid	32.490	2.528%	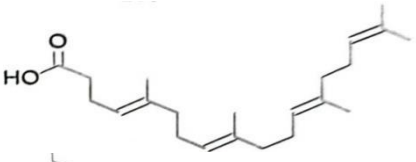
8	Eicosane,7-hexyl	32.915	2.491%	
9	Oxalic acid,allyl pentadecyl ester	34.419	1.696%	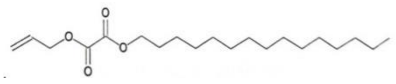
10	Behenic-alcohol	34.495	17.464%	
11	Vitamin E	34.950	23.868%	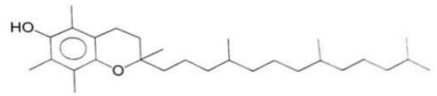
12	1-Eicosanol	35.416	1.628%	

The GC/MS analysis of plant indicated several important components. The GC/MS analysis of *A. nilotica* (Table 1, Fig. 2) revealed following compounds: Bisphenol C, Neophytadiene, Phytol, 17-Pentatriacontene, γ – Sitosterol, α – Amyrin, 5,9,13,17-Tetramethyl 4,8,12,16-octadecatetraenoic acid, Eicosane, 7-hexyl, Oxalic acid, allyl pentadecyl ester, Behenic-alcohol, Vitamin E, 1-Eicosano (Table 1 and Fig. 3). The GC/MS analysis of *E. camaldulensis* revealed several compounds: α – Pinene, Eucalyptol, Eucalyptol, Terpinen-4-ol, α – Terpineol, 1H-Cycloprop[e]azulene,1a,2,3,4a,5,6 ,7b-octahydro-1,1,4,7-tetrametyl- ,[1aR, Aromandendrene, (1R,9R,E)-4,11,11-Trimethyl-8-methylenebicyclo[7.2.0]undec-4-ene, Alloaromadendrene,1H-Cycloprop[e]azulene,1a,2,3,5,6,7, 7a,7b-0ctahydro-1,1,4,7-tetramethyl-,[1Ar], Naphthalene, 12,3,5,6,8a-hexdydro-4,7-dimethyl-1-(1-methylethyl)-,(1S-cis), (-)-Globulol, 1H-Cycloprop[e]azulen-4-0l, decahydro-1,1,4,7-tetramethyl- ,[1aR-(1aα,4β,4aβ,7),1H-Indene,1-ethylideneoctahydro-7a-methyl- ,(1Z,3aα,7aβ), Phytol, γ– Sitosterol, Olean-12-en-3-ol, acetate, (3β), Lupeol (Table 2).

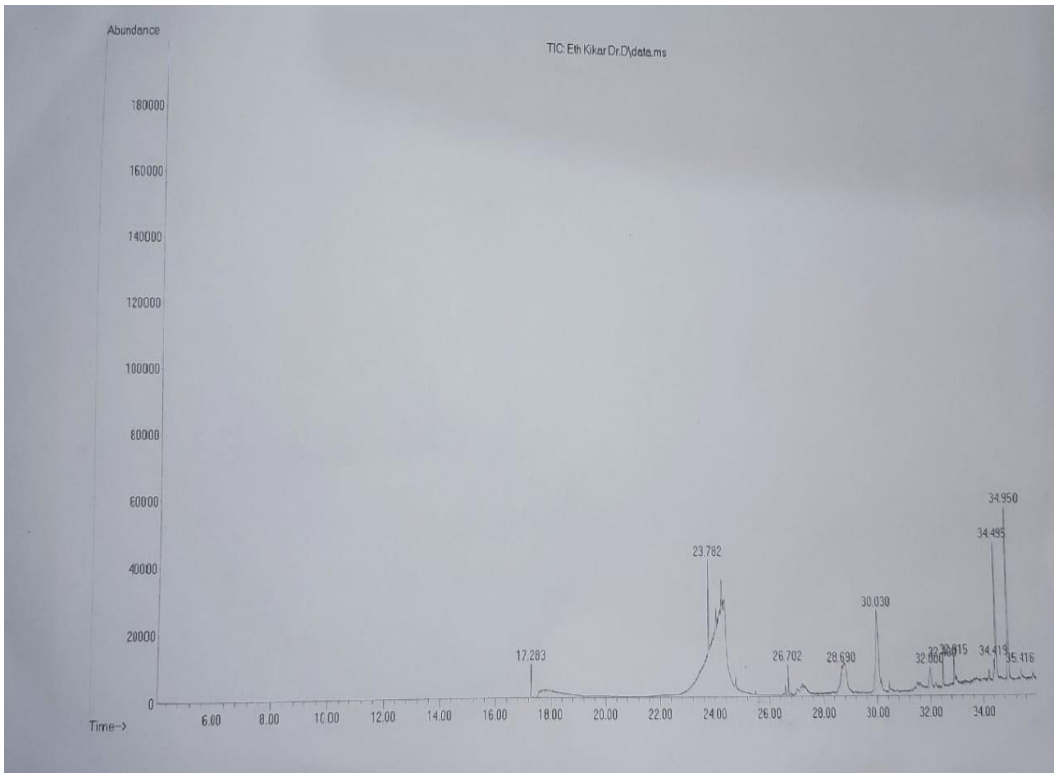

Fig. 2. Compounds identified in GC-MS analysis in *A. nilotica*

Table 2. Phytocompounds analysed in ethanolic extracts of *E. camaldulensis*

Sr #	Phytocompounds	Retention time	Relative percentage composition	Structural formula
1	α – Pinene	5.806	0.691%	
2	Eucalyptol	8.289	7.737%	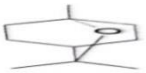
3	Eucalyptol	8.493	57.811%	
4	Terpinen-4-ol	12.189	1.358%	
5	α – Terpineol	12.538	1.749%	
6	1H-Cycloprop[e]azulene,1a,2,3,4a,5,6,7b-octahydro-1,1,4,7-tetrametyl-, [1aR	15.989	0.751%	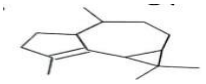
7	Aromandendrene	17.231	1.193%	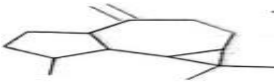
8	(1R,9R, E)-4,11,11-Trimethyl-8-methylenebicyclo [7.2.0]undec-4-ene	17.837	8.062%	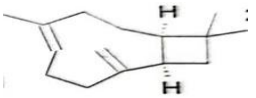
9	Alloaromadendrene	18.227	2.299%	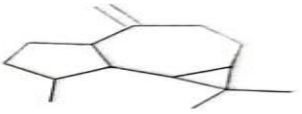
10	1H-Cycloprop[e]azulene, 1a,2,3,5,6,7,7a,7b-0ctahydro-1,1,4,7-tetramethyl-,[1Ar]	18.734	0.960%	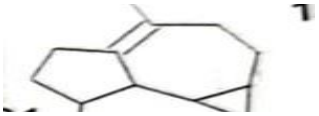
11	Naphthalene,12,3,5,6,8a-hexdydro-4,7-dimethyl-1-(1-methylethyl)-,(1S-cis)	18.845	1.412%	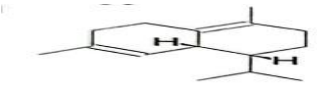

12	(-)-Globulol	19.311	0.667%	
13	1H-Cycloprop[e]azulen-4-0l, decahydro-1,1,4,7-tetramethyl-,[1aR-(1aα,4β,4aβ,7)	20.483	4.810%	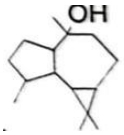
14	1H-Indene,1-ethylideneoctahydro-7a-methyl-,(1Z,3aα,7aβ)	20.605	1.718%	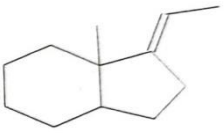
15	Phytol	21.066	0.895%	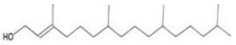
16	γ – Sitosterol	26.708	0.908%	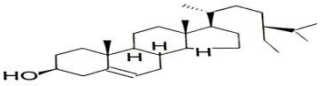
17	Olean-12-en-3-ol, acetate, (3β)	30.030	1.283%	
18	Lupeol	31.033	1.771%	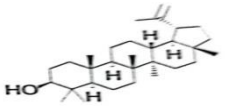

All the concentrations of both the plants were repellent, except 10% concentration of *A. nilotica* (Fig. 4). An observed concentration was notified repellent as twenty-one or more tested insects were found on untreated (UT) filter paper.

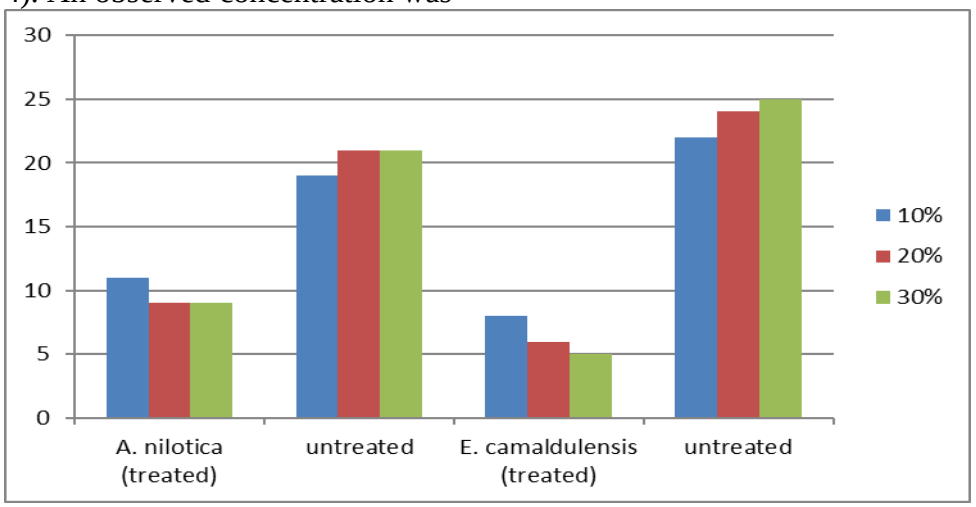

Fig. 4. Repellency test of *A. niolotica* and *E. camaldulensis* against *C. heimi*

Table 3. Two-way ANOVA for mortality of *C. heimi* (workers) after being exposed to *A. nilotica* and *E. Camaldulensis* ethanolic leaf extracts

ANOVA Table	SS (Type III)	Df	MS	F (DFn, DFd)	P value	Significance
Interaction	49.00	2	24.50	F (2,12) =33.92	P<0.0001	Yes
Plants	364.5	1	364.5	F (1,12) = 504.7	P<0.0001	Yes
Concentrations	1625	2	812.7	F (2,12) = 1125	P<0.0001	Yes
Residual	8.667	12	0.7222			

Table4. LC_{50} of *A. nilotica* and *E. camaldulensis* ethanolic extracts against *C. heimi.*

Sr. No.	Plant name	LC_{50}
1.	***A. nilotica***	13.029
2.	***E. camaldulensis***	7.70

DISCUSSION

The plants used in this study to control termites are *A. nilotica* and *E. camaldulensis* which contained biological active compounds. *E. camaldulensis* extracts were more repellent and toxic to *C. heimi* as caused 79.33% mortality at 30% concentration.

No prior research has been documented by using *A. nilotica* extract against termites, although its pesticidal properties are known. Numerous active components found in various parts of *A. nilotica* have been mentioned in diverse literature sources. Despite the absence of specific studies on the termiticidal effects of *A. nilotica* extracts, the promising results warrant further investigation at both laboratory and field levels. It is essential to

identify and evaluate the specific anti-termitic toxicant compounds within the potent extract. Initial findings from this research indicate that *A. nilotica* ethanolic extract exhibits remarkable anti-termitic properties against *C. heimi*.

Pande et al. (1981) reported that the *A. nilotica* (leaves and seeds) carry various components, including crude proteins, phosphorous, tannins, galactose, sulfides, pentosan, arabinose, catechol, galacton, calcium, saponins, and silica. The observed effect of *A. nilotica* extract against termites can be linked to Edriss et al. (2012), who noted its larvicidal effects, on the *Anopheles arabiensis*. Additionally, Vivekanandhan et al. in 2018, documented significant larvicidal activity from the seed pod solvent extract and essential seed oil of *A. nilotica* against 3 mosquito species: *Anopheles stephensi* with 5.239 LC_{50}, *Aedes aegypti* having 3.174 LC_{50} and *Culex quinquefasciatus* having 4.112 LC_{50}.

An extra significant finding is of Edriss et al. (2012), which identified alkaloids, saponins, flavones, tannins, triterpenes, and sterols in the petroleum ether and ethanolic extracts of *A. nilotica*. The tannins in *A. nilotica* are known for their potent biocidal properties (Fagg and Greaves, 1990; Edriss et al., 2012). The current findings align with the research by Baeshen and Baz (2003), which tested *A. nilotica* leaf extract against the *Aedes aegypti* and *Culex pipiens*, observing a remarkable reduction of larvae nearly about 89.8 percent in less than 24 hours and maintaining stability for twelve days. The current findings are consistent with the phytochemical analysis conducted by Solomon & Shittu (2009), which identified various compounds in the ethanolic leaf extract of *A. nilotica*. These compounds include phenols, flavonoids, tannins, alkaloids, triterpenoids, volatile oils, hydrolysable tannins, and saponin glycosides."

The ethanolic extract of *E. camaldulensis* demonstrated notable efficacy against *C. heimi*, with mortality rates increasing in correlation with higher extract concentrations. Jembere et al. (2005) similarly noted that mortality rates rose with increased extract concentration, observing minimal mortality at 10% and maximal mortality at 30%. Qureshi et al. (2016) supported these findings by reporting that the benzene-ethanol extract from the sapwood, heartwood and bark of *E. camaldulensis* exhibited high toxicity towards flagellates in termite species, including *C. heimi*, resulting in significant population reduction ($p < 0.05$). The population of flagellates in *C. heimi*, showed a reduction of 86.66% (908±82.7), 90.6%

(681±214) and 100% (0.0) in the bark, sapwood and heartwood. Furthermore, Alavijeh et al. (2014) corroborated the significant mortality of *E. camaldulensis* extract against pests like *Microcerotermes diversus*, highlighting its efficacy through contact, digestive, and fumigation toxicity.

Additionally, our findings are supported by Siramon et al. (2009), who demonstrated the potent antitermitic properties of *E. camaldulensis* leaf essential oil. They reported significant effectiveness against *C. formosanus* through both contact and fumigation methods, with LC_{50} values ranging from 12.68 to 17.5 mg/g and 12.65 to 17.5 mg/petri dish (100 cm^3), respectively. The extract also exhibited inhibition of acetylcholinesterase activity, impacting the nervous system. Furthermore, Mouna et al. (2021) corroborated these insecticidal properties, noting a 93% mortality rate with a 50% concentration of *E. camaldulensis* extract against *Aphis fabae*.

Among various compounds present in Eucalyptus essential oil, the 1, 8-cineol is the most essential and showed a notable role in insecticidal activity (Duke, 2004). Principally, Eucalyptol was found as an eminent constituent, showing retention time of 8.493 with relative percentage composition of 57.811%. Eucalyptol, the principal active component, present within the leaf extract may be responsible for toxicity against *C. heimi*.

The toxic and repellent effects of these plants are likely influenced by their chemical composition and the insects' susceptibility. To support our findings, we conducted a phytochemical screening, which confirmed the presence of active molecular families, including tannins and saponins.

CONCLUSION

Laboratory bioassay with *A. nilotica* and *E. camaldulensis* indicated their potential to be used as termiticides. Specifically, E. camaldulensis ethanolic extract was strongly repellent and toxic causing highest mortality of *C. heimi* at 30% concentration. The result of the present findings showed that botanical extracts are both economical and effective when used to control termites.

ACKNOWLEDGEMENTS

We are grateful for the facilities provided by Institute of Zoology, University of the Punjab.

CONFLICT OF INTEREST

Authors declare there is no conflict of interest.

REFERENCES

1. Abbas M, Shahid M, Iqbal M, Anjum F, Sharif S, Ahmed S, Pirzada T (2013). Antitermitic activity and phytochemical analysis of fifteen medicinal plant seeds. J. Med. Plants Res. 7(22):1608-1617.

2. Ahmad F, Yang GY, Liang SY, Zhou QH, Gaal HA, Mo JC (2021). Multipartite symbioses in fungus-growing termites (Blattodea: Termitidae, Macrotermitinae) for the degradation of lignocellulose. Insect Sci. 28(6):1512-1529.

3. Ahmed S, Fatima R, Hassan B (2020). Evaluation of different plant derived oils as wood preservatives against subterranean termite *Odontotermes obesus*. Maderas. Ciencia. y tecnología. 22(1):109-20.

4. Ajayi OEO-N, Oyeniyi EA, Elijah OA (2020). Synergism of three botanical termiticides as wood protectants against subterranean termites, *Macrotermes subhyalinus* (Rambur, 1842). J. Basic Appl. Zool. 81:1-2.

5. Aihetasham A, Akhtar MS, Umer M, Rasib KZ, Din MI (2017). Bioactivity of extracts of *Foeniculum vulgare* and *Ocimum basilicum* against *Heterotermes indicola* (Wasmann). Pak. J. Zool. 49 (6).

6. Aihetasham A, Umer M, Akhtar MS, Din MI, Rasib KZ (2015). Bioactivity of medicinal plants *Mentha arvensis* and *Peganum harmala* extracts against *Heterotermes indicola* (Wasmann) (Isoptera). Int. J. Biosci. 7(5):116-26.

7. Alavijeh ES, Habibpour B, Moharramipour S, Rasekh A (2014). Bioactivity of *Eucalyptus camaldulensis* essential oil against *Microcerotermes diversus* (Isoptera: Termitidae). J. Crop Prot. 3(1):1-11.

8. Baeshen RS, Baz MM (2023). Efficacy of *Acacia nilotica*, *Eucalyptus camaldulensis*, and *Salix safsafs* on the mortality and development of two vector-borne mosquito species, *Culex pipiens* and *Aedes aegypti*, in the laboratory and field. Heliyon. 9(5).

9. Brauman A, Majeed MZ, Buatois B, Robert A, Pablo AL, Miambi E (2015). Nitrous oxide (N_2O) emissions by termites: does the feeding guild matter?. PloS one. 10 (12): e0144340.

10. Duke J A (2004). Dr. Duke's Phytochemical and Ethnobotanical databases. Available online at http://www.ars-grin.gov/duke/ (accessed on 9 June, 2008)

11. Edriss AE, Satti AA, Alabjar ZA (2012). Preliminary studies on phytochemicals and larvicidal effects of *Acacia nilotica* L. extracts against

Anopheles arabiensis Patton. Sci. Res. Essay. 7(50):4253-8.

12. Fagg CW, Greaves A (1990). *Acacia nilotica* 1869 – 1988, CABI/OFI Annotated bibliography No. F 42, CAB International, Wallingford, Oyon, UK. 77 p.

13. Hassan B, Ahmed S, Kirker G, Mankowski ME, Misbah-ul-Haq M (2018). Antioxidant effects of four heartwood extractives on midgut enzyme activity in *Heterotermes indicola* (Blattodea: Rhinotermitidae). Environ. Entomol. 47(3):741-8.

14. Hertel H (2000). Finding Alternatives to Persistent Organic Pollutants (POPS) for Termite Management. Global IPM Facility Expert Group Termite Biology Management Stockholm Convention, FAO, Rome, Italy. 118-168.

15. Isman MB (2006). Botanical insecticides, deterrents, and repellents in modern agriculture and an increasingly regulated world. Annu. Rev. Entomol. 51(1): 45-66.

16. Jembere B, Getahun D, Negash M, Seyoum E (2005). Toxicity of Birbira (*Milletia ferruginea*) seed crude extracts to some insect pests as compared to other botanical and synthetic insecticides. In Proceedings of the 11th NAPRECA Symposium on natural products and drug delivery. 9-12.

17. Kassie WB (2019). International Journal of Entomology and Nematology. Int. J. 5(2):135-41.

18. Khan MA, Ahmad W, Paul B, Paul S, Khan Z, Aggarwal C (2016). Entomopathogenic nematodes for the management of subterranean termites. In: Hakeem KR, Akhtar MS, Abdullah SNA (eds) Plant, Soil and Microbes, vol 1. Implications in Crop Science. Springer International Publishing, Switzerland.

19. Khanum TA, Javed S (2020). Virulence of four *Steinernema* species as a biological control agent in controlling the termite, *Coptotermes heimi* (Wasmann)(Isoptera: Rhinotermitidae). EJBPC. 30: 1-4.

20. Meepagala KM, Osbrink W, Sturtz G, Lax A (2006). Plant-derived natural products exhibiting activity against formosan subterranean termites (*Coptotermes formosanus*). Pest Management Science: formerly Pesticide Science. 62(6): 565-570.

21. Mishra P, Verma M, Jha S, Tripathi A, Pandey A, Dikshit A, Sharma S (2021) Biological approaches of termite management: A review. Curr. Bot.12: 121-131.

22. Mouna M, Khadra B, Assia B, Salim L (2021). Insecticidal effect of two aqueous extracts from the leaves of *Salvia officinalis* and *Eucalyptus camaldulensis* against *Aphis fabae*. J. Entomol. Res. 45(2): 268-279.

23. Padwal KG, Chakravarty S, Srivastava CP (2023). Efficacy os Some Plant Extracts against Termites Under Controlled Conditions. Ind. J. Entomol. 14: 1-7.

24. Pande MB, Talpada PM, Patel JS, Shukla PC (1981). Note on the nutritive value of babul (*Acacia nilotica* L.) seeds (extracted). Indian J. Anim. Sci. 51(1): 107-108.

25. Peterson C (2006). Subterranean Termites. Their prevention and control in buildings. USDA Forest Service, Wood Products Insect Research Unit.

26. Prabakar K, Jebanesan A (2004). Larvicidal efficacy of some Cucurbitacious plant leaf extracts against *Culex quinquefasciatus* (Say). Bioresour. Technol. 95(1): 113-114.

27. Qureshi NA, Qureshi MZ, Ashraf A (2016). Comparative protozoacidal activities of different chemical extracts from various parts of three wood species against entozoic flagellates of *Heterotermes indicola* and *Coptotermes heimi*. Int. J. Bio. 8(3): 53-62.

28. Ranjith M, Ramya RS, Boopathi T, Kumar P, Prabhakaran N, Raja M, Bajya DR (2021). First report of the fungus *Actinomucor elegans* Benjamin & Hesseltine belonging to *Odontotermes obesus* (Rambur) (Isoptera: Termitidae) in India. Crop Protection.145:105622.

29. Rasib KZ, Ashraf H (2014). Feeding preferences of *Coptotermes heimi* (Isoptera: Termitidae) under laboratory and field conditions for different commercial and non-commercial woods. Int. J. of Tropi. Insect Sci. 34:115-26.

30. Sattar A, Naeem M, Ehsan-ul-Haq (2014). Efficacy of Plant Extracts Against Subterranean Termites i.e. *Microtermes obesi* and *Odontotermes lokanandi* (Blattodea:Termitidae). Environ. Sci. Biol. Agric. Food Sci. 1: 122.

31. Shafiei Alavije E, Habibpour B, Moharramipour S, Rasekh A (2014). Bioactivity of *Eucalyptus camaldulensis* essential oil against *Microcerotermes diversus* (Isoptera: Termitidae). J. Crop Prot. 3(1):1-11.

32. Siramon P, Ohtani Y, Ichiura H (2009). Biological performance of *Eucalyptus camaldulensis* leaf oils from Thailand against the subterranean termite *Coptotermes formosanus* Shiraki. J. Wood Sci. 55:41-6.

33. Smith VK (1979) Improved techniques designed for screening candidate termiticides on soil in the laboratory. J. Econ. Entomol. 72(6): 877-879.

34. Solomon-Wisdom GO, Shittu GA (2010). In vitro antimicrobial and phytochemical activities of *Acacia nilotica* leaf extract. J. Med. Plants Res. 4(12):1232-4.

35. Uzunovic A, Byrne T, Gignac M, Yang DQ (2008). Wood discolourations and their prevention with an emphasis on bluestain.

36. Van Huis A (2017). Cultural significance of termites in sub-Saharan Africa. J. Ethnobiol. Ethnomed. .13:1-2.

37. Venkateswara Rao J, Parvathi K, Kavitha P, Jakka NM, Pallela R (2005). Effect of chlorpyrifos and monocrotophos on locomotor behaviour and acetylcholinesterase activity of subterranean termites, *Odontotermes obesus*. Pest Manag. Sci. 61(4): 417-421.

38. Vivekanandhan P, Venkatesan R, Ramkumar G, Karthi S, Senthil-Nathan S, Shivakumar MS (2018). Comparative analysis of major mosquito vectors response to seed-derived essential oil and seed pod-derived extract from *Acacia nilotica*. Int. J. Environ. Res. Public Health. 15(2): 388.

LGU Journal of
LIFE SCIENCES

LGU Society of Life Sciences

DOI: https://doi.org/10.54692/lgujls.2024.0803359

Paper Submission: 3rd July 2024; Paper Acceptance: 7th Sep 2024; Paper Publication: 10th Sep 2024

Research Article
Vol 8 Issue 3 July- Sep 2024

LGU J. Life. Sci
ISSN 2519-9404
eISSN 2521-0130

Prevalence and Quantification of Aflatoxin B1 in Broiler Meat and Poultry Feed at Different Zones of Sindh, Pakistan

Abdul Wahid Solangi[1], Atta Hussain Shah[1], Ghulam Shabir Barham[1]*, Mansoor Tariq Samo[2]

1. Department of Animal Products Technology, Sindh Agriculture University Tandojam
2. Department of Veterinary Pathology, Sindh Agriculture University Tandojam

Corresponding Author's Email: gsbarham@sau.edu.pk

ABSTRACT: *This study aimed to assess the prevalence and levels of aflatoxin B1 in broiler meat and feed samples from various zones of Sindh, Pakistan, conducted at Sindh Agriculture University, Tandojam, during 2022-2023. A total of 360 broiler meat and feed samples, with 120 from southern, central, and northern zones, were collected from retail shops and poultry farms. All samples were screened for aflatoxin B1 using the ELISA Bio-Shield Total Extra Sensitive Kit. Negative samples were spiked with 5 and 10g/kg aflatoxin B1 for validation. The southern zone had the highest contamination of aflatoxin B1 in broiler meat (58.33%; 36.50±2.08 µg/Kg) and feed (67.50%; 66.20±1.15 µg/Kg), followed by the central zone (40.00%; 32.60±1.64 µg/Kg) and the northern zone (25.00%; 20.90±2.82 µg/Kg). Contamination levels in feed samples were also higher in the southern zone compared to central (48.30%; 56.25±0.87µg/Kg) and northern (28.30%; 47.55±1.50 µg/Kg) zones. The aflatoxin B1 levels in both meat and feed samples exceeded the FDA-recommended limit of 20 µg/Kg, posing a significant risk to food safety. These findings highlight the urgent need for a monitoring plan to mitigate aflatoxin contamination in broiler meat, poultry products, and feedstuffs across Sindh, Pakistan, to ensure safer food production.*

Keywords: Aflatoxin B1, Broiler meat, Poultry feed, ELISA, Sindh

INTRODUCTION

Poultry industry has been affected with huge monetary fatalities because of higher vulnerability of species to fungal development with toxin production which are painstaking confronts to food security particularly in hot, humid and subtropical regions where environment reached at ambient temperature and humid circumstances are optimal for moulds growth with toxins produced (Gamal, 2013). Among all the feed ingredients used for poultry feed preparation maize corns are more affected to by the mycotoxins especially aflatoxin type B1 all over the world the major and possible reason is the favourable field environment during pre, and post-harvest and storage conditions required for the growth of aflatoxin producing moulds as documented by Richard (2007). Aflatoxin B1 produced by the Aspergillus fungus is one of the most intoxicating toxins detected in poultry chicken, farms animal and other mono-gastric with different concentrations and time diversity (Bovo et al., 2014). Mycological point of view, the toxigenic abilities of all strains of aflatoxin genic species varied qualitatively and quantitatively, only about half of *Aspergillus flavus* strains of moulds produce $>10^6 \mu g/kg^{-1}$ of aflatoxins (Turner et al., 2009). Eighteen (n=18) different types of aflatoxins have been identified, among those the major health concerning members are AFB1, B2 and AFM1 and AFM2 strains of aflatoxins found in meat and milk (Dors et al., 2011; Summia et al., 2020; Hussain et al., 2022). In the environment different types of aflatoxin have been found commonly, four of them; B_1, B_2, G_1 and G_2 are principally perilous for human, birds and livestock as they invent in all major food crops; although human beings are more threatened to aflatoxin exaggerated meat, milk, nuts, grains and their derived products. Additionally, among B1, B2, G1 and G2 isomers of aflatoxins, AFB1 is a highly compelling toxin and carcinogenic. However, chicken rendering to Aflatoxin with tainted poultry and animal feed, different types of aflatoxin B1 and M1 have been found in muscle of thigh region, liver and kidneys and meat (Yunus et al., 2011). In addition to these, aflatoxin type B2 was also has been detected from the liver of broilers and layers due to the ration contaminated with a mixture of aflatoxins resulting lower body weight in broiler and reduction in the egg production and quality with augmented the vulnerability of Salmonellosis, candidacies, and coccidiosis in the poultry birds (Hussain et al., 2010). Among all other types of aflatoxin strains AFB1 is the most virulent type and its beingness reasoning major financial losses in agriculture sector, livestock, feed and poultry industry and produces harmful consequences on the health of human and birds (Beley et al.,

2013). Poultry not only produce toxigenicity but may also lead to retard the growth and quality of meat resulted by utilization of poor contaminated feed and amplified the occurrence of disease in domestic and commercial poultry broiler birds resulting enormous financial losses (Liu et al., 2011). The extent of aflatoxins in broiler muscle (breast, leg) dependents on the load of Fungi and toxin produced in feed as the aflatoxin type B1 concentration is increased in feed, it's residual limit in poultry meat is comprehensively increased than the aflatoxin free meat. Over the 1200 feed ingredients and feed samples collected from Asian countries including Pakistan, Bengal, China, Korea, Malaysia, Philippines, Singapore, Sri Lanka, Thailand and Vietnam for the detection of aflatoxins. Overall average extent of aflatoxin contamination was documented from 109 and 585 µg/Kg, respectively (Wei, 2004), it is surprising to note that, maximum number and extent of contamination of aflatoxin type B1 was recorded in Pakistan. Keeping in the literature cited highlighting the contribution of Pakistan in poultry rearing (11th top poultry producer) as well as share of poultry in Pakistan's meat production (35% of total production), common quality of grain ingredients being used in feed formulation, environmental condition favouring the growth of fungi and limited research on the occurrence of aflatoxin in poultry meat, in the present study an approach has been made to detect the prevalence of aflatoxin B1 in broiler meat and poultry.

MATERIALS AND METHODS

Sampling of broiler meat and poultry feed

One (1) kg each of broiler meat and poultry feed samples were collected from each sample collection point of southern, central and northern zones of Sindh. However, among each zone a total of three study areas (based on farming trend, humid conditions and moderate temperature favoring the fungal growth) were selected. All the collected broiler meat and feed samples were brought to the laboratory and processed for the detection of aflatoxin B1. A flow chart for sampling areas is shown in Fig.1.

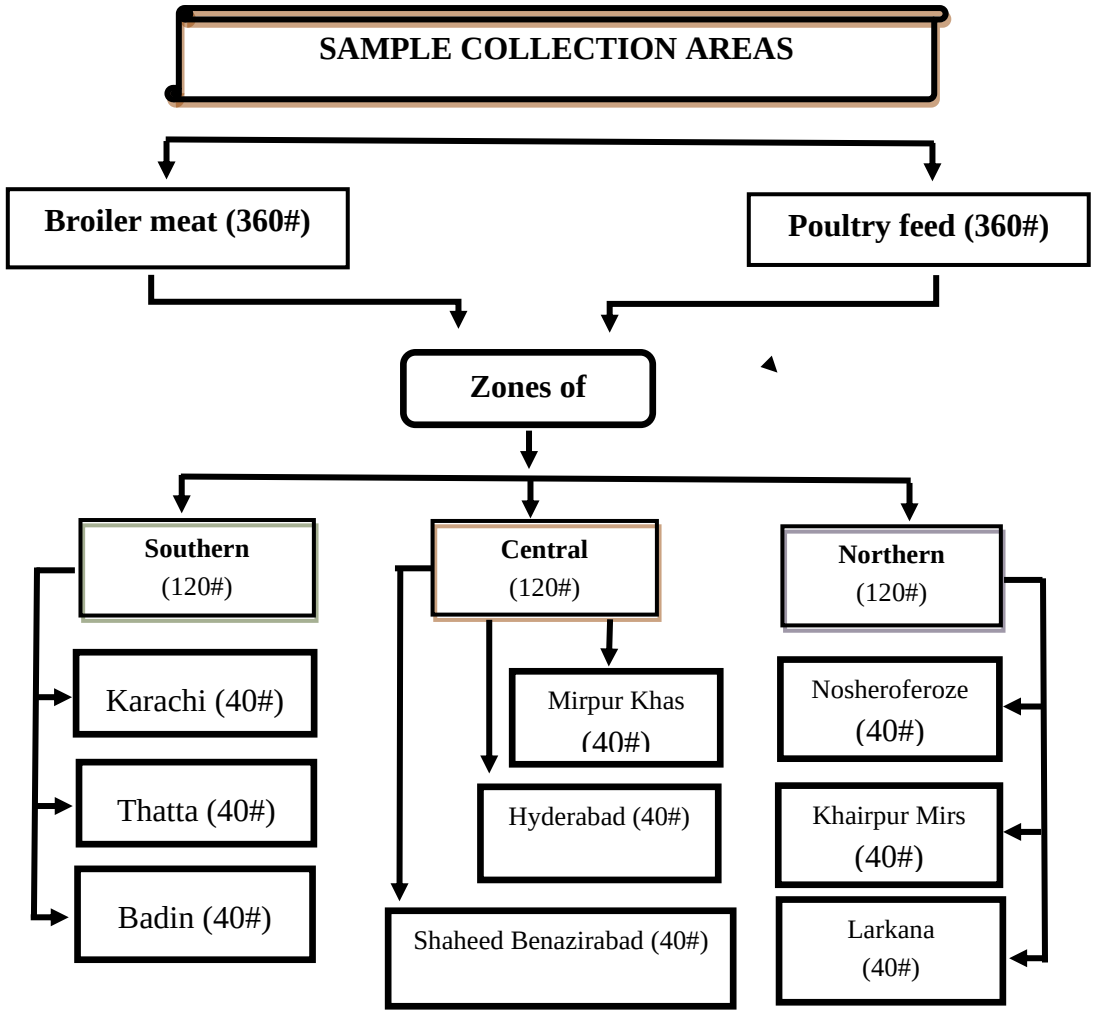

Fig.1: The sampling areas of different zones in Sindh Province

2.2. Experimental procedure for screening of aflatoxin B1 in broiler meat and feed

Present investigation was conducted on the occurrence of aflatoxin B1 in market broiler meat and poultry farms feed from production through ultimate consumption at Sindh province during the years of 2022-2023. Before applying the experimental procedure all the hygienically collected broiler meat and feed samples were transported and stored under chilling (<10°C) conditions at laboratory of Animal Products Technology department, Faculty of Animal Husbandry and Veterinary sciences, Sindh Agriculture University Tandojam. All the collected meat and feed samples of poultry were screened for aflatoxins B_1 by using standard protocol ELISA kit *i.e.* Bio-Shield Total Extra Sensitive kit (Max

Signal® commercial kit; 1055-04, Max Signal®, Bio-Scientific Corporation, Austin, TX, USA), containing 96-well micro-titer plates sensitized with monoclonal antibody specific for AFB1 (ProGnosis Biotech, 2015) as shown in Fig. 2.

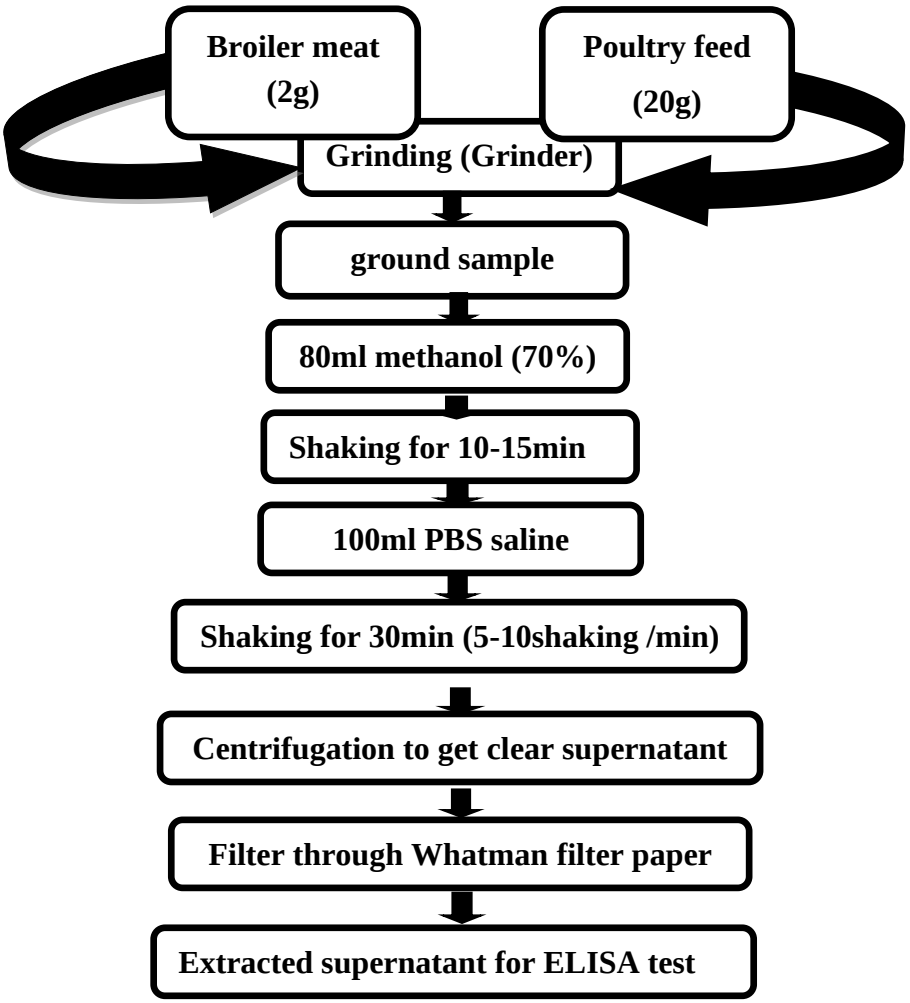

Fig. 2: Protocol for aflatoxin B1 detection in broiler meat and poultry feed

Analysis of aflatoxin B1 in meat and feed samples

50µl of prepared standard solution and both type of samples was taken through automatic pipette and transferred duplicate into the themicro-titer plate wells. Aflatoxin B1-horseradish peroxidase conjugate (100 µL) was poured to each well of plate and it was shaken manually for 1min and for a period of 30min incubated at room temperature. Micro-titer plate wells were completely emptied after incubation and washing has been done three times with 250 µL

of washing solution in each wash and dehydrated by tapping several times on a paper towel layer till the unbound conjugate has been removed completely. After washing Tetramethyl benzidine (100 µL) substrate was added to each well of the plat it was shaken for 1min again and incubated for 15min at room temperature. Subsequently, reaction was stopped by adding enzyme reaction inhibition buffer (100 µL) and the absorbance was directly calculated at 450nm in a BioTek® ELISA plate reader.

Statistical Analysis

Statistical analysis was carried out by applying computer statistical program, Student Edition of Statistix (SXW), Version 8.1 (Copyright 2005, Analytical software-USA). The data was tabulated and analyzed by summary statistics program, in which descriptive statistics was applied to identify the variability within same character of feed and broiler meat samples gathered from all the districts of all three targeted zones of Sindh Province. The data was also evaluated for analysis of variance; where significant variance appeared, the means were additionally computed using least significant difference (LSD) test at 5% level of probability.

RESULTS

Prevalence (%) of Aflatoxin B1 in broiler meat at different zones of Sindh province

In the current research study prevalence and quantification of aflatoxin B1 in broiler meat, among southern, central and northern zones, out of one hundred twenty (n=120) collected broiler meat samples from each zone, 58.33% (n=70) samples at southern, 40.00% (n=48) at central and 25.00% (n=30) at northern zone were found positive for aflatoxin B1, where 41.66% (n=50) 60.00% (n=72) and 75.00% (n=90) meat samples were declared as negative free from aflatoxin B1 contamination at all three zones of Sindh province (Fig. 3).

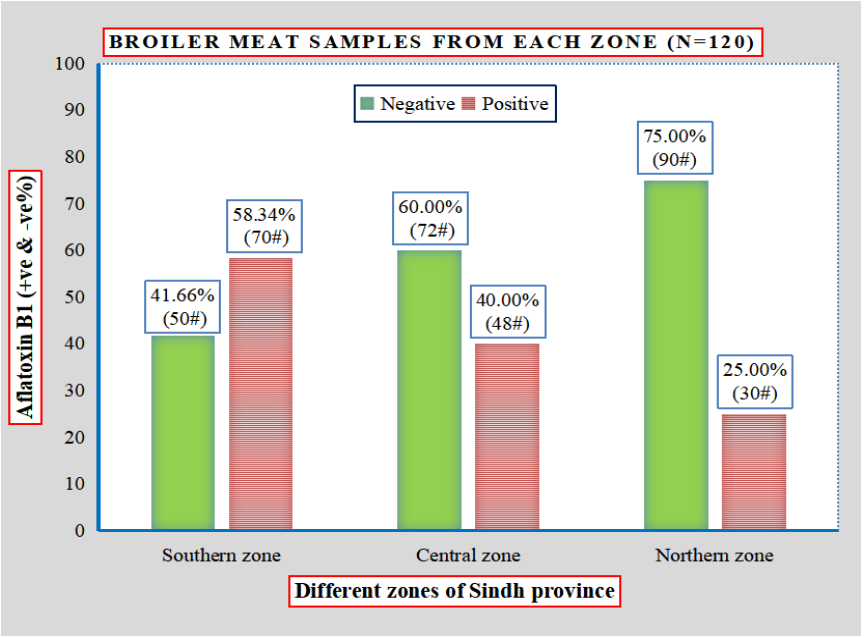

Fig. 3: Prevalence of Aflatoxin B1 in broiler meat at zones of Sindh province

3.2. Occurrence of Aflatoxin B1 in broiler meat at different zones of Sindh

The quantitative level of aflatoxin B1in broiler meat was ranged from 32.50-39.40 and with mean value of 36.50±2.08 µg/Kg at southern zone found significantly (P=0.0104) higher compared to aflatoxin B1 levels at central zone (29.90-35.60 and 32.60±1.64 µg/Kg) and northern (15.20-24.00 and 20.90±2.82 µg/Kg) zones of Sindh province (Fig. 4). Moreover, in current study the average quantitative level of the aflatoxin B1in broiler meat samples at study focused areas (southern, central and northern zones) were recorded more than the critical limits of aflatoxin B1 (20 µg/Kg) in meat and meat products as per recommendations of Food and drug Agency of United states (USFDA, 2000).

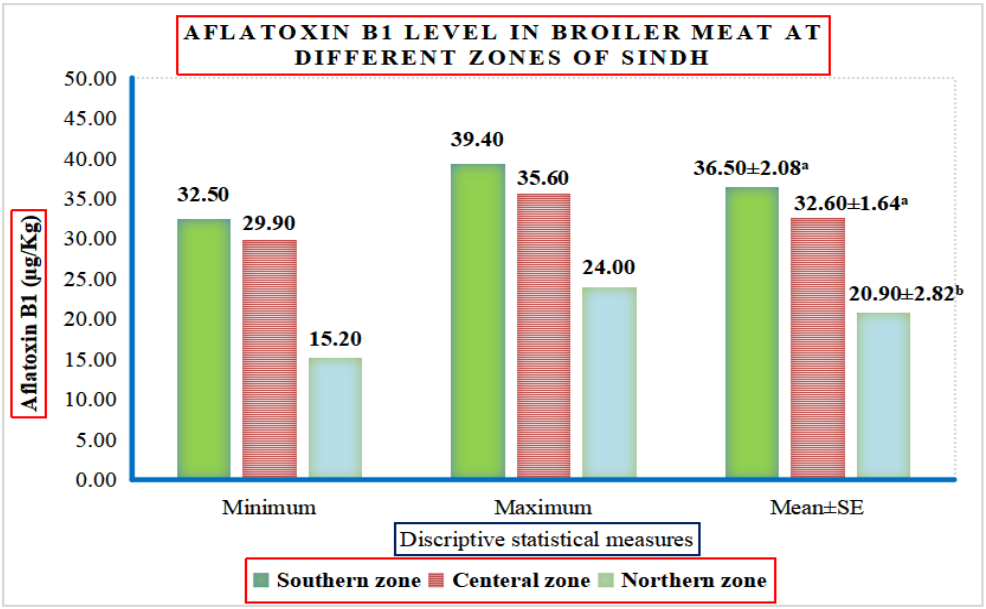

LSD (0.05) = 7.6342 SE±= 2.7496

Fig. 4: Quantitative level of Aflatoxin B1 (µg/Kg) in broiler meat at zones of Sindh province

Prevalence of Aflatoxin B1 in poultry feed at different zones of Sindh province

In the present study during the collection broiler meat samples from different farms at southern, central and northern zones of Sindh province, poultry feed samples were also collected for observing the preponderance and level of aflatoxin B1 in poultry feed. Among all three zones each of southern, central and northern, out of one hundred twenty (n=120) collected feed samples, the highest rate of aflatoxin B1 prevalence was recorded at southern (67.50%; n=81) next by central (48.30%; n=58) while lowest prevalence rate of aflatoxin B1 was noted at northern (28.30%; n=34) zones of Sindh, where 32.50% (n=39) 51.70% (n=72) and 71.86% (n=70) feed samples were found free from aflatoxin B1 contamination at all three zones of Sindh province (Fig. 5).

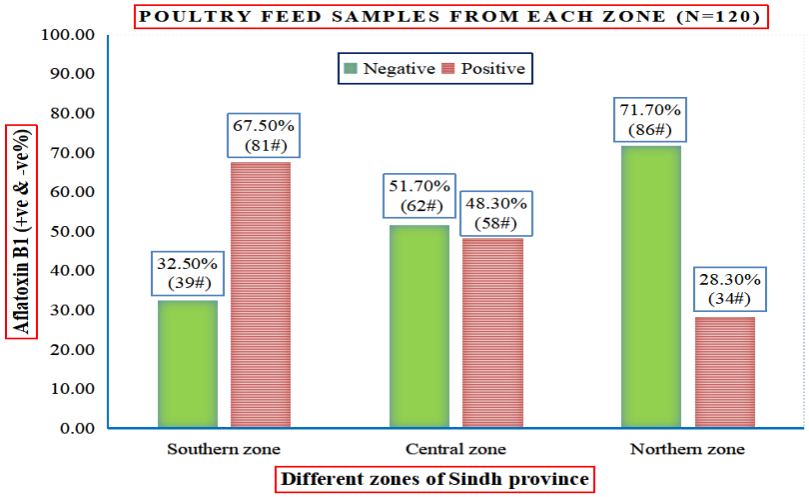

Fig. 5: Prevalence (%) of Aflatoxin B1 in broiler meat in zones of Sindh province

3.4. Occurrence of Aflatoxin B1 in poultry feed at different zones of Sindh

In the current research the quantitative level of aflatoxin B1 in poultry feed samples was ranged from 62.10 to 72.40 µg/Kg with average value of 66.20±1.15 µg/Kg at southern zone found significantly (P=0.0001) higher than the ranges and mean values of aflatoxin B1 in central (53.40, 60.10 and 56.25±0.87 µg/Kg) and northern (41.10, 52.60 and 47.55±1.50 µg/Kg) zones of Sindh province respectively (Fig. 6).

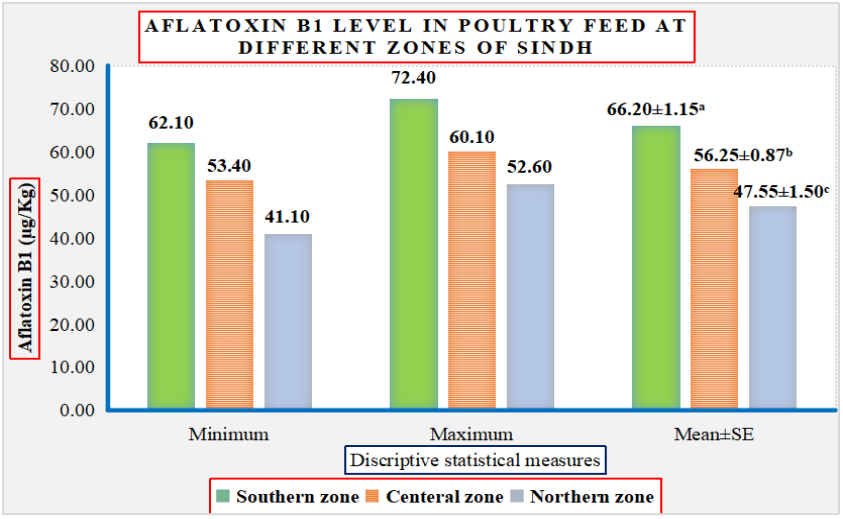

LSD (0.05) = 0.7265 SE± = 0.3427

Fig. 6: Quantitative level of Aflatoxin B1 (µg/Kg) in broiler meat at zones of Sindh province

DISCUSSION

Prevalence and quantitative level of aflatoxin B1 in broiler meat

The presence of aflatoxins in food and food products of animal and plant origin symbolizes a vital and major danger to the consumer health. Prevalence and occurrence of major toxic compound namely aflatoxin B1 broiler muscle and edible organs collateral to the exposure of poultry birds by means of feed and its ingredients as reported in the previous scientific studies (Sineque et al., 2017). Mainly aflatoxin B1 is famous natural intoxicant known as most virulent, toxic and cancerous growth compound (Bbosa et al., 2013) responsible for induce liver cancer (Feddern et al., 2013; Du et al., 2019) not only produce cancer cells also initiate production of metabolite compounds having analogous cyanogenetic properties (Bbosa et al., 2013), which create the curiosity for the monitoring of aflatoxins and their metabolites in chicken meat and poultry feed stuffs. In the current study higher prevalence and contamination level of aflatoxin B1 was noted at southern zone (58.33%; 36.50±2.08 µg/Kg) than central (40%; 32.60±1.64 µg/Kg) and northern (25%; 20.90±2.82 µg/Kg) zones of Sindh, Pakistan (fig. 3 and 4). Parallel to current results, 35% aflatoxin B1 with extent of 3.23 µg/Kg in chicken meat samples has been reported by Iqbal et al. (2014) from Pakistan, 45% chicken liver, 32% gizzard and 25% from 60 with 2.24 µg/Kg levels of aflatoxin B1 at Egypt was reported by researchers. Elsayed et al. (2018) reported 25.71, 48.57 and 77.1% prevalence of aflatoxin in luncheon, ground meat and meat sausages, while in another study 8.57% with 8µg/Kg quantitative level of aflatoxin B1 was also recorded by researchers. 0.25-0.331µg/Kg dietetic B1 residual level in the meat and edible offal (liver & kidney) was reported by Yunus (2011) in the flock fed with contaminated ration. Findings of Karmi (2019) showed variations in the extent of aflatoxins in meat products with 20µg/Kg (80%) residual level in basterma, 24 µg/Kg (96%) in meat burger, 23 µg/Kg (92%) in luncheon, 19 µg/kg (76%) in minced meat and 22 µg/Kg (88%) concentration of aflatoxin B1 was recorded in kofta meat samples. Filazi et al. (2010) have reported the major cause of aflatoxins in meat of broiler was the consumption of contaminated ration, when broiler chicken has been exposed to aflatoxins B1 along with trace of B1 and M1 aflatoxins have been found in meat and edible parts (liver and kidney) of broiler (Herzallah, 2009). However, the average quantitative level of the aflatoxin B1in broiler meat samples in all selected areas of Sindh were

recorded more than the critical limits of aflatoxin B1 (20 µg/Kg) in meat and meat products as per recommendations of Food and drug Agency of United States (USFDA, 2000). Researchers reported higher extent of contaminated meat and feed samples with aflatoxins which crossing the critical limits of 2µg/Kg for B1 and 4.2µg/Kg for total aflatoxins, therefore, it might be simply expected that these food sources pretense carcinogenic effects in the body of consumers and that extent of aflatoxins foods of animal origin should be examined for the reason that of these toxins are very much harmful and threatened to consumer health. The major sources of aflatoxins contamination in the food commodities were possibly the contaminated environment where moulds are omnipresent in air, soil, water, feeds and processing materials, respectively **(**Greco et al., 2014). However, according to the FDA and United state standards the safe level of aflatoxin B1 in a food is recommended <20 µg/Kg (USFDA, 2000). Maximum extent and contamination level of aflatoxin B1 in broiler meat samples found in the current study did not match with the critical limits of European community and many other countries, those have obligatory level of 2ng/g aflatoxin B1 as maximal tolerance level in consumable food for the human (Ortatatli et al., 2005).

Prevalence and quantitative level of aflatoxin B1 in poultry feed

Aflatoxin producing Aspergillus mould is a filth fungus species which has been acknowledged as a major source of grains contamination which are used in poultry diets. The growth of these moulds is facilitated by the ambient humid conditions and produce bioscience combat-ready cell toxic aflatoxins. Mainly all the poultry feed stuff like maize, rice, wheat, pistachios, cottonseed, copra groundnuts are prone to the contamination of these fungus taxonomic categories (Attia et al., 2016). In the current study highest prevalence rate and quantitative level of aflatoxin B1 was recorded at southern (67.50%; 66.20±1.15 µg/Kg) followed by central (48.30%; 56.25±0.87 µg/Kg), while lowest percent and level of aflatoxin in poultry feed samples was noted at northern (28.30%; 47.55±1.50 µg/Kg) zone of Sindh province (fig. 5 and 6). High rate of aflatoxin B1 prevalence with 100% positive samples at Balakot, 96% at Mansehra and 80% poultry feed samples were found contaminated with aflatoxin B1 at Oghi region of northern Pakistan with the average range of 34 to 86.2 µg/Kg, respectively as documented by the Naveed et al. (2022). Around the Globe, different frequencies and

contamination levels of aflatoxin have been reported in various studies. 88.2% of poultry feed samples were analysed through indirect competitive ELISA and found positive for aflatoxin B1 in Brazil (Rossi et al., 2012). The trend of current results for the prevalence and contamination level of aflatoxin B1 in poultry feed samples varied significantly at zone level. Factors like ambient temperature and humid environment could be the optimal chances for the growth of molds and production of aflatoxins in food stuffs (Abidin et al., 2017). Such a high prevalence and contamination level of aflatoxin B1 in feed samples detected during present study might be because of improper storage of broiler and layer feedstuff and lack of awareness for proper storage at poultry farms. Likewise, high levels of aflatoxin B1 in commercial poultry feed ingredients were documented by Anjum et al. (2012) samples gathered from a particular area of Pakistan. 66.6% aflatoxin B1 positive poultry feed samples from Morocco. 60% prevalence of positive samples with >10 µg/Kg aflatoxins in India and 7 to 160 ppb contamination level of aflatoxin B1 in the poultry feed samples in Bangladesh. Secondary metabolites (Aflatoxins) of *Aspergillus flavus* are the most common and prevalent contaminant found in poultry feed among both developed and underdeveloped countries of the world (Hern and ez-Ramirez et al., 2021). Rashid et al. (2012) reported higher frequency of positive (91.66%) poultry feed samples with contamination level of 47.64±2.55 µg/Kg, these figures of contamination level were differed from the current results (56.70±1.63 µg/Kg) at Pakistan. The existence of the aflatoxin type B1 is normally reported in the cereals like peanuts, corn, rice, soya beans which are been considered to be basic dietetic ingredients of the poultry ration, and the acceptable level of B1 type of aflatoxins in poultry feed is extremely low and consequently due to the contamination aflatoxin type B1 in the poultry feed is at a high risk resulting presence of toxins in broiler meat and its edible by-products (Fouad et al., 2019). Food and Drug Administration recommended 20 µg/Kg maximum permissible limit of aflatoxin B for feed and ration (USDFA, 2000), while the tolerable level of aflatoxins (4 µg/kg for total aflatoxins and 2 µg/kg for AFB1) for human consumption was suggested much lesser compared to animal feed (Kehinde et al., 2015).

CONCLUSION

In the present study it is concluded that among all three zones of Sindh province of Pakistan, the average prevalence percent and

quantitative levels of aflatoxin B1 in broiler meat and poultry feed samples were found significantly ($P<0.05$) higher at southern zone compared to central zone and northern zones. Nevertheless, the extents of aflatoxin B1 in broiler meat and feed samples among all three zones were found more than the critical limits of aflatoxin B1 (20µg/Kg) in meat and poultry feed. In this situation there is a prompt need to execute a monitoring plan to eradicate the entry of aflatoxin B1 residues in meat its products and poultry feed stuffs, that economical and cost-effective approach seem to be wrathful for developed food safety at different zones of Sindh, Pakistan.

Conflict of Interest

There is no conflict of interest shown by the research manuscript authors.

ACKNOWLEDGEMENT

Authors are highly graceful to Department of Animal Products Technology, Faculty of Animal Husbandry and Veterinary Sciences, Sindh Agriculture University Tandojam, Pakistan for facilitating and providing the healthy working environment for the appliance of current research work.

REFERENCES

1. Abidin Z, Khatoon A, Arooj N, Hussain S, Ali S, Manzoor AW, Saleemi MK (2017). Estimation of ochratoxin A in poultry feed and its ingredients with special reference to temperature conditions. Brit. Poult. Sci. 58(3): 251-255.
2. Anjum MA, Khan, SH, Sahota AW, Sardar R (2012). Assessment of aflatoxin B1 in commercial poultry feed and feed ingredients. J. Ani. Plant Sci. 22(2): 268-272.
3. Attia YA, Abd Al-Hamid AE, Allakany HF, Al-Harthi MA, Mohamed NA (2016). Necessity of continuing of supplementation of non-nutritive feed additive during days 21-42 of age following 3 weeks of feeding aflatoxin to broiler chickens. J. Appl. Ani. Res. 44(1): 87-98.
4. Bbosa GS, Kitya D, Ogwal-Okeng J (2013). Aflatoxins metabolism, effects on epigenetic mechanisms and their role in carcinogenesis. SCIRP 5 (10A): 14-34.
5. Beley MAJ, Teves FG, Reina M, Madamba SB (2013). Isolation of fungal species and detection of aflatoxin from soymilk products using ELISA method. Int. Res. J. Biol. Sci. 2(5): 45-48.
6. Binder EM, Tan, LM, Chin LJ, Handl J, Richard J (2007). Worldwide occurrence of mycotoxins in commodities, feeds and feed ingredients. Ani. Feed Sci. and Techol. 137(3-4): 265-282.
7. Bovo F, Franco LT, Rosim RE, Oliveira CAFD. (2014). Ability of a *Lactobacillus*

rhamnosus strain cultured in milk whey based medium to bind aflatoxin B1. Food Sci. and Technol. 34, 566-570.

8. Du X, Schrunk, DE, Imerman PM, Smith L, Francis K, Tahara J, Rumbeiha WK (2019). Evaluation of a diagnostic method to quantify aflatoxins B1 and M1 in animal liver by high-performance liquid chromatography with fluorescence detection. J. AOAC Inter. 102(5): 1530-1534.
9. Elsayed ME, Algammal AM, El-Diasty EM, Abouelmaatti RR, Abbas SM (2018). Prevalence of Aspergillus spp and Aflatoxins in luncheon, minced meat and sausage. Glob. Ani. Sci. J. 6(2): 17-23.
10. Feddern V, Dors GC, Tavernari FDC, Mazzuco H, Cunha A, Krabbe EL, Scheuermann GN (2013). Aflatoxins importance on animal nutrition. Aflatoxins-Recent Adv. and Fut. Prosp., 171-195.
11. Filazi A, Sinan INCE, Temamogullari F (2010). Survey of the occurrence of aflatoxin M1 in cheeses produced by dairy ewe's milk in Urfa city, Turkey. Ankara University of Veterinary Fakultesi Dergisi. 57(3): 197-199.
12. Fouad AM, Ruan D, El-Senousey HK, Chen W, Jiang S, Zheng C (2019). Harmful effects and control strategies of aflatoxin b1 produced by *Aspergillus flavus* and *Aspergillus parasiticus* strains on poultry. Toxins, 11(3): 176.
13. Gamal RE (2013). Mycological studies on chicken meat and their products. MV Sc. (Doctoral dissertation, Thesis Faculty of Vet. Med. Suez Canal Univ., Egypt).
14. Greco MV, Franchi ML, Rico Golba SL, Pardo AG, Pose GN (2014). Mycotoxins and mycotoxigenic fungi in poultry feed for food-producing animals. The Sci. World J. (1): 1-9.
15. Hernandez-Ramirez JO, Merino-Guzman R, Tellez-Isaias G, Vazquez-Duran A, Mendez-Albores A (2021). Mitigation of AFB1-related toxic damage to the intestinal epithelium in broiler chickens consumed a yeast cell wall fraction. Front. Vet. Sci. 8: (1) 677-965.
16. Herzallah SM (2009). Determination of aflatoxins in eggs, milk, meat and meat products using HPLC fluorescent and UV detectors. Food Chem. 114(3): 1141-1146.
17. Hussain A, Yasmeen R, Hafeez F, Saeed K (2023). Monitoring of Aflatoxins in

Broiler, Quail and Ostrich feed samples. Sci. Rep. Life Sci. 4(2).

18. Hussain Z, Khan MZ, Khan A, Javed I, Saleemi MK, Mahmood S, Asi MR (2010). Residues of aflatoxin B1 in broiler meat: Effect of age and dietary aflatoxin B1 levels. Food Chem. Toxicol. 48(12): 3304-3307.
19. Iqbal SZ, Nisar S, Asi MR, Jinap S (2014). Natural incidence of aflatoxins, ochratoxin A and zearalenone in chicken meat and eggs. Food Cont. 43, 98-103.
20. Kehinde MT, Oluwafemi F, Itoandon EE, Orji FA Ajayi OI (2014). Fungal profile and aflatoxin contamination in poultry feeds sold in Abeokuta, Ogun State, Nigeria. Niger. Food J. 32(1): 73-79.
21. Kotinagu K, Mohanamba T, Kumari LR (2015). Assessment of aflatoxin B1 in livestock feed and feed ingredients by high-performance thin layer chromatography. Veter. World. 8(12): 1396.
22. Liu R, Jin Q, Tao G, Shan L, Huang J, Liu Y, Wang S (2010). Photo degradation kinetics and byproducts identification of the Aflatoxin B1 in aqueous medium by ultra-performance liquid chromatography–quadrupletime-of-flight mass spectrometry. J. Mass Spect. 45(5): 553-559.
23. Naveed M, Haleem KS, Ghazanfar S, Tauseef I, Bano N, Adetunji CO, Paray BA (2022). Quantitative estimation of aflatoxin level in poultry feed in selected poultry farms. Bio. Med. Res. Inter. 2022.
24. Ortatatli M, Oguz H, Hatipoglu F, Karaman M (2005). Evaluation of pathological changes in broilers during chronic aflatoxin (50 and 100ppb) and clinoptilolite exposure. Res. Vet. Sci. 78(1): 61-68.
25. Rashid N, Bajwa MA, Rafeeq M, Khan MA, Ahmad Z, Tariq MM, Abbas F (2012). Prevalence of aflatoxin B1 in finished commercial broiler feed from west central Pakistan, pp: 6-10.
26. Richard, J. L. (2007). Some major mycotoxins and their mycotoxicoses - An overview. Inter. J. Food Microbiol. 119(1-2): 3-10.
27. Rossi CN, Takabayashi CR, Ono MA, Saito GH, Itano EN, Kawamura O, Ono, EYS (2012). Immunoassay based on monoclonal antibody for aflatoxin detection in poultry feed. Food Chem. 132(4): 2211-2216.
28. Sineque AR, Macuamule CL, Dos Anjos, FR (2017). Aflatoxin B1 contamination in

chicken livers and gizzards from industrial and small abattoirs, measured by ELISA technique in Maputo, Mozambique. Inter. J. Envir. Res. Publ. Health. 14(9): 951-958.

29. Summia K, Yasmeen R, Nisa A, Djeffal A, Jabeen T (2020). Estimation of Aflatoxins in Cattle Feed Used in and Around Lahore District. Biol. 66(1): 185-191.
30. Turner NW, Subrahmanyam S, Piletsky SA (2009). Analytical methods for determination of mycotoxins: a review. Anal. Chem. Acta, 632(2): 168-180.
31. US, Food and Drug Administration. (2000). Guidance for industry: action levels for poisonous or deleterious substances in human food and animal feed. USFDA, Washington, DC.
32. Wei G (2004). Biomin mycotoxin survey in the Asia-Pacific Region. Biomin Singapore Lab Reports. 35-80.
33. Yunus AW, Razzazi-Fazeli E, Bohm J (2011). Aflatoxin B1 in affecting broiler's performance, immunity, and gastrointestinal tract: A review of history and contemporary issues. Tox. 3(6): 566-590.

LGU Journal of
LIFE SCIENCES

LGU Society of Life Sciences

DOI: https://doi.org/10.54692/lgujls.2024.0803360
Paper Submission: 28th July 2024; Paper Acceptance: 5th Sep 2024; Paper Publication: 10th Sep 2024

Research Article
Vol 8 Issue 3 July- Sep 2024

LGU J. Life. Sci
ISSN 2519-9404
eISSN 2521-0130

Impact of PGPR on Spinach Growth Concerned with Industrial Effluents Contaminated with Chromium

Muhammad Ramzan[1], Sehrish Anwar*[1], Danish Manzoor[2], Asif Ali Kaleri[2], Hafiz Arslan Mustafa[3], Naseeruddin[4], Asadullah Azhar[2], Waqar Ahmed Rajput[2], Irum Sadiq[5], Ameer Hyder Laghari[2], Hameer Kolhi[2]

1. Department of Agronomy, Pir Mehr Ali Shah Arid Agriculture University, Rawalpindi, Pakistan
2. Department of Agronomy, Sindh Agriculture University, Tandojam, Pakistan.
3. Institute of Soil and Environmental Sciences, University of Agriculture, Faisalabad, Pakistan
4. Department of Agronomy Baluchistan Agriculture College Quetta
5. Department of PBG, Sindh Agriculture University, Tandojam, Pakistan

Corresponding Author's Email: sehrishanwar32@gmail.com

ABSTRACT: *Heavy metal pollution in soil poses a significant threat to the environment and human health as it accumulates throughout the food chain. Remediation of soil contamination involves biological, chemical, and physical methods. Plant growth-promoting rhizobacteria inoculation helps some plants stabilize heavy metals in polluted soil by forming chelates with the metals. An experiment was conducted to examine the impact of Plant growth-promoting rhizobacteria on spinach growth and heavy metal stability in polluted soil with industrial effluents. The study found that Plant growth-promoting rhizobacteria (S1 and S2) enhanced growth and yield parameters, with fresh weights reaching 18% and 14%, highest dry weights at 10% and 40%, and longest roots at 11%. The treatment with Plant growth-promoting rhizobacteria S1 recorded the highest SPAD values (27%). Chemical parameters revealed that Cr levels in roots peaked in treatments without PGPR. The results concluded that PGPR can effectively remediate heavy metal-contaminated soils and industrial effluent-irrigated soils used for food crop growth.*

Keywords: Spinach**,** Soil, Heavy metal, PGPR, Plant growth

INTRODUCTION

Spinach (*Spinacia oleracea* L.) is considered an important nutritional vegetable. It is considered a vital component of a diet because it provides many micronutrients such as Mn (manganese), Mg (magnesium), Fe (iron), K (potassium), and folic acid, with small amounts of vitamins A, B2, K, and C (Sarwar et al., 2023). Furthermore, spinach exhibits strong antioxidant activity, primarily because it contains flavonoids, a key component of water-soluble polyphenols. Spinach also has anti-carcinogenic, antioxidant, and antimicrobial activities (Hartmanand and Tringe 2019; Shilev et al., 2020). Moreover, adding spinach to the diet can reduce the post-ischaemic stroke in the brains of rats. Potentially due to its anti-apoptosis and antioxidant effects as well as its anti-inflammatory properties (Zaheer et al., 2020). Research has demonstrated that individuals consuming spinach or carrots more than twice a week have a lower risk of breast cancer recurrence and prostate cancer propagation compared to those who did not (Tirry et al., 2021). Moreover, early research documented that the people who consumed spinach had a lower risk of developing cancer than those who didn't consume any (Shah and Daverey 2020; Ali et al., 2023). Metal pollution in soil has become a significant hazard to agriculture, not only in Pakistan but also globally. It has risen dramatically in recent years, and it is now one of the aspects affecting agricultural production (Alengebawy et al., 2021; Jalal et al., 2023). Furthermore, high levels of heavy metal pollution severely damage the ecosystem; the term HMs (heavy metal) refers to a metallic substance that has a greater density than others and is dangerous even in small quantities (Shahid et al., 2020; Karnwal et al., 2023). According to Renu et al. (2021), heavy metal substances are defined as those that have a density greater than 5 g/cm3, a specific gravity greater than four, and an atomic weight ranging from 63.54 to 200.5 g/mol. Both natural and anthropogenic activities can introduce heavy metals into the environment. Human activities that contribute to heavy metal pollution include mining activities, the use of pesticides containing high quantities of metals, the use of heavy metal-contaminated sludge in agro-ecosystems, and metallurgical and electronic processing (Tchounwou et al., 2012; Jamil et al., 2022). The natural sources of heavy metal pollution include the movement of dust from the mainland, the identification of metal-bearing rocks, and volcanic activity (Ahmad et al., 2021). The addition of microbes to the soil can aid in HM remediation by reducing their availability. Plant growth-promoting rhizobacteria can significantly decrease HM stress in plants by producing siderophores,

indole-3-acetic acid (IAA), organic acids, 1-aminocyclopropane-1-carboxylate (ACC) deaminase, and phytohormones (De Andrade et al., 2023). Other mechanisms may involve complexation, chelation, immobilization, and enzymatic transformation of HMs. Thus, plant growth-promoting rhizobacteria is the best alternative to chemical fertilizers and can contribute to sustainable agricultural production (Jamil et al., 2024). Various chemical and physiological methods, such as the reverse process of osmosis, reduction process, and ion-exchange process, are available to mitigate the harmful impact of heavy metals (HMs) (Batool et al., 2015). However, these remedial methods are costly and decrease the fertility of soil. Plant growth-promoting rhizobacteria is another method to reduce heavy metal pollution. The bacteria in the rhizosphere can enhance the developmental process of plants in various ways, including by fixing nitrogen, producing siderophores, solubilizing phosphorous, and enhancing the symbiotic process of plants. This plant growth-promoting rhizobium can perform three different roles, like production of specific substances, plant protection from diseases, and improved nutrient absorption (Sami et al., 2023).

MATERIALS AND METHODS

The Institute of Soil and Environmental Sciences, University of Agriculture Faisalabad, set up a pot experiment in the wire house to study the effect of industrial effluent and PGPR on spinach growth, using a completely randomized design (CRD). Six different treatments were used, including industrial effluent and PGPR, along with a control, and three replications were done. All pots were irrigated with water as and when needed. Every week, weeds were removed to promote better germination and growth. The recommended doses of nitrogen (N), potassium (K), and phosphorus (P) were provided by using urea, DAP, and sulphate of potash (SOP). All the recommended agronomic practices were carried out till crop maturity.

NPK Recommended for Spanish

A fertilizer with a 20-10-10 ratio may be more appropriate for Spanish, as they require a higher nitrogen concentration for lush development.

Making Samples

A dose of samples for the experiment were prepared by growing Cr-tolerant strains in LB broth media. To achieve this, we autoclaved the LB broth medium at 121 °C and 15 psi pressure for 20 minutes, followed by the inoculation of the plant growth-promoting rhizobacteria (U17) strain. Before being used for seed inoculation, it was shifted in a shaking incubator at 28 ˚C for 2 to 3 days.

T1 represents the control group (no industrial effluent and no PGPR), T2 represents the industrial effluent (50 mL/pot), T3 represents S1 (PGPR alone), T4 represents S2 (PGPR combined with industrial effluent), T5 represents S1 + industrial effluent, and T6 represents S2 + industrial effluent. The spinach crop was used as a test crop.

STATISTICAL ANALYSIS

The collected data had been submitted to an ANOVA (analysis of variance) using the computer program Statistix-8.1 (Statistics, 2006). LSD was employed to examine treatment variations at ($P<0.05$).

RESULTS

Shoot fresh weight

The plant's fresh weight revealed that the application of industrial effluent resulted in a minimum value of 40.33 g (Fig. 1). Compared to the control, applying industrial effluent suppressed spinach growth by 8%. The application of metal-resistive strains was observed better under normal and contaminated conditions.

However, under contaminated conditions with industrial effluents, the applications of strains S1 and S2 promoted plant growth" to improve the structure and reduce redundancy. While the application of plant growth-promoting rhizobacteria (S1) was observed to be more effective under contamination conditions, strain (S1) increased the shoot fresh weight of spinach by 23% under contaminated conditions with industrial effluents, while the strain (S2) increased the shoot fresh weight of spinach by 25% compared to the respective control. Overall, the findings revealed that plant growth-promoting rhizobacteria strains were improving crop growth in contaminated soil with industrial effluents.

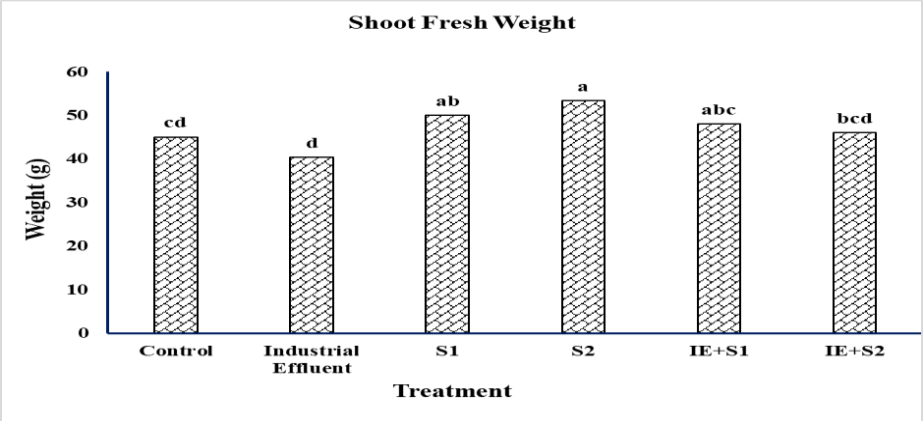

Fig. 1. Effect of industrial effluents and Plant growth-promoting rhizobacteria on shoot fresh weight

Shoot dry weight

According to the shoot dry weight industrial effluent application had a minimum value of 7 g (Fig. 2). The application of industrial effluent reduced spinach growth by 14% compared to the control. However, under contaminated conditions with industrial effluents, the applications of strains S1 and S2 promoted plant growth" to improve the structure and reduce redundancy. Under contamination conditions, the application of S1 yielded superior results, enhancing the shoot dry weight of spinach by 83% when combined with industrial effluents. Strain S2 significantly enhanced the dry weight of spinach by 50% compared to its reference control. The overall findings showed that plant growth-promoting rhizobacteria strains were effective in improving the growth of spinach under contaminated soil.

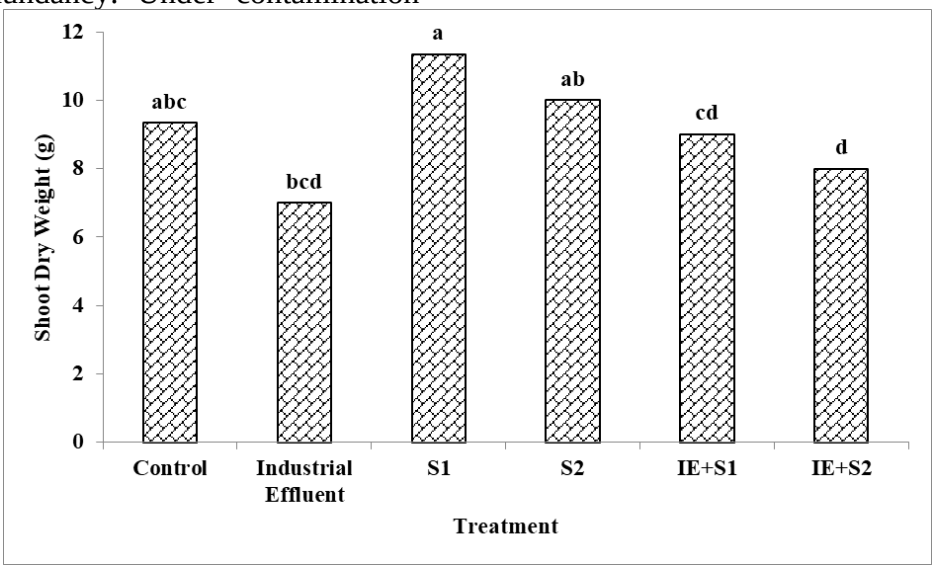

Fig. 2. Effect of industrial effluents and plant growth-promoting rhizobacteria on shoot dry weight

Root Fresh Weight (g)

When applying industrial effluent without the use of plant growth-promoting Rhizobacteria strains or other industrial effluents, we measured a minimum mean value of 9.66 g based on the root fresh weight data in Figure 3. Applying industrial effluent results in 21% slower spinach growth compared to the control group. However, under contaminated conditions with industrial effluents, the applications of strains S1 and S2 promoted plant growth" to improve the structure and reduce redundancy. Conversely, the control group did not use any plant growth-promoting rhizobacteria strain. However, the application of plant growth-promoting rhizobacteria strains (S1 and S2)

increased plant growth by 17% and 20%, respectively, under polluted conditions containing industrial effluents. Thus, we deduced that rhizobacteria strains that promote plant growth improved crop growth in polluted soil.

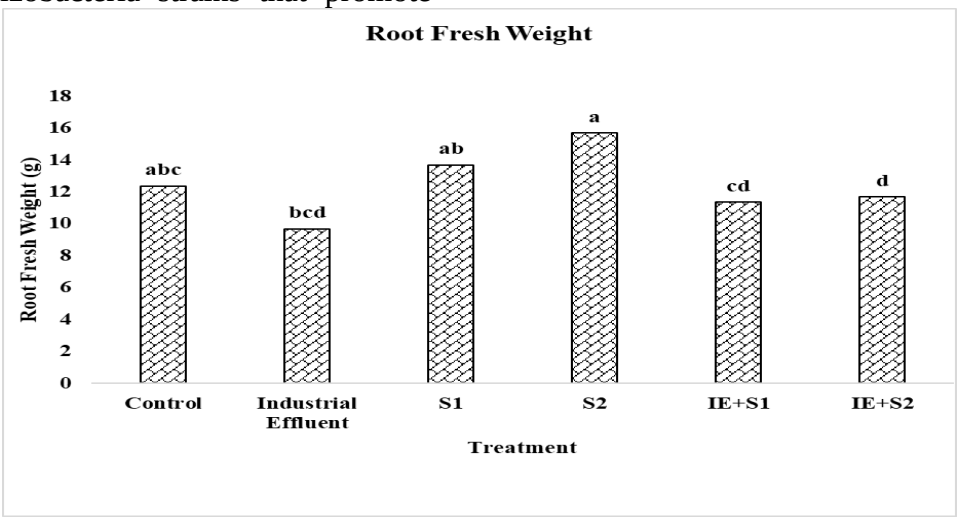

Fig. 3. Effect of industrial effluents and plant growth-promoting rhizobacteria on Root Fresh Weight

Root Dry weight (g)

The data on plant root dry weight indicated that the application of industrial effluent yielded a minimum value of 1 g (Fig. 4). Compared to the control, applying industrial effluent suppressed spinach growth by 39%. We observed better results with the application of metal-resistive strains under both normal and contaminated conditions. However, under contaminated conditions with industrial effluents, the applications of strains S1 and S2 promoted plant growth" to improve the structure and reduce redundancy. While the application of plant growth-promoting rhizobacteria (S1) was observed to be better under contamination conditions, S1 increased the root dry weight of spinach by 33% under contaminated conditions with industrial effluents, and strain (S2) increased the dry weight of spinach by 40% as compared to its respective control. Overall, the findings revealed that plant growth-promoting rhizobacteria strains were improving crop growth in contaminated soil with industrial effluents.

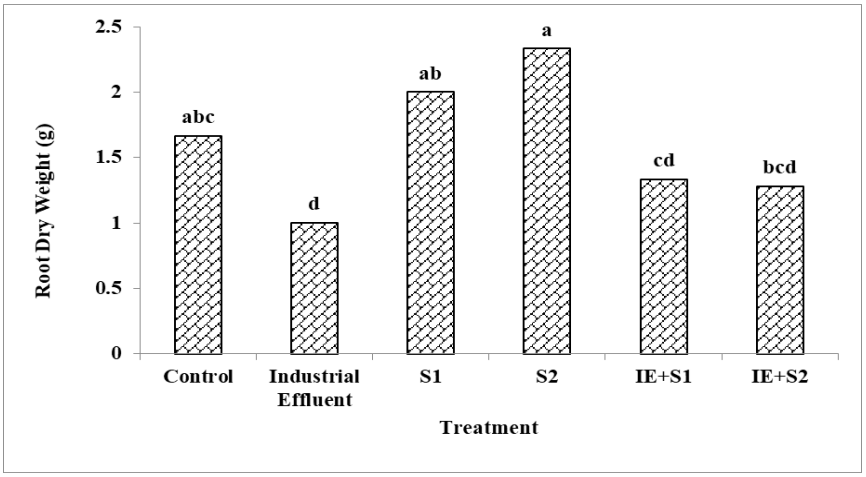

Fig. 4. Effect of industrial effluents and plant growth-promoting rhizobacteria on root dry weight

Shoot Length (cm)

The data presented in Fig. 5 regarding shoot length cm indicated a minimum value of 5.4 cm for the application of industrial effluents. The application of industrial effluent reduced spinach growth by 22% compared to the control. However, the application of S1 resulted in a 50% increase in the plant's growth compared to the control. However, under contaminated conditions with industrial effluents, the applications of strains S1 and S2 promoted plant growth" to improve the structure and reduce redundancy. Under contamination conditions, the application of S1 showed superior results, enhancing spinach shoot length by 48% when combined with industrial effluents. In contrast to its perspective control, strain S2 enhanced the shoot length cm of spinach by 60%. Overall, the findings showed that plant growth-promoting rhizobacteria strains were effective in improving spinach growth in contaminated soil.

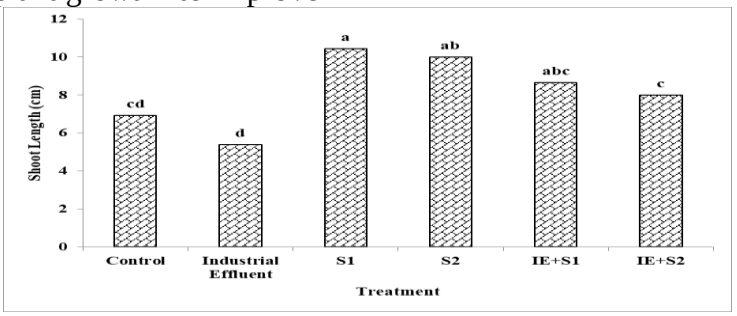

Fig. 5. Effect of industrial effluents and plant growth-promoting rhizobacteria on shoot length

Root length (cm)

The data on root length cm in Figure (6) revealed that the application of industrial effluent, without the use of plant growth-promoting rhizobacteria strains or

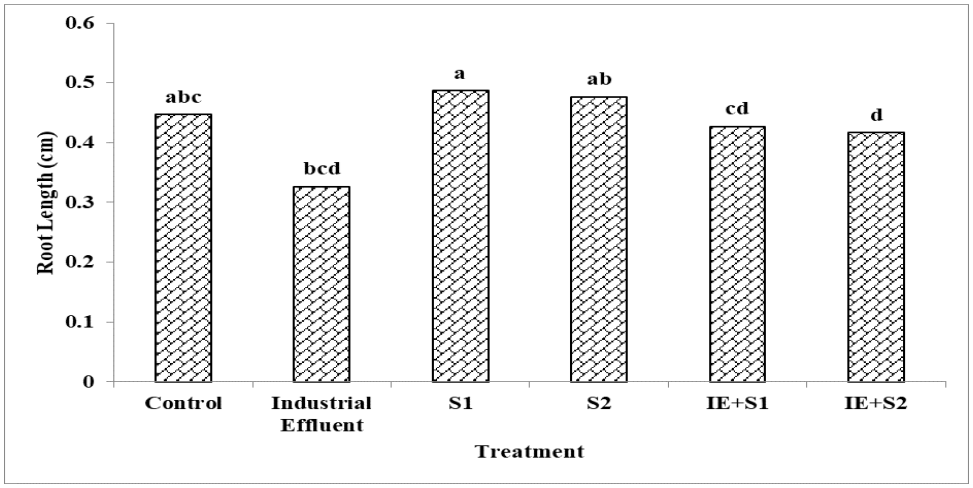

Fig. 6. Effect of industrial effluents and plant growth-promoting rhizobacteria on root length

industrial effluents, resulted in a minimum mean value of 0.32 cm. The application of industrial effluent retards the growth of spinach by 14% as compared to control. However, under contaminated conditions with industrial effluents, the applications of strains S1 and S2 promoted plant growth" to improve the structure and reduce redundancy. The use of plant growth-promoting rhizobacteria strains S1 and S2, on the other hand, increased plant growth by 14% and 8%, respectively, when industrial wastewater was present. Therefore, we concluded that the application of plant growth-promoting rhizobacteria strains enhanced crop growth in contaminated soil.

Total Nitrogen in Shoot

The plant's fresh weight indicated that an application of industrial effluent resulted in a minimum value of 0.32% (Fig. 7). Compared to the control, the application of industrial effluent suppressed spinach growth by 26%. The application of metal-resistive strains was observed better under normal and contaminated conditions. However, under contaminated conditions with industrial effluents, the applications of strains S1 and S2 promoted plant growth" to improve

the structure and reduce redundancy. Under contaminated conditions with industrial effluents, the application of S1 performed better, increasing the total nitrogen in shoot of spinach by 31%, while strain S2 increased the total nitrogen in shoot in the spinach by 25% compared to its respective control. The overall findings revealed that plant growth-promoting rhizobacteria strains were improving crop growth in contaminated soil with industrial effluents.

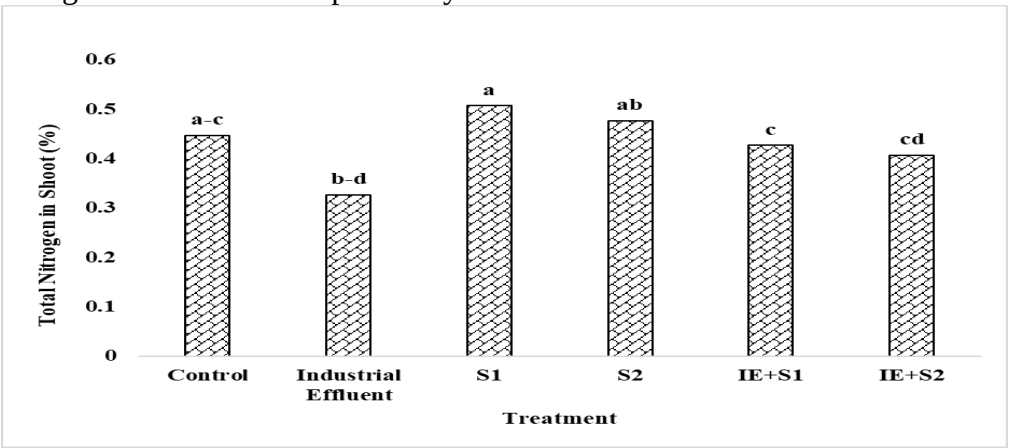

Fig. 7. Effect of industrial effluents and plant growth-promoting rhizobacteria on total Nitrogen in Shoot

Total Nitrogen in Root

The total nitrogen in root data revealed that industrial effluent application had a minimum value (0.32%) (Fig. 8). The application of industrial effluent reduced spinach growth by 11% compared to the control. However, under contaminated conditions with industrial effluents, the applications of strains S1 and S2 promoted plant growth" to improve the structure and reduce redundancy. Application of S1 was observed better when used in contaminated conditions, strain S1 gave better results, increasing the total nitrogen in root and the spinach root take up to 15%. On the other hand, strain S2 made the spinach 19% heavier than the control group. Findings showed that plant growth-promoting rhizobacteria strains were effective at improving spinach growth in contaminated soil.

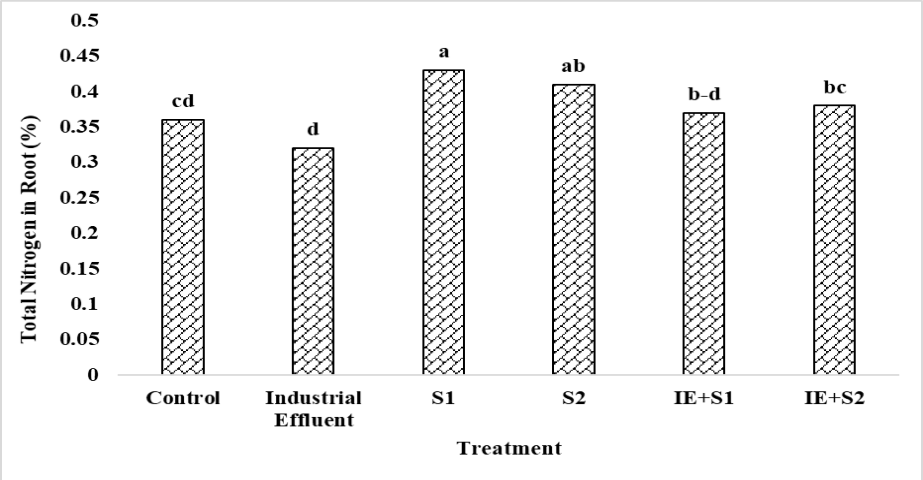

Fig. 8. Effect of industrial effluents and plant growth-promoting rhizobacteria on total Nitrogen in root

Phosphorus in Shoot

The data on phosphorus in shoot as presented in Fig. 9, revealed that the application of industrial effluent, without the use of plant growth-promoting Rhizobacteria strains and industrial effluents, yielded a minimum mean value of 0.11%. Compared to the control, applying industrial effluent retards spinach growth by 31%. However, under contaminated conditions with industrial effluents, the applications of strains S1 and S2 promoted plant growth" to improve the structure and reduce redundancy. This was different from the control, which did not use the plant growth-promoting rhizobacteria strain. However, under contaminated conditions with industrial effluents, the applications of strains S1 and S2 promoted plant growth by 27% and 45%, respectively. Therefore, we concluded that plant growth-promoting rhizobacteria strains enhanced crop growth in contaminated soil.

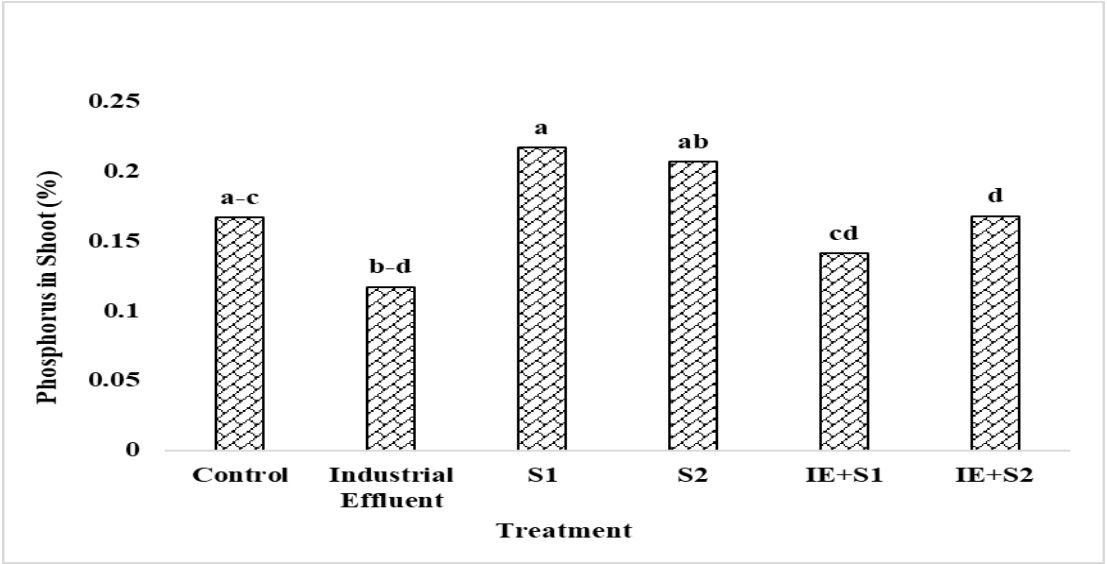

Fig. 9: Effect of industrial effluents and plant growth-promoting rhizobacteria on Phosphorus content in Shoot

Phosphorus in Root

A Fig. 10 data on phosphorus in root revealed that the application of industrial effluent resulted in a minimum value (0.1166%). Compared to the control, applying industrial effluent suppressed spinach growth by 35%. The application of metal-resistive strains was observed better under normal and contaminated conditions. However, under contaminated conditions with industrial effluents, the applications of strains S1 and S2 promoted plant growth" to improve the structure and reduce redundancy. In an experiment where industrial wastewater was present, strain S1 did better, increasing the phosphorus in root of spinach by 45%. On the other hand, strain S2 increased the amount of phosphorus in the spinach root by 63% compared to the control. It was revealed that strains of plant growth-promoting rhizobacteria were improving crop growth in contaminated soil with industrial effluents.

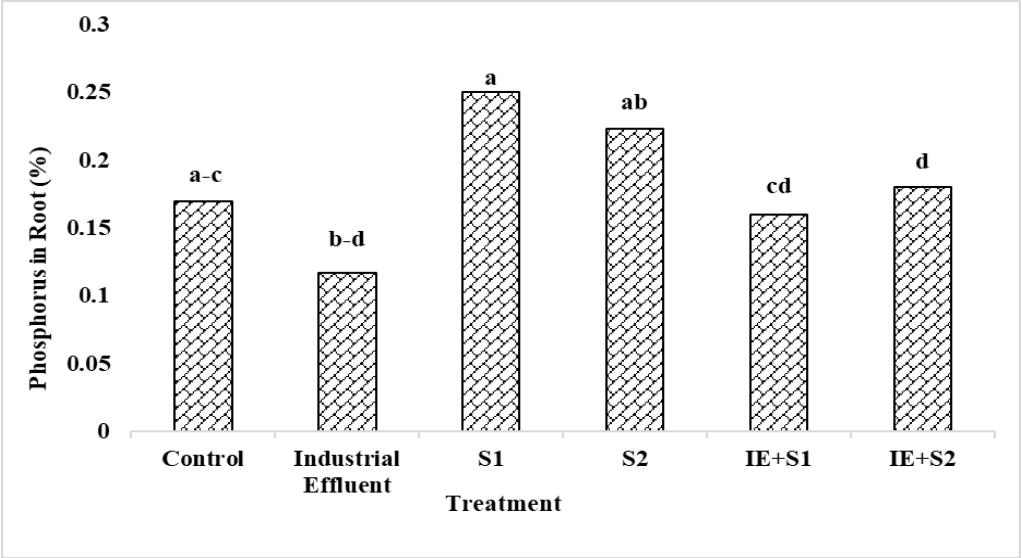

Fig. 10. Effect of industrial effluents and plant growth-promoting rhizobacteria on Phosphorus content in Root

Potassium in Shoot

The Potassium in shoot data shown in Figure (11) revealed that the application of industrial effluents had a minimum value (0.4%). The application of industrial effluent reduced spinach growth by 24% compared to control. However, under contaminated conditions with industrial effluents, the applications of strains S1 and S2 promoted plant growth" to improve the structure and reduce redundancy. Under contamination conditions, the application of S1 yielded better results, and when combined with industrial effluents, S1 enhanced the Potassium in shoot of spinach by up to 21%. Strain S2 boosted potassium levels in the spinach shoot by 17% in comparison to the control. Overall, the findings showed that plant growth-promoting rhizobacteria strains were effective in improving spinach growth in contaminated soil.

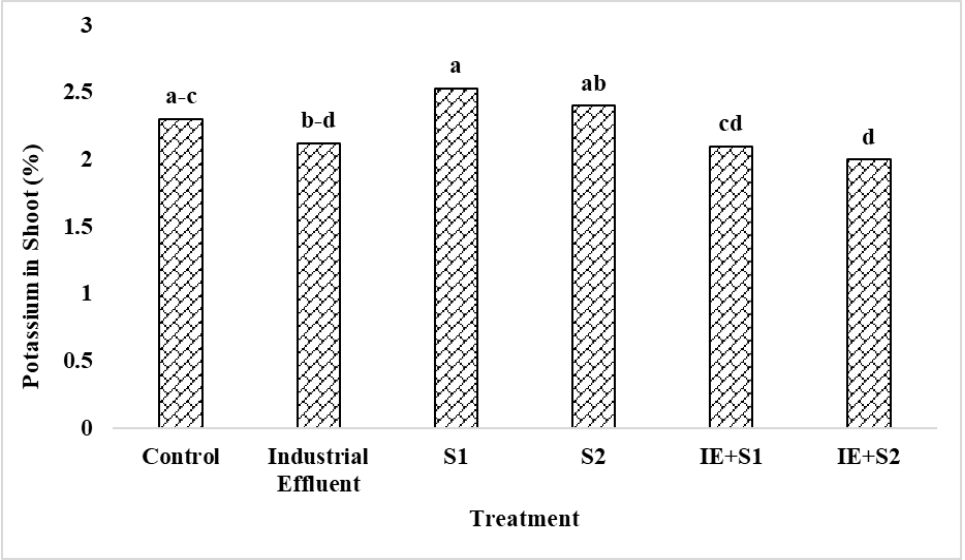

Fig. 11. Effect of industrial effluents and plant growth-promoting rhizobacteria on Potassium content in Shoot

Potassium in Root

Fig. 12 showed Potassium in root that the application of industrial effluent, without the use of plant growth-promoting rhizobacteria strains and industrial effluents, results in a minimum mean value of potassium in root (0.2%). Compared to the control, applying industrial effluent retards spinach growth by 32%. However, the application of S1 boosted plant growth by 65% and S2 enhanced plant yield by 47%, respectively, compared to the control, which did not use any plant growth-promoting rhizobacteria strain. However, under contaminated conditions with industrial effluents, the applications of strains S1 and S2 promoted plant growth by 36% and 28%, respectively. Therefore, we concluded that rhizobacteria strains that promote plant growth enhanced crop growth in contaminated soil.

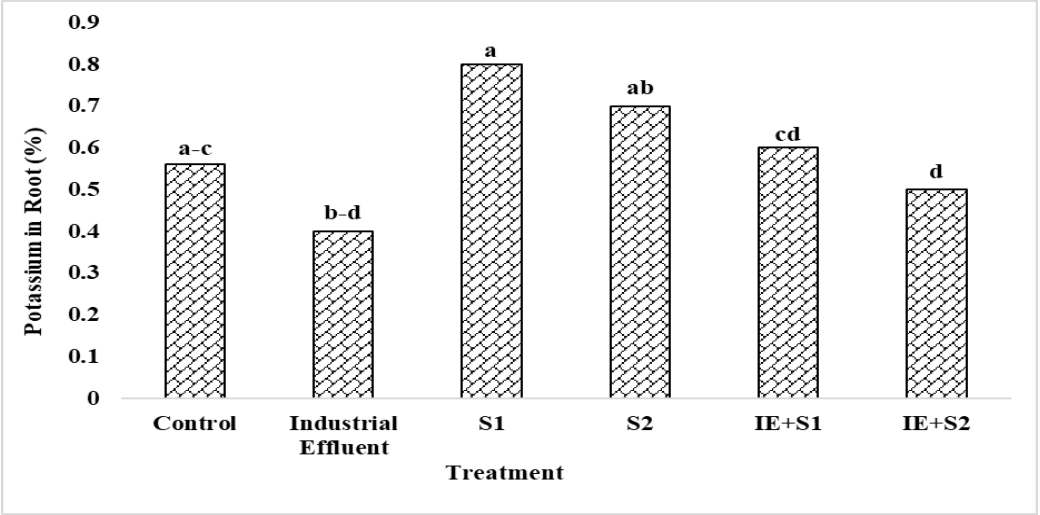

Fig. 12. Effect of industrial effluents and plant growth-promoting rhizobacteria on Potassium content in Root

DISCUSSION

The first sign of heavy metal poisoning is thought to be a reduction in biomass output and plant height (Chen et al., 2019). Heavy metal toxicity may occur at any stage of plant development, including the vegetative and reproductive stages. When the level of heavy metal in the soil rises, it becomes directly accessible to plants (Han et al., 2021; Khaliq et al., 2022; Gupta et al., 2023). Plants absorb metals, which affect plant metabolism and prevent the absorption of other necessary elements. Compared to other methods, using different metal-tolerant plant growth-promoting rhizobacteria strains alone or together successfully makes the plant stronger, less likely to contract diseases, taller, less susceptible to biotic and abiotic stressors, and less likely to absorb and accumulate metals. In this study, applying plant growth-promoting rhizobacteria (Strain 1) without any other external factors resulted in a 50% improvement in plant height. A study by Dubey et al. (2018) validates my findings, demonstrating a 20% rise in plant height compared to soils irrigated with metal-contaminated industrial effluents. Researchers reported the same results: using plant growth-promoting rhizobacteria in spinach crops leads to increased plant

heights. The application of plant growth-promoting rhizobacteria (Strain1 and Strain2) resulted in the highest fresh and dry weights of shoots compared to the normal control. The obtained results aligned with the findings of Cordero et al. (2018), Shameer (2018), and Mala et al. (2020) who also observed an increase in root fresh and dry weight upon the application of plant growth-promoting rhizobacteria strains in industrial effluent soils. The application of industrial effluents blocked important nutrients within the plants, resulting in a decrease in the fresh and dry weight of the shoots. Abiotic stress can alter a plant's defence mechanisms. However, plant growth-promoting rhizobacteria and their combinations increased plant biomass production and enhanced plant defence mechanisms against abiotic stress. They also doubled the fresh and dry weight of shoots by lowering metal uptake and increasing mineral nutrient uptake. The quantity of roots and their penetration into the soil determine plant erection and stability. Roots in regular soil travel a long distance in quest of vital nutrients. The presence of metals in the soil negatively affects the structure of the roots, leading to a restricted root zone. Consequently, the industrial effluent roots exhibited reduced root length, root freshness, and dry weight compared to the control roots, which did not receive plant growth-promoting rhizobacteria or industrial effluent treatment. plant growth-promoting rhizobacteria -1, plant growth-promoting rhizobacteria -2, and their combinations significantly reduced metal absorption in plants. The plant growth-promoting rhizobacteria (Strain 1 and Strain 2) showed the maximum root length and root fresh and dry weights in comparison to all other treatments. This was the same outcome as Paredes et al. (2018), Fu et al. (2020) and Hussain et al. (2021). Where no plant growth-promoting rhizobacteria were used to reduce heavy metal buildup in plants, the concentration of heavy metals in industrial effluents rose in plant control treatment. Zafar-ul-Hye et al. (2018) applied plant growth-promoting rhizobacteria (Strain 1 and Strain 2) to reduce metal accumulation in wheat, confirming my findings that industrial effluents increased plant metal accumulation, but the

application of plant growth-promoting rhizobacteria made plants more resistant to metals and reduced their accumulation. These findings are consistent with those of Gonzalez et al. (2021), who found that plant growth-promoting rhizobacteria may reduce metal toxicity in regions irrigated with industrial effluents.

CONFLICT OF INTEREST

There is no conflict of interest shown by the research manuscript authors.

ACKNOWLEDGEMENT

Authors are highly graceful to their department of affiliations.

CONCLUSION

The study demonstrated that Cr-contaminated industrial effluents negatively affect spinach growth by reducing plant height, shoot, and root fresh weights. However, the application of plant growth-promoting rhizobacteria significantly improved these growth parameters, including nutrient uptake of N, P, and K. Thus, rhizobacteria inoculation effectively mitigates heavy metal toxicity and enhances spinach growth under contaminated soil conditions.

REFERENCES

1. Ahmad M, Ahmad I, Nazli F, Mumtaz MZ, Latif M, Al-Mosallam MS, El-Shafei AA (2021). Lead-tolerant bacillus strains promote growth and antioxidant activities of spinach (Spinacia oleracea) treated with sewage water. Agron. 11(12): 2482.
2. Alengebawy A, Abdelkhalek ST, Qureshi SR, Wang MQ (2021). Heavy metals and pesticides toxicity in agricultural soil and plants: Ecological risks and human health implications. Toxic. 9(3): 42.
3. Ali A, Alghanem SMS, Al-Haithloul HAS, Muzammil S, Adrees M, Irfan E, Abeed AH (2023). Co-application of copper nanoparticles and metal-tolerant Bacillus sp. for improving growth of spinach plants in chromium contaminated soil. Chemo. 345: 140495.
4. Batool R, Yrjala K, Hasnain S (2015). Alleviation of phyto-toxic effects of chromium by inoculation of chromium (VI) reducing Pseudomonas aeruginosa Rb-1 and Ochrobactrum intermedium Rb-2. Int. J. Agric. Biol. 17: 21-30.
5. Chen D, Shao Q, Yin L, Younis A, Zheng B (2019). Polyamine function in plants: metabolism, regulation on development, and

roles in abiotic stress responses. Front. Plant Sci. 9: 1945.

6. Cordero I, Balaguer L, Rincon A, Pueyo JJ (2018). Inoculation of tomato plants with selected PGPR represents a feasible alternative to chemical fertilization under salt stress. J. Plant Nut. Soil Sci. 181(5): 694-703.
7. De Andrade LA, Santos CHB, Frezarin ET, Sales LR, Rigobelo EC (2023). Plant growth-promoting rhizobacteria for sustainable agricultural production. Microorgan. 11(4): 1088.
8. Dubey S, Shri M, Gupta A, Rani V, Chakrabarty D (2018). Toxicity and detoxification of heavy metals during plant growth and metabolism. Environ. Chem. Lett. 16: 1169-1192.
9. Fu SC, Liu JM, Lee KI, Tang FC, Fang KM, Yang CY, Chen YW (2020). Cr (VI) induces ROS-mediated mitochondrial-dependent apoptosis in neuronal cells via the activation of Akt/ERK/AMPK signaling pathway. Toxicol. Vitro. 65: 104795.
10. Gonzalez D, Blanco C, Probanza A, Jimenez PA, Robas M (2021). Evaluation of the PGPR capacity of four bacterial strains and their mixtures, tested on Lupinus albus var. dorado seedlings, for the bioremediation of mercury-polluted soils. Processes. 9(8): 1293.
11. Gupta S, Pandey S (2023). Plant growth-promoting rhizobacteria to mitigate biotic and abiotic stress in plants. Sustain. Agric. Rev. Microbi. Proc. Agric. 60: 47-68.
12. Han L, Zhang H, Xu Y, Li Y, Zhou J (2021). Biological characteristics and salt-tolerant plant growth-promoting effects of an ACC deaminase-producing Burkholderia pyrrocinia strain isolated from the tea rhizosphere. Arch. Microbiol. 203: 2279-2290.
13. Hartman SG, Tringe SG (2019). Interactions between plants and soil shaping the root microbiome under abiotic stress. Biochem. J. 476: 2705-2724.
14. Hussain I, Saleem MH, Mumtaz S, Rasheed R, Ashraf MA, Maqsood F, Rehman M, Yasmin H, Ahmed S, Ishtiaq M, Anwar S, Ali S (2021). Choline chloride mediates chromium tolerance in spinach (*Spinacia oleracea L.*) by restricting its uptake in relation to morpho-physio-biochemical attributes. J. Plant Growth Regul. 1–21.

15. Jalal A, da Silva Oliveira CE, Galindo FS, Rosa PAL, Gato IMB, de Lima BH, Teixeira Filho MCM (2023). Regulatory mechanisms of plant growth-promoting rhizobacteria and plant nutrition against abiotic stresses in Brassicaceae family. Life. 13: 211.
16. Jamil M, Malook I, Rehman SU, Aslam MM, Fayyaz M, Shah G, Abeed AH (2024). Inoculation of heavy metal-resistant bacteria alleviated heavy metal-induced oxidative stress biomarkers in spinach (*Spinacia oleracea L.*). BMC Plant Biol. 24(1): 221.
17. Jamil N, Hyder S, Valipour M, Yasir M, Iqbal R, Roy R, Ahmed A (2022). Evaluation of the bioremediation potential of *Staphylococcus lentus* inoculations of plants as a promising strategy used to attenuate chromium toxicity. Sustain. 14(20): 13056.
18. Karnwal A, Shrivastava S, Al-Tawaha ARMS, Kumar A, Kumar A (2023). PGPR-mediated breakthroughs in plant stress tolerance for sustainable farming. J. Plant Grow. Regul. 1-17.
19. Khaliq MA, Javed MT, Hussain S, Imran M, Mubeen M, Nasim W, Abdo HG (2022). Assessment of heavy metal accumulation and health risks in okra (*Abelmoschus Esculentus L.*) and spinach (*Spinacia Oleracea L.*) fertigated with wastewater. Int. J. Food Contaminat. 9(1): 11.
20. Mala JGSM, Takeuchi S, Sujatha D, Mani U (2020). Microbial chromate reductases: novel and potent mediators in chromium bioremediation - a review. Appl. Microbiol. Theory Technol. 32–44.
21. Naili F, Neifar M, Elhidri D, Cherif H, Bejaoui B, Aroua M, Cherif A (2018). Optimization of the effect of PGPR–based biofertilizer on wheat growth and yield. Biomet. Biostat. Int. J. 79(1): 226-232.
22. Paredes-Paliz K, Rodriguez VR, Duarte B, Caviedes MA, Mateos-Naranjo E, Redondo Gomez S, Pajuelo E (2018). Investigating the mechanisms underlying phytoprotection by plant growth-promoting rhizobacteria in Spartina densiflora under metal stress. Plant Biol. 20(3): 497-506.
23. Renu, Sarim KM, Sahu U, Bhoyar MS, Singh DP, Singh UB, Manna MC (2021). Augmentation of metal-tolerant bacteria elevates growth and reduces metal toxicity in spinach. Bioremed. J. 25(2): 108-127.

24. Sarwar MJ, Shabaan M, Asghar HN, Ayyub M, Ali Q, Zulfiqar U, Elshikh MS (2023). Interaction of chromium (Cr) resistant plant growth promoting rhizobacteria with compost to phytostabilize Cr in spinach rhizosphere. Plant Stress. 10: 100261.
25. Shah V, Daverey A (2020). Phytoremediation: A multidisciplinary approach to clean up heavy metal-contaminated soil. Environ. Technol. Innovat. 18: 100774.
26. Sami H, Ashraf K, Sultan K, Alamri S, Abbas M, Javied S, uz Zaman Q (2023). Remediation potential of biochar and selenium for mitigating chromium-induced stress in spinach to minimize human health risk. S. Afric. J. Bot. 163: 237-249.
27. Shilev S, Babrikova I, Babrikov T (2020). Consortium of plant growth-promoting bacteria improves spinach (*Spinacea oleracea L.*) growth under heavy metal stress conditions. J. Chem. Technol. Biotechnol. 95(4): 932-939.
28. Shahid M, Javed MT, Tanwir K, Akram MS, Tazeen SK, Saleem MH, Chaudhary HJ (2020). Plant growth-promoting Bacillus sp. strain SDA-4 confers Cd tolerance by physio-biochemical improvements, better nutrient acquisition, and diminished Cd uptake in *Spinacia oleracea L.* Physiol. Mol. Biol. Plants. 26: 2417-2433.
29. Shameer S, Prasad TNVKV (2018). Plant growth-promoting rhizobacteria for sustainable agricultural practices with special reference to biotic and abiotic stresses. Plant Growth Reg. 84: 603-615.
30. Tchounwou PB, Yedjou CG, Patlolla AK, Sutton DJ (2012). Heavy metal toxicity and the environment. Mol. Clin. Environ. Toxicol. 3(10): 133-164.
31. Tirry N, Kouchou A, El Omari B, Ferioun M, El Ghachtouli N (2021). Improved chromium tolerance of Medicago sativa by plant growth-promoting rhizobacteria (PGPR). J. Gen. Eng. Biotechnol. 19: 1-14.
32. Yanez-Yazlle MF, Romano-Armada N, Rajal VB, Irazusta VP (2021). Amelioration of saline stress on chia (*Salvia hispanica L.*) seedlings inoculated with halotolerant plant growth-promoting bacteria isolated from hypersaline environments. Front. Agron. 3: 665798.

33. Zaheer IE, Ali S, Saleem MH, Noor I, El-Esawi MA, Hayat K, Wijaya L (2020). Iron–lysine mediated alleviation of chromium toxicity in spinach (*Spinacia oleracea L.*) plants in relation to morpho-physiological traits and iron uptake when irrigated with tannery
wastewater. Sustainab. 12(16): 6690.
34. Zafar-Ul-Hye M, Shahjahan A, Danish S, Abid M, Qayyum MF (2018). Mitigation of cadmium toxicity induced stress in wheat by ACC-deaminase containing PGPR isolated from cadmium polluted wheat rhizosphere. Pak. J. Bot. 50(1): 1727-1734.

LGU Journal of
LIFE SCIENCES

LGU Society of Life Sciences

DOI: https://doi.org/10.54692/lgujls.2024.0803362
Paper Submission: 24th July 2024; Paper Acceptance: 7th Sep 2024; Paper Publication: 10th Sep 2024

Research Article
Vol 8 Issue 3 July- Sep 2024

LGU J. Life. Sci
ISSN 2519-9404
eISSN 2521-0130

Comparison of Mycobacterium tuberculosis Strains with H37Rv Using Whole Genome Sequence Analysis to Identify Virulence Factors and Phylogenetic Relationships

Saba Kabir[1], Muhammad Asif Rasheed[2], Abdul Rehman[3]*

1. Department of Microbiology, Faculty of Science and Technology, University of the Central Punjab, Lahore Pakistan
2. Department of Biosciences, COMSATS University Islamabad, Sahiwal Campus, 57000, Sahiwal, Pakistan
3. Institute of Microbiology and Molecular Genetics, University of the Punjab, Quaid Azam Campus, Lahore Pakistan

Corresponding Author's Email: rehman.mmg@pu.edu.pk

ABSTRACT: *Mycobacterium tuberculosis (Mtb) poses a significant disease burden in developing countries, largely due to the rising issue of drug resistance. In Pakistan, the genetic and molecular characteristics of resistant strains have not been thoroughly analyzed or compared with the reference Mtb strain, H37Rv, to understand the molecular and genetic epidemiology. Mtb employs various strategies to resist anti-tuberculosis drugs, and antimicrobial resistance, including single and multidrug resistance, has increased extensively in developing nations like Pakistan. In this study, the whole genomes of three Mtb strains (335, 335-2, and 311) were uploaded to the Rapid Annotation Subsystems Technology (RAST) server to retrieve coding DNA sequences (CDS). The RAST server identified 4,454, 4,445, and 4,396 CDS for Mtb strains 335, 335-2, and 311, respectively. Mutation analysis was performed using NCBI nucleotide BLAST and CLUSTAL Omega, comparing the sequences with the H37Rv reference strain. The analysis revealed 909, 832, and 1,135 mutations in the 335, 335-2, and 311 strains, respectively. Phylogenetic analysis based on the most virulent protein (EccC3) indicated a close resemblance between all three strains and the H37Rv strain. Furthermore, Mycobacterium canettii (accession number WP_203037448.1) was identified as the closest related bacterium to the studied strains and H37Rv.*

Keywords: Mutations, XDR-TB, Drug-resistant TB, Tuberculosis

INTRODUCTION

There are more than 1.5 million cases of tuberculosis (TB) in Pakistan which is caused by *Mycobacterium tuberculosis* (*Mtb*). The molecular existence of this pathogen has been evidenced back to 17,000 years The prevalence of *Mtb* infections is currently very high in Pakistan which is mainly due to poverty, undiagnosed cases, failure to define the accurate case definitions at the clinics, unawareness, misreporting, and lack of intensive active surveillance (Siddiqui et al., 2019). The developed countries are very successful in controlling these kinds of challenges and efficiently reducing the incidence of *Mtb* (Aftab et al., 2021), but even then, despite newer methods for diagnosis and treatment, TB is still among the top 10 deadly infectious diseases (Sandhu, 2011). This is because *Mtb* uses several strategies to resist the action of anti-TB drugs (Yasmin et al., 2014).

Additionally, antimicrobial resistance prevalence in terms of single and multiple drug resistance has already been extensively increased in developing countries including Pakistan (Gao et al., 2018; Wang et al., 2018; Desai and Joshi 2019; Kabir et al., 2020). Furthermore, these drug-resistant strains also pose higher susceptibility to cause various types of mutations in the *Mtb* strains which is also becoming a serious public health concern for the medical sciences (Yar et al., 2018; Mukati et al., 2019; Sharma et al., 2020). Therefore, it is imperative to explore all the possible resistance strains of *Mtb* so that counteractions at molecular levels can be established to prevent the occurrence of *Mtb* resistance genes (Jabbar et al., 2019; Kabir et al., 2021).

The emergence of drug resistance in tuberculosis is due to the collective contribution of the various mechanisms. Mainly, two factors i.e., internal and external are concerned with enhancing resistance to MTB. The genetic mutation acquisition, presence of drug efflux pumps, modification of drug target enzymes, low drug permeability through cell envelope, drug inactivation, and the fitness cost are the internal factors connected with resistance strategies in bacteria (da Silva et al., 2011; Gygli et al., 2017; Swain et al., 2020; Allue Guardia et al., 2021). On the other hand, factors concerning social determinants in a population of tuberculosis patients are called external factors (Nguyen et al., 2018).

The genetic studies and analysis of molecular patterns of identified strains of *Mtb* are essential to monitor the prevalence of specific strains of *Mtb* in Pakistan (Ali et al., 2011; Jabbar et al., 2019). The extent of genetic variability, mutations, diversity, and measured resistance level can be studied through comparative genomic studies to identify drug-resistant genes in different isolated strains of

Mtb in Pakistan (Jabbar et al., 2019; Kabir et al., 2023). Bioinformatics tools such as rapid annotation subsystems technology (RAST) utilize the genetic sequences to predict genes for elaborative protein sequencing and inform virulence factor databases through genetic comparison with the reference strains of *Mtb* (Ilina et al., 2013; Jia et al., 2017). These and similar other tools also predict the possible reasons behind the genetic mutations and drug resistance in *Mtb* strains (Khan et al., 2019). Given this context, the present study has been designed to compare the whole genome of 3 strains of *Mtb i.e.* 335, 335-2, and 311 with reference strain of *Mtb* H37Rv.

MATERIALS AND METHODS

Uploading of Genome Sequences at RAST

The genomes of the strains i.e. 335, 335-2, and 311 used in the current study were obtained from a recently published work (Kabir et al., 2019). The genomes of studied strains i.e. 335, 335-2, and 311 were uploaded one by one on the Rapid Annotation using Subsystems Technology (RAST) for getting complementary DNA sequences (CDS) of DNA and protein. The RAST server supports the data and procedures established within the SEED framework (http://pubseed.theseed.org/) to provide high-quality functional annotation. The RAST supports both the automated annotation and the analysis of the genome. Annotated genomic information was obtained through the SEED viewer which offers a wide set of information to browse, compare, and download for genome. The result consists of domain, genus, species, strains, genome size, and number of contigs. The procedure of finding gene location and coding regions in the genome was performed by aligning the submitted genomes against the reference genomes. Hence, the filtering and trimming were performed by the server based on reference genomes. After the genome sequence, annotation is necessary to make it useful. The SEED viewer gave genomic information in graphically and tabulated form.

Analysis of Gene Prediction

In computational biology, gene finding refers to the procedure of identifying
the regional genomic DNA that encodes genes. It comprises RNA genes (non-coding), protein-coding genes, and other functional elements (regulatory regions). Gene prediction of *Mtb* was done through the RAST server in the presence of reference genome H37Rv.

DNA Sequence Alignment analysis

Sequence alignment is a process of arranging the sequence of DNA, RNA, or protein to know similar regions having functional, structural, or evolutionary relationships. CLUSTAL Omega

was used for multiple sequence alignment among 3 *Mtb* strains and the reference strain H37Rv.

Analysis through Virulent Factor Database

The mutated sequences were obtained from CLUSTAL Omega and BLAST alignment and uploaded on the virulence factor database (http://www.mgc.ac.cn/VFs/) through which we get the bit score and E values of the most virulent genes. The list of all virulent genes was arranged in descending order to get the highest bit scored gene at the top. Finally, the most virulent gene was BLAST against other organisms excluding *Mtb* to check its evolutionary relationship.

Construction of phylogenetic tree

The phylogenetic tree provides an evolutionary relationship of the specific gene of one organism to the other organisms. For this purpose, molecule evolutionary genomic analysis (MEGA X**)** software was employed. FASTA files of drug resistance genes in 3 *Mtb* strains and reference genome (H37Rv) were aligned and converted to a mega format to build the tree. The files were opened in Mega X one by one and then alignment was made by a CLUSTAL Omega with falling parameter gap penalty 10, gap extension penalty 0.1, multiple alignments having gap opening penalty 1.0, and gap extension penalty. 0.2, protein weight matrix Gonnet, Residue specific penalties on, hydrophilic penalties on, gap separation distance 4, end gap separation off, use negative metrics of and delay divergence. Cut off 30% and the gaps contacts were removed for the aligned sequences and then the data were exported to mega format. The mega format file was opened, and phylogenetic trees were constructed by having an analysis of phylogenetic reconstruction, and maximum likelihood.

RESULTS

Genome annotation and features

High-quality functional annotation of *Mtb* was obtained from the RAST server. Results showed information about sequence size, shortest contig size, number of contigs, % GC content, longest contig size, median sequence size, mean sequence size, L50 value, and N50 value. This information is illustrated in Table 1.

Table 1: Genome annotation and analysis in 3 different Mtb strains

Statistic	As uploaded			As splitting into scaffolds		
	***Mtb* 335**	***Mtb* 335-2**	***Mtb* 311**	***Mtb* 335**	***Mtb* 335-2**	***Mtb* 311**
Sequence size	4406929	4392079	4399363	4406929.	4392079	4399363
Number of contigs	237	224	194	237	224	194
GC content (%)	65.7	65.7	65.7	65.7	65.7	65.7
Shortest contig size	92	92	104	92	92	104
Median sequence size	2245	6594	6594	2245	6594	6594
Mean sequence size.	18594.6	19607.5	22677.1	18594.6	19607.5	22677.1
Longest contigs size	199215	174386	178690	199215	174386	178690
N50 value	62939	61172	64257	62939	61172	64257
L50 value	-	26	24	-	26	24

RAST server provided 4454, 4445, and 4396 CDS of DNA/protein for *Mtb* 335, 335-2, and 311 strains, respectively. DNA sequences were then compared for mutation analysis using NCBI nucleotide BLAST and CLUSTAL omega against H37Rv reference strain and obtained 909, 832, and 1135 mutated regions in *Mtb* 335, 335-2, and 311 strains, respectively. Most of the mutations were due to single nucleotide polymorphism (SNPs). Moreover, some mutations were related to the resistance genes of the bacteria including mutations in gyrA and EthA in *Mtb* 335 strain, mutations in katG, gyrA, embB, embC, and EthA in *Mtb* 335-2 strain, and mutations in katG, embA, embB, embC and EthA in *Mtb* 311 strain.

Predicted virulence factors in *Mtb* 335 strain

When the DNA sequences of *Mtb* were compared with reference genome H37Rv we get the most mutated sequences. After getting the mutated sequences, we checked out the most virulent sequences in those mutated sequences through the virulence factor database (VFDB) which shows the bit score and e-values of sequences. The bit score and e-values define how much the sequence is virulent. Based on bit score and e-values 20, 19, and 20 virulence-related factors for *Mtb* 335, 335-2, and 311 strains, respectively. The VFDB analysis showed that the most virulent protein was EccC3 which is a component of the Type VII secretion system as mentioned in Table 2.

Table 2: Results of virulence factor database in *Mtb* strain. The most virulent protein found was FtsK/SpoIIIE family protein EccC3, the component of the Type VII secretion system ESX-3

Strain	Sequence no.	length	bit score
335	fig|6666666.737179.peg.1587	3993	7908
335-2	fig|6666666.737181.peg.2161	3993	7908
311	fig|6666666.736742.peg.2371	3993	7908

Phylogenetics analysis

The construction of a phylogenetic tree takes place to check the evolutionary relationship of *Mtb* 335, *Mtb* 335-2, and *Mtb* 311 strains with other species based on the most virulent protein i.e. EccC3 which is a component of the Type VII secretion pathway. This has provided us the opportunity to observe which proteins have the same mutated protein sequence, are interlinked to each other, and belong to the same family. Phylogenetics analysis of Mtb strains and the reference strain H37rV was performed using a maximum likelihood algorithm. Furthermore, the closest related bacteria with studied strains and H37Rv found was *Mycobacterium canettii* with accession number WP_203037448.1. From a phylogenetic point of view, strains that are closely related to each other have more similarities. The results of the phylogenetic analyses are shown in Fig. 1.

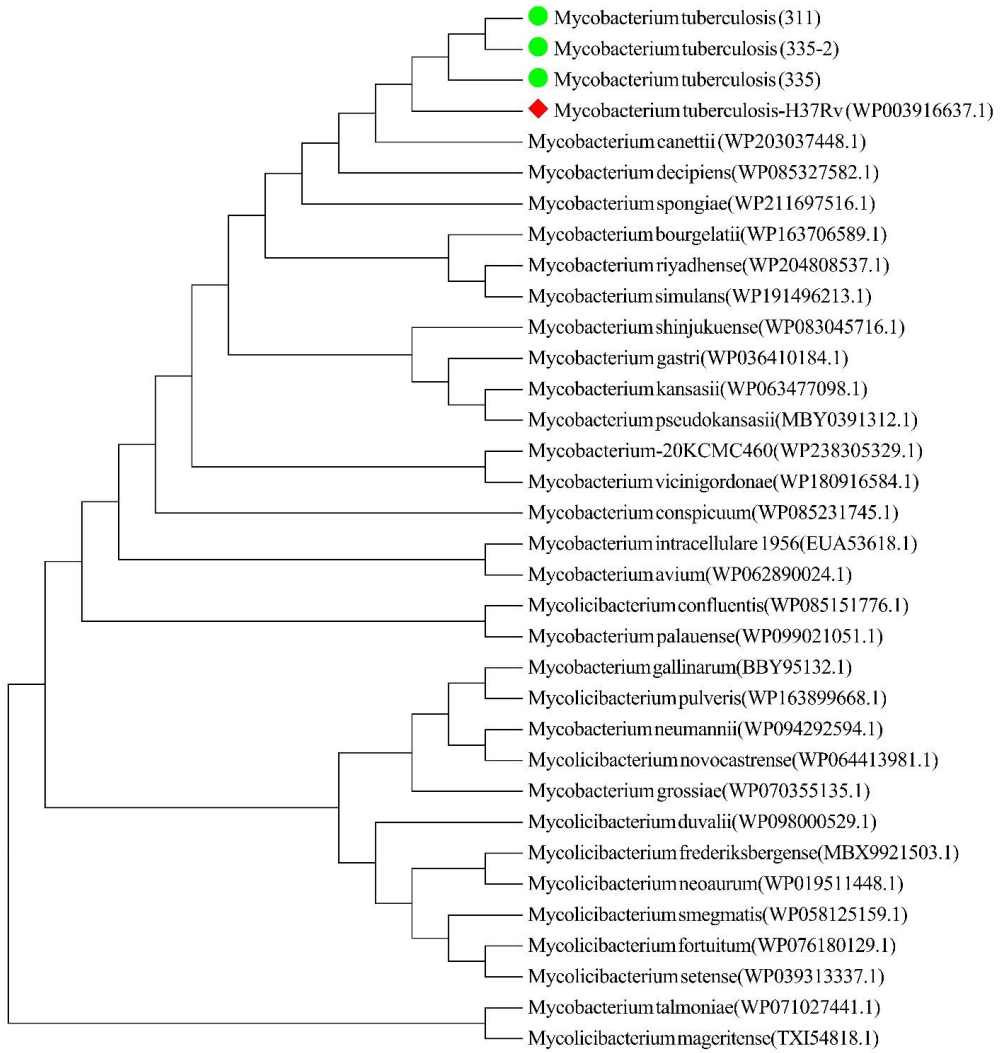

Fig. 1: Phylogenetics analysis of Mtb strains and the reference strain H37rV. The analysis is based on the most virulent protein i.e. EccC3 which is a component of Type VII secretion system. The analysis was performed using maximum likelihood algorithm. The closely related bacteria found was *Mycobacterium canettii* with accession number WP_203037448.1

DISCUSSION

In the current investigation, genomes of 3 *Mtb* strains (335, 335-2, and 311) were individually compared with the reference genome H37Rv of *Mtb*. All strains not only showed similarity to the reference genome but also shared several characteristics with the pathogenic reference genome. The CLUSTAL Omega tool generated multiple sequence alignments among 3 or more sequences. The alignment was carried out in genes that had 99% identity to the reference strain of *Mtb*. Mutation

analysis by CLUSTAL Omega provided 909, 832, and 1135 mutated regions in *Mtb* 335, 335-2, and 311 strains, respectively. Comparison of virulence factors encoded in *Mtb* 335, 335-2, and 311 strains reported multiple clades which showed phylogenetic lineage between these species' clades. These clades were based on structural or functional similarity. The prime objectives of the study were to identify the mutation and compare it with the reference genome, phylogenetic analysis, evolutionary relationships among *Mtb* strains, and evolutionary comparison among other bacteria and *Mtb* 335-2 strain.

Bloom and Cadarette (2019) described that bacterial pathogens pose major threats to public health worldwide in the 21st century. Current work on bacterial pathogenesis has increased considerably our information about the pathways of the disease occurrence at the molecular level over (Chen et al., 2005). To enhance future work, it is essential to create a database collectively providing the virulence factors (VFs) of different medically important bacterial pathogens (Chen et al., 2005). The virulence factor database (VFDB) provides current information on virulence factors from different pathogenic bacterial species. VFDB can be used by browsing each genus or by using keywords. VFDB gives a unified gateway for VFs from various bacterial pathogens (Chen et al., 2005). Forrellad et al. (2013) reported that a variety of virulence factors have been produced in MTBC members in response to the host's immune reaction

Pule et al. (2016) reported that bacterial EPs are responsible for providing resistance against various anti-TB drugs by pressing out the drug molecules that enter the cell. Isoniazid, the most potent first-line anti-TB drug, is resisted due to overexpression of the MmpL7 protein (Pasca et al., 2005). The efflux-mediated resistance can be decreased using efflux inhibitors. Drug efflux pumps i.e., reserpine (Shaheen et al., 2019), verapamil (de Souza et al., 2020), chlorpromazine, and thioridazine (Rodrigues et al., 2012) show reduced activity against various inhibitors.

As mentioned in Table 2, the most virulent protein found in the bacteria was EccC3 (a component of the Type VII secretion system ESX-3) based on the highest bit score in VFDB. The 4 ESX conserved protein constituents (EccB3, EccC3, EccD3, and EccE3) are involved in making secretion machinery of the ESX-3 system of *Mycobacterium tuberculosis* (Famelis et al., 2019). Out of these 4 constituents, EccC3 (Uniprot ID: P9WNA9) is a malleable arrangement of 4 ATPase domains and has been crosslinked with its neighbouring (EccD3) protein's small hydrophilic domain. Its 4 ATPase domains are connected to the

bacterial cell membrane via a stem domain. Next to the stem domain another unknown function domain (DUF) is considered an ATPase domain that is necessary for ESX-3 secretory pair release (Famelis et al., 2019). The conformational alterations in the stem domain which is stimulated by the binding of substrate/stimulant at the posterior end of EccC3 lead to hydrolysis of ATP in the DUF and hence, secretory pair discharge through the periplasm (Famelis et al., 2019). Moreover, Costa et al., declared that the structural design of type VII secretion pathways (T7SS) varies significantly from the other known secretory apparatuses (Costa et al., 2015). This study furnishes the comprehension of secretory pathways conformation that will be expedient for the novel antimicrobial tactics designed to hit bacterial virulence (Famelis et al., 2019).

CONCLUSION

This investigation reveals that the genomes of three Mtb strains (335, 335-2, and 311) were uploaded to the RAST server, which identified 4,454, 4,445, and 4,396 coding DNA sequences (CDS) for each strain, respectively. Phylogenetic analysis based on the most virulent protein (EccC3) showed a close relationship between all three strains and the H37Rv reference strain. Additionally, *Mycobacterium canettii* (accession number WP_203037448.1) was identified as the closest related bacterium to the studied strains and H37Rv. These findings can support researchers in utilizing the identified virulent genes for developing vaccines and new treatment strategies against these resistant Mtb strains.

CONFLICT OF INTEREST

The authors have no competing interests.

FUNDING SOURCE

No funding was received for this project.

ETHICAL APPROVAL STATEMENT

Not applicable

REFERENCES

1. Aftab A, Afzal S, Qamar Z, Idrees M (2021). Early detection of MDR *Mycobacterium tuberculosis* mutations in Pakistan. Sci. Rep. 11(1): 16736.
2. Ali A, Hasan R, Jabeen K, Jabeen N, Qadeer E, Hasan Z (2011). Characterization of mutations conferring extensive drug resistance to *Mycobacterium tuberculosis* isolates in Pakistan. Antimicrob. Agents Chemother. 55(12): 5654-5659.
3. Allue Guardia A, Garcia JI, Torrelles JB (2021). Evolution of drug-resistant Mycobacterium tuberculosis strains and their adaptation to the human lung environment. Front. Microbiol. 12: 137.
4. Bloom DE, Cadarette D (2019). Infectious Disease Threats in the Twenty-First Century: Strengthening the Global

Response. Front. Immunol. 10: 549.
5. Chen L, Yang J, Yu J, Yao Z, Sun L, Shen Y, Jin Q (2005). VFDB: a reference database for bacterial virulence factors. Nucl. Acids Res. 33(Database issue): D325-8.
6. Costa TR, Felisberto-Rodrigues C, Meir A, Prevost MS, Redzej A, Trokter M, Waksman G (2015). Secretion systems in Gram-negative bacteria: structural and mechanistic insights. Nat. Rev. Microbiol. 13(6): 343-359.
7. da Silva PEA, Von Groll A, Martin A, Palomino JC (2011). Efflux as a mechanism for drug resistance in *Mycobacterium tuberculosis*. FEMS Immunol. Med. Microbiol. 63(1): 1-9.
8. de Souza JVP, Murase LS, Caleffi-Ferracioli KR, Palomo CT, de Lima Scodro RB, Siqueira VLD, Cardoso RF (2020). Isoniazid and verapamil modulatory activity and efflux pump gene expression in *Mycobacterium tuberculosis*. Int. J. Tuberc. Lung Dis. 24(6): 591-596.
9. Desai U, Joshi JM (2019). Extrapulmonary drug-resistant tuberculosis at a drug-resistant tuberculosis center, Mumbai: Our experience–Hope in the midst of despair. Lung India: Official Organ of Indian Chest Society 36(1): 3.
10. Famelis N, Rivera-Calzada A, Degliesposti G, Wingender M, Mietrach N, Skehel JM, Fernandez-Leiro R, Böttcher B, Schlosser A, Llorca O, Geibel S (2019). Architecture of the mycobacterial type VII secretion system. Nat. 576(7786): 321-325.
11. Forrellad MA, Klepp LI, Gioffré A, Sabio y García J, Morbidoni HR, de la Paz Santangelo M, Cataldi AA, Bigi F (2013). Virulence factors of the *Mycobacterium tuberculosis* complex. Virul. 4(1): 3-66.
12. Gao Y, Zhang Z, Deng J, Mansjö M, Ning Z, Li Y, Li X, Hu Y, Hoffner S, Xu B (2018). Multi-center evaluation of GenoType MTBDR*sl* line probe assay for rapid detection of pre-XDR and XDR Mycobacterium tuberculosis in China. J. Infect. 77(4): 328-334.
13. Gygli SM, Borrell S, Trauner A, Gagneux S (2017). Antimicrobial resistance in *Mycobacterium tuberculosis*: mechanistic and evolutionary perspectives. FEMS Microbiol. Rev. 41(3): 354-373.
14. Ilina EN, Shitikov EA, Ikryannikova LN, Alekseev DG, Kamashev DE, Malakhova MV, Parfenova TV, Afanas'ev MV, Ischenko DS, Bazaleev NA, Smirnova TG, Larionova EE, Chernousova LN, Beletsky AV, Mardanov AV, Ravin NV, Skryabin KG, Govorun VM (2013). Comparative genomic analysis of *Mycobacterium tuberculosis* drug-resistant

strains from Russia. PLoS One. 8(2): p. e56577.

15. Jabbar A, Phelan JE, de Sessions PF, Khan TA, Rahman H, Khan SN, Cantillon DM, Wildner LM, Ali S, Campino S, Waddell SJ, Clark TG (2019). Whole genome sequencing of drug resistant *Mycobacterium tuberculosis* isolates from a high burden tuberculosis region of North West Pakistan. Sci. Rep. 9(1): 14996.
16. Jia X, Yang L, Dong M, Chen S, Lv L, Cao D, Fu J, Yang T, Zhang J, Zhang X, Shang Y, Wang G, Sheng Y, Huang H, Chen F (2017). The Bioinformatics analysis of comparative genomics of *Mycobacterium tuberculosis* complex (MTBC) provides insight into dissimilarities between intraspecific groups differing in host association, virulence, and epitope diversity. Front. Cell Infect. Microbiol. 7(1): 88.
17. Kabir S, Ejaz H, Hussain SZ, Rasheed MA, Junaid K, Rehman, A (2023). Effect of tellurite on growth of extensively drug resistant (XDR) *Mycobacterium tuberculosis* and action on mycobacterial drug efflux pump. J. King Saud. Uni. Sci. 35(4): 102629
18. Kabir S, Junaid K, Rehman A (2021). Variations in rifampicin and isoniazid resistance associated genetic mutations among drug naïve and recurrence cases of pulmonary tuberculosis. Int. J. Infect. Dis. 103: 56-61.
19. Kabir S, Tahir Z, Mukhtar N, Sohail M, Saqalein M, Rehman A (2020). Fluoroquinolone resistance and mutational profile of gyrA in pulmonary MDR tuberculosis patients. BMC Pulm. Med. 20: 1-6.
20. Khan MT, Ali S, Khan AS, Ali A, Khan A, Kaushik AC, Irfan M, Chinnasamy S, Zhang S, Zhang YJ, Cui Z, Wei AJ, Wang Y, Zhao M, Liu K, Wang H, Zeb MT, Wei DQ (2019). Insight into the drug resistance whole genome of *Mycobacterium tuberculosis* isolates from Khyber Pakhtunkhwa, Pakistan. Infect. Genet. Evol. 92: 104861.
21. Mukati S, Julka A, Varudkar HG, Singapurwala M, Agrawat JC, Bhandari D, Jain A (2019). A study of clinical profile of cases of MDR-TB and evaluation of challenges faced in initiation of second line Anti tuberculosis treatment for MDR-TB cases admitted in drug resistance tuberculosis center. Indian J. Tuberc. 66(3): 358-363.
22. Nguyen QH, Contamin L, Nguyen TVA, Bañuls AL (2018). Insights into the processes that drive the evolution of drug resistance in *Mycobacterium tuberculosis.* Evol. Appl. 11(9): 1498-1511.

23. Pasca MR, Guglierame P, De Ross, E, Zara F, Riccardi G (2005). *mmpL7* gene of *Mycobacterium tuberculosis* is responsible for isoniazid efflux in *Mycobacterium smegmatis*. Antimicrob. agents Chemother. 49(11): 4775-4777.
24. Pule CM, Sampson SL, Warren RM, Black PA, van Helden PD, Victor TC, Louw GE (2016). Efflux pump inhibitors: targeting mycobacterial efflux systems to enhance TB therapy. J. Antimicrob. Chemother. 71(1): 17-26.
25. Rodrigues L, Machado D, Couto I, Amaral L, Viveiros M (2012). Contribution of efflux activity to isoniazid resistance in the Mycobacterium tuberculosis complex. Infect. Genet. Evol. 12(4): 695-700.
26. Sandhu GK (2011). Tuberculosis: current situation, challenges and overview of its control programs in India. J Glob Infect Dis. 3(2): 143-50.
27. Shaheen A, Afridi WA, Mahboob S, Sana M, Zeeshan N, Ismat F, Rahman M (2019). Reserpine is the new addition into the repertoire of AcrB efflux pump inhibitors. Mol. Biol. 53**(**4): 596-605.
28. Siddiqui S, Brooks MB, Malik AA, Fuad J, Nazish A, Bano S, Becerra MC, Hussain H (2019). Evaluation of GenoType MTBDRplus for the detection of drug-resistant *Mycobacterium tuberculosis* on isolates from Karachi, Pakistan. PLoS One. 14(8): e0221485.
29. Swain SS, Sharma D, Hussain T, Pati S (2020). Molecular mechanisms of underlying genetic factors and associated mutations for drug resistance in *Mycobacterium tuberculosis*. Emerg. Microb. Infect. 9(1): 1651-1663
30. Wang Z, Xie T, Mu C, Sun R, Wang C, Zhao H, Ju H (2018). Performance of sequencing in predicting ofloxacin resistance in *Mycobacterium tuberculosis* from positive Bactec MGIT 960 cultures. Ann. Clin. Lab. Sci. 48(1): 69-74.
31. Yar AM, Zaman G, Hussain A, Changhui Y, Rasul A, Hussain A, Bo Z, Bokhari H, Ibrahim M (2018). Comparative genome analysis of 2 *Mycobacterium tuberculosis* strains from Pakistan: insights globally into drug resistance, virulence, and niche adaptation. Evol. Bioinform. Online, 14: 1176934318790252.
32. Yasmin M, Gomgnimbou MK, Siddiqui RT, Refrégier G, Sola C (2014). Multi-drug resistant Mycobacterium tuberculosis complex genetic diversity and clues on recent transmission in Punjab, Pakistan. Infect Genet Evol. 27: 6-14.

LGU Journal of
LIFE SCIENCES

LGU Society of Life Sciences

DOI: https://doi.org/10.54692/lgujls.2024.0803363
Paper Submission: 24th July 2024; Paper Acceptance: 7th Sep 2024; Paper Publication: 10th Sep 2024

Research Article
Vol 8 Issue 3 July- Sep 2024

LGU J. Life. Sci
ISSN 2519-9404
eISSN 2521-0130

Structural and Functional Annotations of Hypothetical Proteins of *Candida auris* for Novel Drug Target Identification: An in-silico Approach

Qamar Abbas[1], Sana Batool[2], Muhammad Zaid[1], Mahnoor Mushtaq[1], Maham Ijaz[2], Ayman Naeem[1], Ali Munir[2], Arslan Hamid[3], Naeem Mahmood Ashraf[4], Hina Batool[1]*

1. Department of Life Sciences, University of Management and Technology, Pakistan
2. School of Biological Sciences, University of the Punjab, Lahore, Pakistan.
3. University of Bonn, Germany
4. School of Biochemistry and Biotechnology, University of the Punjab, Lahore, Pakistan

Corresponding Author's Email: hinabatool198@gmail.com

ABSTRACT: *Candida auris is an emerging fungal pathogen that causes severe invasive infections in healthcare facilities which are difficult to control and treat due to its resistance to major antifungal drugs. A large fraction of C. auris proteins are uncharacterized and hypothetical, and structural and functional characterization of these proteins can aid in the selection of novel drug targets. The present study involves a computational approach for the structural and functional characterization of hypothetical proteins from Candida auris. After the sequence retrieval, hypothetical proteins were predicted for physiochemical properties and subcellular localization, structurally modeled using I-TASSER, quality assessed through Verify3D, ERRAT, and PROCHECK, and functionally annotated to reveal conserved domains and roles in pathogen pathways. Finally, the immunogenic assessments, non-human homologous analysis, and druggability analysis reveal three hypothetical proteins of C. auris (KND95408.2, KND95415.2, and KND95429.2) as novel drug targets. Furthermore, the stable conformations of these selected drug targets with the minimum root mean square deviations (RMSD) and fluctuation (RMSF) were analyzed by MD simulations. Conclusively, the functional annotations of these hypothetical proteins can help in understanding the disease mechanisms at the molecular level, as well as provide new targets for drug development against Candida auris.*

Keywords: Candida auris, Drug targets, In silico analysis, Candidiasis

INTRODUCTION

Recently, several fungal infections have posed significant health concerns (Almeida et al., 2019). *Candida auris* is an emerging fungus that presents a serious global health threat causing severe illness in hospitalized and immunocompromised patients (Du et al., 2020). According to recent statistics, *C. auris* infects thousands of individuals globally, and the infectivity rate has gradually increased over the last decade (Vila et al., 2020). The pathogen is associated with many invasive infections of the ear, urinary system, skin, bone, wounds, bloodstream, and lower respiratory tract (Horton and Nett, 2020). Since its first isolation in 2009 from the ear canal of an infected female in Japan, the infectious outbreaks of *C. auris* have covered 45 countries with a mortality rate of 72% (Cândido et al., 2020; D'Ambra, 2019; Dahiya et al., 2020). Due to the nosocomial origin of these infections, the principal sources for the outspread of this infection include contaminated surfaces in hospitals and other healthcare settings (Bandara and Samaranayake, 2022). The pathogen colonizes the patient's skin, and the mucosal surfaces, contaminating the surroundings, leading to rapid transmission into the environment (Büyüktuna et al., 2019).

The excessive use of antibiotics and antifungal agents, a recent history of surgery, prolonged stay in the Intensive Care Unit (ICU), use of indwelling lines, central venous catheters, and feeding tubes are the main risk factors associated with *C. auris* infections (Thomas-RŘddel et al., 2022). *Candida auris* can also co-infect individuals infected with other pathogens, as in the case of COVID-19, where infected patients who were on ventilators acquired coinfection of *C. auris*, complicating the diagnosis, treatment, and prognosis, and increasing disease symptoms and mortality (Calvo et al., 2021).

Several antifungal agents, including echinocandins, fluconazole, and polyenes, have been proven effective against *C. auris*. However, the resistance of *C. auris* to these agents has increased the infection rates leading to increased mortalities and morbidities (Fang et al., 2021). Consequently, there is a need to

develop new treatment options to curtail the increasing infection rate of *C. auris* (Ré et al., 2021). In several emerging pathogens, the molecular functions of some proteins are unknown, and these uncharacterized proteins are known as hypothetical proteins (HPs). The functional annotation of these uncharacterized proteins helps in understanding their roles in different pathways and to identify novel drug targets for these pathogens (Omeershffudin and Kumar, 2019). Thus, in addition to the known proteins, the hypothetical proteins of emerging pathogens need to be analyzed for their potential drug target abilities (Chirgadze et al., 2022).

Recently, the uncharacterized proteins from many deadly pathogens have been suggested as ideal drug candidates for controlling their infections (Abbasi et al., 2022). Several computational tools are available for the structural and functional annotations of HPs, physicochemical characterization, protein network and pathway analysis, and molecular interaction exploration (Prabhu et al., 2020). Moreover, the computational screening of uncharacterized proteins may help in probing the potential drug targets, followed by measuring their affinities to various therapeutic agents. Therefore, screening the proteome of drug-resistant pathogens for discovering novel drug targets would be a new strategy to cater to the increased infectivity rates of these pathogens (Shamsinejad et al., 2022). The whole genome analysis of *C. auris* indicates that this pathogen contains over 5500 genes. Currently, 8357 proteins are reported, out of which many proteins are hypothetical (Jain et al., 2022).

The present study involves a computational strategy for the structural and functional characterization of the hypothetical proteins of *Candida auris* and subsequently screening for potential drug target proteins. The selected proteins should be essential for the survival of the pathogen and should not be homologous to the human proteome. The conformational stabilities of selected drug

targets were determined using molecular dynamics simulations. This study suggests novel drug targets for the pathogen *C. auris*, which may help in designing new and effective treatment options against this deadly pathogen. Further experimental confirmation through wet-lab analysis is needed.

MATERIALS AND METHODS

Selection of HPs and their Sequence Retrieval

The hypothetical proteins of *Candida auris* and their sequence in the FASTA format were retrieved from the NCBI database (https://www.ncbi.nlm.nih.gov/) (Schoch et al., 2020). After the sequence retrieval, the sequence homology analysis of hypothetical proteins was performed using the BLASTp server (Wu et al., 2019). The proteins having homology with the structurally and functionally characterized proteins were selected for the downstream analysis.

Physiochemical Characterization of Selected HPs

The physicochemical parameters of selected HPs, including molecular weight, extinction coefficient, theoretical pI, instability index, aliphatic index, and Grand Average of Hydropathy (GRAVY), were analyzed via the online Expasy ProtParam (https://www.web.expasy.org/protparam) (Duvaud et al., 2021).

Subcellular Localization

The cellular location of proteins provides information about their function and helps predict the protein-protein interactions, which reveals these proteins' involvement in various signalling pathways (Wang and Chen, 2022). Based on this, the subcellular localization of selected hypothetical proteins was assessed using the CELLO2GO (http://cello.life.nctu.edu.tw/cello2go/) online server. CELLO is a computer program that uses BLAST to find homologous protein sequences in an in-house database annotated with the Gene Ontology database. It is used to study domains of proteins as cellular components, molecular functions, and biological processes (Yu et al., 2014). Furthermore, the presence of signal peptide was predicted by the SignalIP (5.0) server (http://www.cbs.dtu.dk/services/SignalP/) (Almagro Armenteros et al., 2019).

Secondary and Tertiary Structure Prediction

For secondary structure predictions of hypothetical proteins, SOPMA (https://npsa-prabi.ibcp.fr/NPSA/npsa_sopma.html), GOR1V (NPSA/npsa_gor4.html), and PSIPRED (http://www.bioinf.cs.ucl.ac.uk.) were used This tool exploits a combined approach based on the clustering process and reports biological and molecular functions based on Gene Ontology dependent similarities. Moreover, the 3D structures of selected HPs were constructed using the I-TASSER server (Zhang, 2008). The quality of protein models was evaluated via Verify3D, ERRAT, and PROCHECK programs of the SAVES server (https://saves.mbi.ucla.edu/).

Functional characterization of HPs

The functional characterization of hypothetical proteins was based on the conserved domain and motif analysis (Dhanyalakshmi et al., 2016). For conserved domain analysis, the NCBI CDD (www.ncbi.nlm.nih.gov/structure/cdd/docs/cdd) server and the online Pfam (https://www.pfam.xfam.org) server were used, while motif analysis, was performed using InterProScan (Ebi.ac.UK/InterPro/) Among these, the CDD compares a query sequence against position-specific score matrices using RPS-BLAST (Reverse Position Specific BLAST), resulting in the alignment of these proteins with conserved domains present in CDD (Marchler-Bauer et al., 2015). The Pfam is a protein family database with annotations and multiple sequence alignments based on Hidden Markov Models (Bateman et al., 2004). Motifs are highly conserved secondary structural elements present in protein families that define the functions of these proteins (Serçinoğlu and Ozbek, 2020). For motif analysis, InterProScan combines various methods for recognizing the protein footprints from the InterPro consortium (Paysan-Lafosse et al., 2022). After domain and motif analysis, hypothetical proteins' possible molecular and biological functions were assessed using the Argot 2.5 database (http://www.medcomp.medicina.unipd.it/Argot2-5/help.php). This tool predicts the function of the protein by its amino acid sequence in a significant manner by using a neural network approach. This combined approach is based on clustering and reports biological and molecular functions based on Gene Ontology-

dependent similarities. (Reijnders, 2022).

Antigenicity Predictions

VaxiJen server (http://www.jenner.ac.uk/VaxiJen9-) was used to check the antigenicity of hypothetical proteins. The potential antigenic fungal proteins were selected at the VaxiJen score greater than 0.5 (Zaharieva et al., 2019).

Screening for Non-human Homologous HPs

To avoid the possibility of autoimmune reactions, the drug-target proteins of *C. auris* should not be homologous to the host proteins. Therefore, only non-human homologous proteins were considered for further analysis (Khan et al., 2022). For the homology analysis, the hypothetical proteins of *C. auris*, the BLASTp analysis against humans was performed and proteins homologous to the human proteome were excluded from the analysis.

Eessentiality Analysis of Selected Non-Human Homologous Hps

Essential genes are those that are crucial for the survival of organisms. For essential gene analysis, the protein sequences of hypothetical proteins were subjected to the Database of Essential Genes (DEG), followed by the screening of proteins encoded by the essential genes at an e-value threshold of 0.0001 (Luo et al., 2021).

Druggability Analysis of Essential Non-human Homologous HPs

The essential and non-human homologous hypothetical proteins were screened against the drug bank database (https://go.drugbank.com/stats) to identify the potential drug candidates that can bind with selected drug targets. The drug bank database contains 14624 drugs, including 4243 approved drugs, 2687 biotechnology drugs, 2725 approved small molecular drugs, and 6677 experimental drugs. The matching of a hypothetical protein to a drug molecule in the drug bank database indicates its druggable properties, while the proteins not matching the existing drugs might be the novel drug targets (Murugan et al., 2020).

Molecular Dynamics Simulations

Molecular Dynamic (MD) simulations were performed using GROMACS software through the LINUX interface (Gomes et al., 2022). The simulations were carried out at 100ns production phase. The trajectory analysis was based on the Root Mean Square Deviations (RMSD), Root Mean Square Fluctuation (RMSF), Solubility Accessible Area, Radius

of gyration (R_g), and hydrogen bonds. These parameters helped in assessing the conformational stabilities of the candidate proteins.

RESULTS

Protein Selection and Sequence Retrieval

Initially, fifty hypothetical proteins of *Candida auris* were selected for analysis. After the sequence homology analysis by BLASTp, twelve out of fifty proteins, showing significant homology to already characterized proteins and having a percentage identity score of greater than 50 were selected for further analysis (Table 1).

Physiochemical Characterization of HPs

The physicochemical characterization of HPs by Expasy ProtParam revealed different parameters, including molecular weight, pI, instability index, aliphatic index, and GRAVY value (Table 1). Among all twelve proteins, the KND95425.2 showed the highest molecular weight of 76374.50 Da. The isoelectric points of six HPs were above 7, while the remaining six had pI values less than 7. The instability index determines the stability of proteins, and the GRAVY value describes the hydrophobicity of proteins (Guruprasad et al., 1990; Kyte and Doolittle, 1982). The instability index value of eight HPs was greater than 40, indicating the unstable nature of these proteins, while four proteins were found to be stable with values less than 40. The GRAVY values of HPs were negative, indicating the hydrophilic nature of these proteins (Table 1).

Table 1. Physicochemical characterization, subcellular localization, and signal peptide prediction by using EXPASY ProtParam, CELLO2GO, and Signal IP 6.0 respectively for selected hypothetical proteins of *Candida* auris

Sr. No	Accession Ids	Physicochemical parameters					Subcellular localization	
		M.W	pI	Instability Index	Aliphatic Index	Gravy value	CELLO2GO	Signal IP 6.0
1	KND95391.2	16848.78	9.98	43.18	81.70	-0.387	Mitochondrial	No
2	KND95421.2	9751.54	10.88	37.3	70.00	-1.106	Nuclear	No
3	KND95408.2	58138.2	6.15	32.11	107.11	-0.365	Plasma membrane	No
4	KND95415.2	75853.51	8.55	54.40	80.94	-0.419	Nuclear	No

5	KND95425.2	76374.50	8.98	44.05	88.19	-0.404	Nuclear	No
6	KND95429.2	25758.28	6.03	42.18	89.69	-0.539	Nuclear	No
7	KND95462.2	64704.18	6.01	27.01	85.25	-0.345	Mitochondrial	No
8	KND95435.2	23986.09	5.18	41.05	74.71	-0.764	Nuclear	No
9	KND95434.2	52689.61	5.05	53.86	74.63	-0.375	Nuclear	No
10	KND95471.2	41927.46	9.50	46.55	68.27	-0.965	Nuclear	No
11	KND95463.2	15148.27	9.68	48.89	71.88	-0.833	Nuclear	No
12	KND95448.2	69670.96	6.97	39.76	89.39	-0.196	Mitochondrial	No

Subcellular localization

Table 1 demonstrates the results of subcellular localization and signal peptide prediction of selected HPs. Three proteins, KND95462.3, KND95448.2, and KND95391.2, have scored for the mitochondrial location, while KND95408.2 was found to be associated with the plasma membrane. All remaining proteins were localized in the nuclear region (Fig. 1). SignalIP v.6.0 tool revealed that none of these proteins had signal peptides (Table 1).

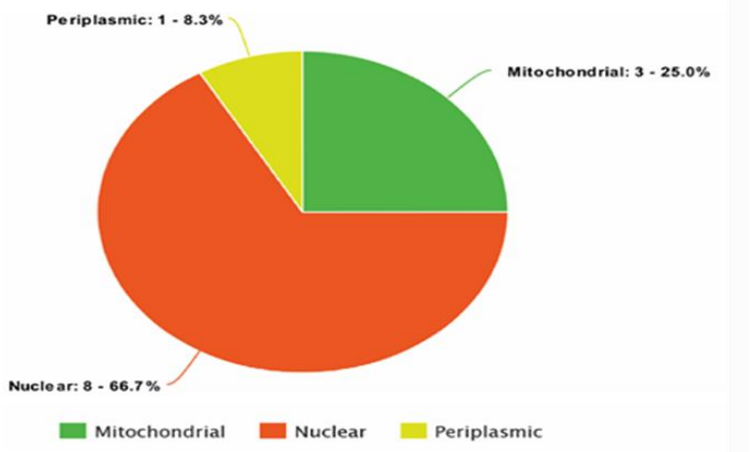

Fig. 1. Subcellular localization prediction of twelve HPs of *Candida auris* using CELLO2GO program

Structure modeling and validation

The secondary structure predictions through **SOPMA, GOR1V,** and **P SIPRED** reveal the percentage of alpha-helix, beta-sheet, and coils/loops in these proteins (Geourjon and Deleage, 1995; McGuffin et al., 2000; Sen et al., 2005). All these servers heralded that the HPs have a higher percentage of alpha helix and loops than the β-sheets (Fig. 2).

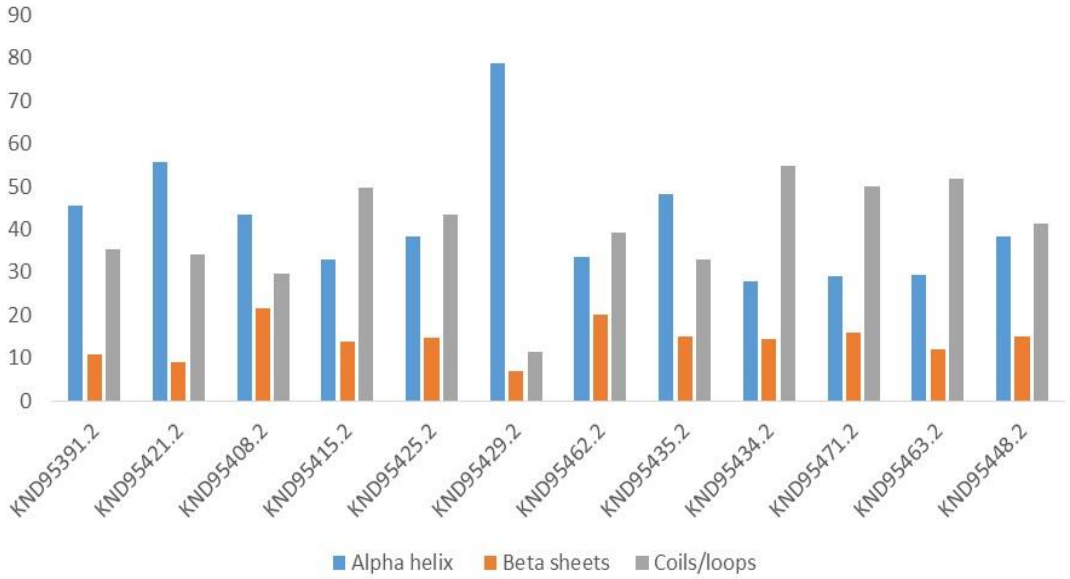

Fig. 2. Secondary structure prediction of HPS. The blue color indicates the alpha helix, the red color shows the percentage of beta-sheet, and the green color indicates coils/loops

For 3D structure modeling of HPs, an I-TASSER server was used that employs sequence-to-structure matching and then structure-to-function homology matching, thus predicting the structure and functions of the protein (Yang et al., 2015). The selection of accurate protein models was based on their C-score and TM-score. C-score is a confidence score for assessing the quality of predicted models that range from -5 to -2. Likewise, the TM score >0.5 indicates a good quality model (Steyerberg et al., 2010). Out of all protein models generated by I-TASSER, the protein model with a high C-score and TM-score was considered accurate. The 3D structures of HPs were visualized using the PyMOL server and are displayed in (Fig. 3).

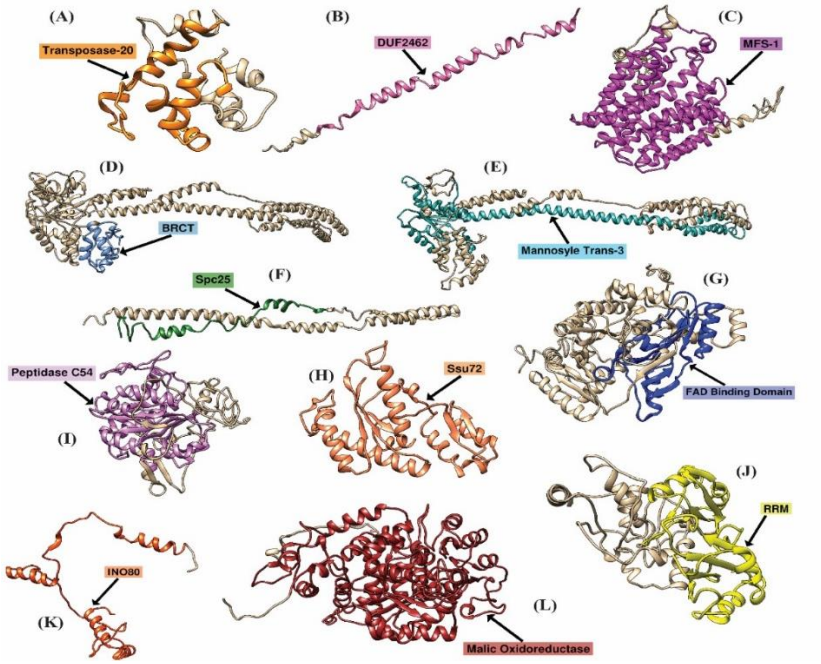

Fig. 3. Visualization of 3D models of HPs constructed by I-TASSER by using PYMOL and along conserved domain present in each HPs are named and highlighted in different colors in the models

After the 3D structure modeling, protein structures were validated through SAVES server version 6.0 using verify 3D, ERRAT, and PROCHECK (Dym et al., 2012; Eisenberg et al., 1997; Laskowski et al., 1993). The Verify 3D determines the compatibility of the protein model with its amino acid sequence providing a 3D-1D score. Protein models with a 3D-1D score greater than 0.2 were considered more compatible with their sequence (Eisenberg et al., 1997). ERRAT determines the overall quality factor of protein models considering all non-bonded atomic interactions. The higher ERRAT score indicates higher quality, and the generally accepted threshold for a high-quality protein model is >50 (Dym et al., 2012). Likewise, the Ramachandran plot depicts the statistical distributions of amino residues, based on their torsion angles, in the allowed and the favorable portions of the plot, giving insight into the conformation of the protein model. Based on these parameters, the protein models of all HPs were found to be accurate and of good quality (Laskowski et al., 1993) (Fig. 4).

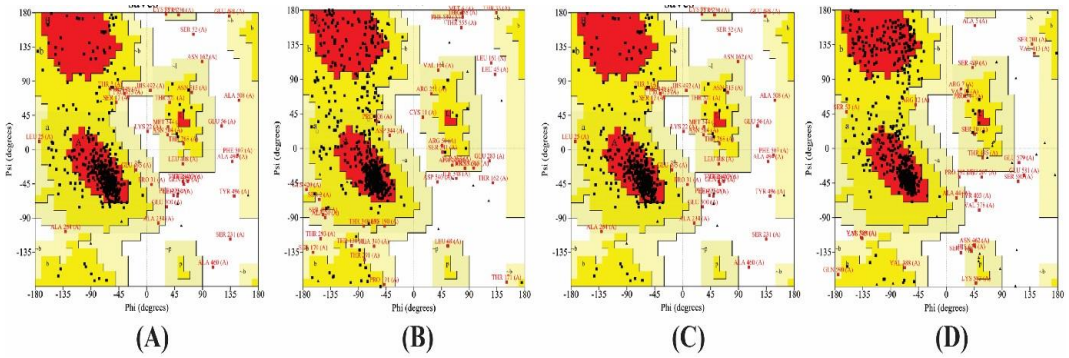

Fig. 4. Ramachandran Plot of 4 more compatible HPs (**A**= (KND95391.2, **B**= KND95435.2, **C**=KND95434.2, **D**=and KND95448.2)

Conserved domain analysis and functional assessments

NCBI conserved domain database (CDD), Pfam, and InterProScan were used to identify the conserved domains in the hypothetical proteins of *C. auris* (Bateman et al., 2004; Marchler-Bauer et al., 2015; Paysan-Lafosse et al., 2022). Several domains including, transposase-20- superfamily, DUF2462 superfamily, major facilitator superfamily (MFS), BRCT family, mannosyl transferase, chromosome segregation protein, Spc25 (Spindle –Spc25, D-lactate dehydrogenase [cytochrome], FAD linked oxidases, C-terminal domain, FAD-binding domain, RNA polymerase II subunit, Peptidase_C54, RNA recognition motif, oxaloacetate, and decarboxylating malate dehydrogenase, were identified in the HPs. The respective domains in these HPs are highlighted in their 3D structures (Fig. 3). After the conserved domain analysis, the functional annotation of hypothetical proteins was carried out using Argotv2.5, where the cut-off value of > 200 indicates the significant involvement of the protein in the predicted function (Torres et al., 2021). The functional annotation of HPs asserted their significant involvement in diverse biological pathways, including the catalysis of transposition, oxidoreductase activity, transmembrane transporter activity, DNA-directed DNA polymerase activity, nucleotide transferase activity, Flavin adenine dinucleotide activity, malate dehydrogenase, nucleic acid binding, hydrolase, and peptidase activity.

Antigenicity prediction

The antigenicity analysis marked six of the twelve proteins as potentially antigenic with a VaxiJen score greater than 0.5 (Fig.

5). The six proteins predicted as non-antigenic were excluded from the further analysis because these proteins could not be the drug targets.

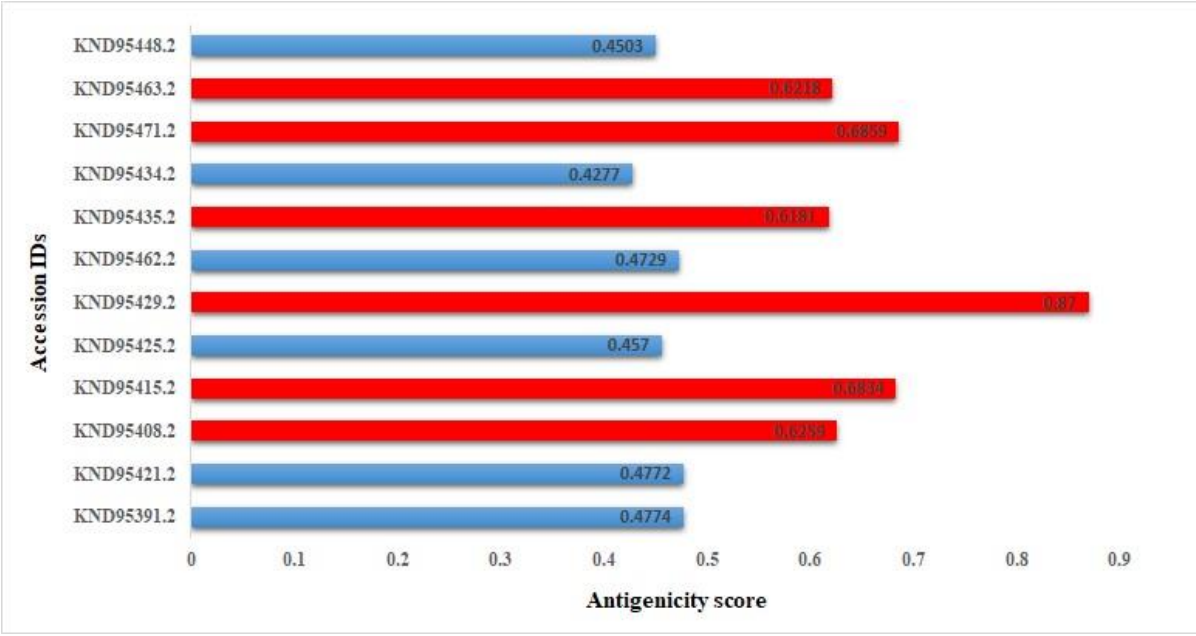

Fig. 5. Antigenicity prediction of HPs by using the VaxiJen server. The six proteins highlighted in red are marked as antigenic with a VaxiJen score greater than 0.5, while the blue-labeled proteins are non-antigenic

Screening of non-human homologous proteins

A notable feature of the drug candidate is that it should not be homologous to the host proteome to avoid cross-reactivity in hosts (Pourhajibagher and Bahador, 2016). Therefore, the homology analysis of selected immunogenic proteins against the human proteome was performed using BLASTp. The results revealed that three proteins have significant homology with human proteome (Fig. 6). The three human homologous proteins were excluded from analysis, and three non-human homologous HPs were further analyzed to probe the potential drug targets.

Essentiality analysis of selected non-human homologous HPs

After the homology analysis with the human proteome, the essentiality analysis reveals that three non-human homologous proteins are also crucial for the survival of *Candida auris* thus, these three HPs were selected as the drug targets for *C. auris* and were subjected to druggability analysis (Fig. 6).

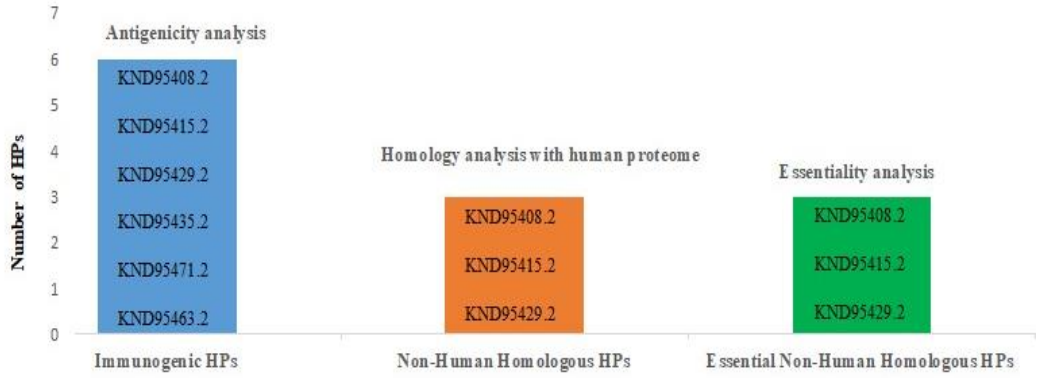

Fig. 6: The immunogenic, non-human homologous and essential hypothetical proteins of *Candida auris*

Druggability Analysis of Essential Non-Homologous Hypothetical Proteins

The druggability analysis of three selected non-human homologous and essential proteins marked them as novel drug targets having no affinity with the already available drug molecules (Table 2).

Table 2: Druggability analysis of essential non-homologous hypothetical proteins by Drug Bank.

Sr.No	Protein Accession ID	Druggability analysis
1	KND95408.2	Novel
2	KND95415.2	Novel
3	KND95429.2	Novel

Molecular dynamics simulations

MD simulations of the three selected drug target proteins showed in (Fig. 7). The combined analysis of Root Mean Square Deviations (RMSD), Root Mean Square Fluctuation (RMSF), Surface Accessible Area, Radius of gyration (Rg), and the hydrogen bonds shows the stable conformations of three proteins with the different fluctuations over time. The protein KND95408.2 remains compact with the least fluctuations, while the proteins KND95415.2 and KND95429.2 show marginal deviations without undergoing any drastic changes in confirmations.

MD simulations depict that the selected candidates are the best potent drug targets depending on

the nature of the proteins determined by multiple sequence alignment after detecting their homologs. As KND95408.2 is a membrane transporter having a compact nature it showed less variation and fluctuations in its structure and remained stable over time. While the protein, KND95415.2 has a significant role in DNA damage repair, cell cycle regulation, and checkpoint control so, the fluctuation and conformational changes in its structure depict its nature and give confidence about the promising results. Respectively, KND95429.2 proteins despite their small size have high fluctuation and conformational changes that synchronize with their functional characterization as it has significant importance in cell division, maintenance of genome stability, and repair of double-stranded DNA breaks. The nature of proteins along with their function co-relate with the conformational changes detected by MD simulations.

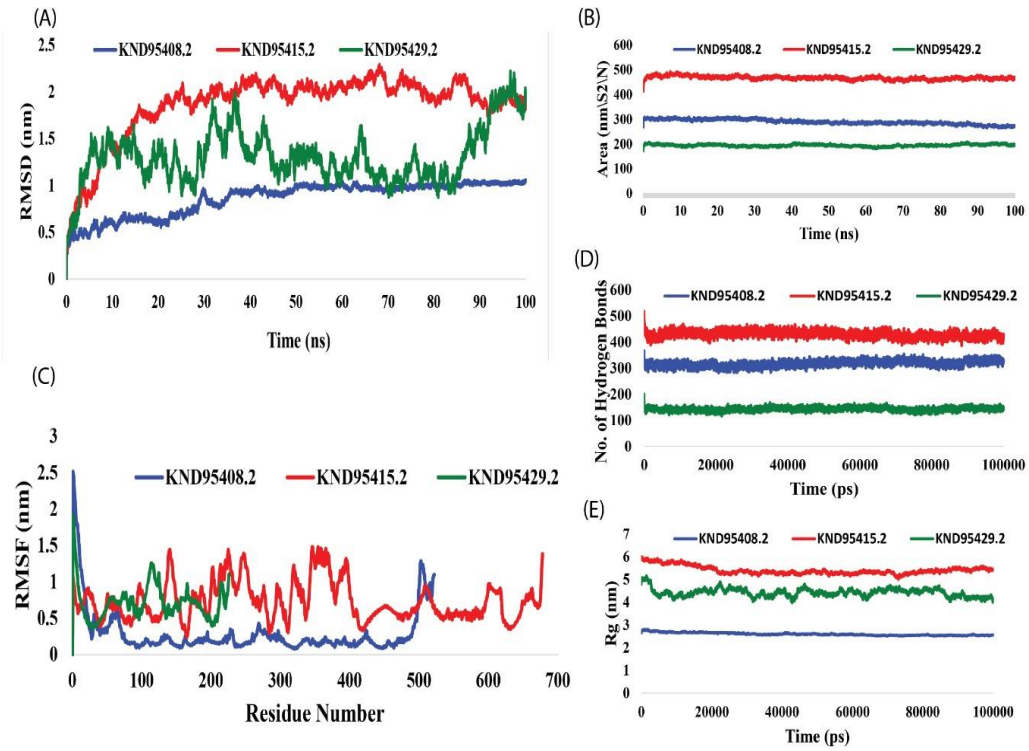

Fig. 7: Simulation analysis of hypothetical proteins of *Candida auris* using GROMACS. (A) RMSD at 100ns shows significant conformational changes in Red and Green proteins, while Blue remains more stable (B) Solubility Accessible Area reflects protein stability with hydrophobic core exposure (C) RMSF at 100ns indicates higher flexibility in Red and Green proteins, with Blue being less flexible (D) Number of Hydrogen Bonds indicates greater compactness in the larger Red protein (E)

Radius of Gyration shows Green protein is short and flexible with a large radius, while Blue is compact with a small radius. Red protein is the largest and most flexible

DISCUSSION

Candida auris cause infections, collectively known as candidiasis (Du et al., 2020), and due to its resistance to antifungal drugs and high mortality rate, the Center for Disease Control and Prevention (CDC) has declared this pathogen a superbug (D'Ambra, 2019). The emergence of drug resistance in *C. auris* demands the exploration of new treatment options to combat this pathogen (Jain et al., 2022). The structural and functional characterization of hypothetical proteins can pave the way, to identify new potential drug targets facilitating drug development (Prabhu et al., 2020). Many novel drug targets have been identified for various pathogens from their uncharacterized proteins (Ahamed et al., 2021; Araújo et al., 2020; Hafsa et al., 2022; Pranavathiyani et al., 2020). Since a large portion of the proteome of *C. auris* remains structurally and functionally uncharacterized, the structural and functional annotations of these proteins would help to determine the novel therapeutic targets of this pathogen (Rossato and Colombo, 2018). The present study employs various computational algorithms to characterize hypothetical proteins from *C. auris* to discover novel therapeutic targets from these uncharacterized proteins. Initially, fifty hypothetical proteins of *C. auris* were retrieved from the NCBI database. The hypothetical proteins showing significant sequence similarity to the already characterized proteins were screened through BLASTp analysis because the structurally and functionally characterized proteins having homology with the uncharacterized proteins might help to infer the structure and function of hypothetical proteins (Ahmed et al., 2018). Out of fifty hypothetical proteins, twelve homolog proteins were considered for further analysis, whose physicochemical characterization provides insights into the chemical nature, stability, and molecular attributes (Panda and Chandra, 2012). The Expasy ProtParam tool revealed that one hypothetical protein (KND95425.2) has the highest molecular weight of 76 kDa, and the GRAVY values of all twelve hypothetical proteins were negative, indicating the non-polar nature of these proteins (Table 1). As the function of a protein is directly or indirectly related to its subcellular localization, which indicates that two proteins are

mitochondrial, one protein is the plasma membrane protein, and all remaining proteins are nuclear. None of these hypothetical proteins shows the presence of signal peptide as predicted by the SignalIP (6.0) server (Table 1 and Fig. 1). Structure modeling of the proteins is crucial to evaluate their molecular and biological functions in cells, thus assisting in drug target identification (Zhang, 2009). The secondary structural modeling of HPs reveals the significant presence of alpha-helix and coils/loops, then beta-sheets (Fig. 2). After the 2D structure predictions, the tertiary structures of proteins were modeled using I-TASSER, followed by the quality assessment of protein structures. The protein structure validation through these programs revealed that the selected models have minimum steric hindrance with most of their amino acid residues in favorable and allowed regions of the Ramachandran plot (Fig. 4). The functional annotation of the hypothetical protein is a prerequisite for a better understanding of biological processes and finding potential drug targets from them (Loewenstein et al., 2009). NCBI conserved domain database, Pfam, and InterProScan revealed the presence of evolutionarily conserved domains in these proteins; moreover, the Argot 2.5 server revealed the involvement of all hypothetical proteins in the crucial biological pathways (Fig. 3).

The pathogenic proteins of microbes play a pivotal role in the initial interaction between the pathogen and the host. Consequently, these proteins are frequently prioritized as suitable drug targets. In addition to their immunogenic nature, a drug target protein must also be crucial for the survival of the pathogen. Furthermore, these proteins should not have similarities with the host proteins, which otherwise may cause the cross reactivity. Considering these points the selected hypothetical proteins were analyzed for their immunogenic nature, homology with the human proteome, and their essentiality in the survival of pathogen (Qureshi et al., 2021; Sauna et al., 2020). The immunogenic predictions through the VaxiJen server revealed six proteins as antigenic (Fig. 5). The homology analysis marked three among the six antigenic proteins as non-human homologous, and essentiality analysis indicated that three non-human homologous proteins are also essential for the survival

of *C. auris* (Fig. 6). Therefore, the three immunogenic, non-human homologous, and essential proteins were declared as the potential drug target proteins for *C. auris* (Table 2). Finally, the similarity search against the Drug Bank database showed that all three immunogenic, essential, and non-human homologous hypothetical proteins have no significant similarity with compounds in the Drug Bank database; therefore, these proteins are novel drug targets (Table 2). The Molecular dynamic simulations show the thermodynamically stable conformation of the selected hypothetical proteins, thereby validating their suitability as promising drug targets (Fig. 7). Based on this *in silico* screening, characterization, and simulation analysis KND95408.2, KND95415.2, and KND95429.2 are potential drug targets, but they need further wet-lab characterization to confirm their suitability as drug targets.

CONCLUSION

The structural and functional characterization of hypothetical proteins is crucial for understanding their role in biochemical/physiological pathways and screening novel therapeutic targets. The present study employs an *in-silico* approach to identify novel drug targets from hypothetical proteins of *Candida auris* that are found to be essential for this pathogen and are non-human homologous. However, these proteins need further wet lab characterization before their use in drug designing.

ACKNOWLEDGMENT

Authors are thankful for the online available open access databases which were used in this research. The research was self-supported by the authors.

ETHICAL STATEMENT

This study is a computational work. No humans or animals were used during the study. Therefore, ethical approval was not necessary.

CONFLICT OF INTEREST

Authors declare no conflict of interests.

DATA AVAILABILITY

The data that supports the findings of this study are available on request by the corresponding author.

REFERENCES

1. Abbasi, B. A., Dharan, A., Mishra, A., Saraf, D., Ahamad, I., Suravajhala, P., and Valadi, J. (2022). In

silico characterization of uncharacterized proteins from multiple strains of *Clostridium difficile*. *Frontiers in Genetics*, 13, 878012.

2. Ahamed, N. A., Panneerselvam, A., Arif, I. A., Abuthakir, M. H. S., Jeyam, M., Ambikapathy, V., Health, P. (2021). Identification of potential drug targets in human pathogen *Bacillus cereus* and insight for finding inhibitor through subtractive proteome and molecular docking studies. *Journal of Infection and Public Health*, 14(1), 160-168.
3. Ahmed, M. S., Shahjaman, M., Kabir, E., and Kamruzzaman, M. J. B. (2018). Structure modeling to function prediction of uncharacterized human protein C15orf41. *BMC Bioinformatics*, 14(5), 206.
4. Almagro Armenteros, J. J., Tsirigos, K. D., Sønderby, C. K., Petersen, T. N., Winther, O., Brunak, S., ... Nielsen, H. J. (2019). SignalP 5.0 improves signal peptide predictions using deep neural networks. *Nature Biotechnology*, 37(4), 420-423.
5. Almeida, F., Rodrigues, M. L., and Coelho, C. (2019). The still underestimated problem of fungal diseases worldwide. *Frontiers in Microbiology*, 10, 214.
6. Araújo, C. L., Blanco, I., Souza, L., Tiwari, S., Pereira, L. C., Ghosh, P., Folador, A. (2020). In silico functional prediction of hypothetical proteins from the core genome of *Corynebacterium pseudotuberculosis* biovar ovis. *PeerJ*, 8, e9643.
7. Bandara, H., and Samaranayake, L. J. (2022). Emerging strategies for

environmental decontamination of the nosocomial fungal pathogen *Candida auris*. *Journal of Medical Microbiology*, 71(6), 001548.

8. Bateman, A., Coin, L., Durbin, R., Finn, R. D., Hollich, V., Griffiths-Jones, S., Sonnhammer, E. L. (2004). The Pfam protein families' database. *Nucleic Acids Research*, 32(suppl_1), D138-D141.
9. Büyüktuna, S. A., Hasbek, M., Elaldı, N., Gözel, M. G., Çelik, C., Engin, A., Bakır, M. (2019). Epidemiological analysis of nosocomial *Candida* infections: Experience of a university hospital. *Clinical Microbiology and Infection*, 41(2), 318-327.
10. Cândido, E. d. S., Affonseca, F., Cardoso, M. H., and Franco, O. L. (2020). Echinocandins as biotechnological tools for treating *Candida auris* infections. *Journal of Fungi*, 6(3), 185.
11. Chirgadze, Y., Boshkova, E., Kargatov, A., Chirgadze, N., and Dynamics. (2022). Functional identification of 'hypothetical protein' structures with unknown function. *Journal of Biomolecular Structure and Dynamics*, 1-5.
12. D'Ambra, M. (2019). CDC alert for hospital infections due to *Candida auris* multiresistant. *Clinical Translational Gastroenterology*, 2, 150-152.
13. Dahiya, S., Chhillar, A. K., Sharma, N., Choudhary, P., Punia, A., Balhara, M., Parmar, V. S. (2020). *Candida auris* and nosocomial infection. *Current Drug Targets*, 21(4), 365-373.

14. Dhanyalakshmi, K., Naika, M. B., Sajeevan, R., Mathew, O. K., Shafi, K. M., Sowdhamini, R., and N. Nataraja, K. (2016). An approach to function annotation for Proteins of Unknown Function (PUFs) in the transcriptome of Indian mulberry. *PLoS ONE*, 11(3), e0151323.
15. Du, H., Bing, J., Hu, T., Ennis, C. L., Nobile, C. J., and Huang, G. (2020). *Candida auris*: Epidemiology, biology, antifungal resistance, and virulence. *PLoS Pathogens*, 16(10), e1008921.
16. Duvaud, S., Gabella, C., Lisacek, F., Stockinger, H., Ioannidis, V., and Durinx, C. (2021). Expasy, the Swiss Bioinformatics Resource Portal, as designed by its users. *Nucleic Acids Research*, 49(W1), W216-W227.
17. Dym, O., Eisenberg, D., and Yeates, T. (2012). ERRAT.
18. Eisenberg, D., Lüthy, R., and Bowie, J. U. (1997). [20] VERIFY3D: assessment of protein models with three-dimensional profiles. In Methods in enzymology (Vol. 277, pp. 396-404). Elsevier.
19. Fang, J., Huang, B., and Ding, Z. (2021). Efficacy of antifungal drugs in the treatment of oral candidiasis: A Bayesian network meta-analysis. *Journal of Pharmaceutical Design*, 125(2), 257-265.
20. Geourjon, C., and Deleage, G. (1995). SOPMA: significant improvements in protein secondary structure prediction by consensus prediction from multiple alignments. *Bioinformatics*, 11(6), 681-684.

21. Gomes, D. E. B., Gomes, P. S., and Bernardi, R. C. (2022). QwikMD 2.0: bridging the gap between sequence, structure, and protein function. *Biophysical Journal*, 121(3), 132a.
22. Guruprasad, K., Reddy, B. B., and Pandit, M. W. (1990). Correlation between stability of a protein and its dipeptide composition: a novel approach for predicting in vivo stability of a protein from its primary sequence. *Protein Engineering*, 4(2), 155-161.
23. Hafsa, U., Chuwdhury, G., Hasan, M. K., Ahsan, T., and Moni, M. A. (2022). An in silico approach towards identification of novel drug targets in *Klebsiella oxytoca*. *Infection, Genetics and Evolution*, 31, 100998.
24. Horton, M. V., and Nett, J. E. (2020). *Candida auris* infection and biofilm formation: going beyond the surface. *Clinical Candida Mycology Research*, 7(3), 51-56.
25. Jain, M., Jain, A., Khare, B., Jain, D. K., Khan, R., and Jain, D. (2022). An update on the recent emergence of *Candida auris*. *American Journal of Dermatological and Health Sciences*, 2(1), 14-19.
26. Khan, K., Jalal, K., Khan, A., Al-Harrasi, A., and Uddin, R. (2022). Comparative metabolic pathways analysis and subtractive genomics profiling to prioritize potential drug targets against *Streptococcus pneumoniae*. *Frontiers in Microbiology*, *12*, 4384.
27. Kyte, J., and Doolittle, R. F. (1982). A simple method for displaying the hydropathic character of a protein. *Journal of*

Molecular Biology, *157*(1), 105-132.

28. Laskowski, R. A., MacArthur, M. W., Moss, D. S., and Thornton, J. M. (1993). PROCHECK: A program to check the stereochemical quality of protein structures. *Journal of Applied Crystallography*, *26*(2), 283-291.
29. Loewenstein, Y., Raimondo, D., Redfern, O. C., Watson, J., Frishman, D., Linial, M., ... Tramontano, A. (2009). Protein function annotation by homology-based inference. *Genome Biology*, *10*(2), 1-8.
30. Luo, H., Lin, Y., Liu, T., Lai, F.-L., Zhang, C.-T., Gao, F., and Zhang, R. (2021). DEG 15, an update of the Database of Essential Genes that includes built-in analysis tools. *Nucleic Acids Research*, *49*(D1), D677-D686.
31. Marchler-Bauer, A., Derbyshire, M. K., Gonzales, N. R., Lu, S., Chitsaz, F., Geer, L. Y., Hurwitz, D. I. (2015). CDD: NCBI's conserved domain database. *Nucleic Acids Research*, *43*(D1), D222-D226.
32. McGuffin, L. J., Bryson, K., and Jones, D. T. (2000). The PSIPRED protein structure prediction server. *Bioinformatics*, *16*(4), 404-405.
33. Murugan, N. A., Kumar, S., Jeyakanthan, J., and Srivastava, V. (2020). Searching for target-specific and multi-targeting organics for COVID-19 in the DrugBank database with a double scoring approach. *Scientific Reports*, *10*(1), 1-16.
34. Omeershffudin, U. N. M., and Kumar, S. (2019). In silico approach for mining of potential drug targets

from hypothetical proteins of bacterial proteome. *International Journal of Microbiology Open Access*, *4*(4), 145-152.

35. Panda, S., and Chandra, G. (2012). Physicochemical characterization and functional analysis of some snake venom toxin proteins and related non-toxin proteins of other chordates. *Bioinformatics*, *8*(18), 891.
36. Paysan-Lafosse, T., Blum, M., Chuguransky, S., Grego, T., Pinto, B. L., Salazar, G. A., Colwell, L. J. (2022). InterPro in 2022. *Nucleic Acids Research*.
37. Pourhajibagher, M., and Bahador, A. (2016). Designing and in silico analysis of PorB protein from *Chlamydia trachomatis* for developing a vaccine candidate. *Drug Research*, *66*(09), 479-483.
38. Prabhu, D., Rajamanikandan, S., Anusha, S., Chowdary, M. S., Veerapandiyan, M., and Jeyakanthan, J. (2020). In silico functional annotation and characterization of hypothetical proteins from *Serratia marcescens* FGI94. *BioBiotechnology*, *47*(4), 319-331.
39. Pranavathiyani, G., Prava, J., Rajeev, A. C., and Pan, A. (2020). Novel target exploration from hypothetical proteins of *Klebsiella pneumoniae* MGH 78578 reveals a protein involved in host-pathogen interaction. *Frontiers in Cell and Infection Microbiology*, *109*.
40. Qureshi, N. A., Bakhtiar, S. M., Faheem, M., Shah, M., Bari, A., Mahmood, H. M., ... Jamal, S. B. (2021). Genome-based drug target identification in human pathogen *Streptococcus*

gallolyticus. *Frontiers in Genetics*, *12*, 564056.

41. Ré, A. C. S., Martins, J. F., Cunha-Filho, M., Gelfuso, G. M., Aires, C. P., and Gratieri, T. (2021). New perspectives on the topical management of recurrent candidiasis. *Drug Development and Research*, *11*(4), 1568-1585.
42. Reijnders, M. J. (2022). Wei2GO: Weighted sequence similarity-based protein function prediction. *Protein Science*, *10*, e12931.
43. Rossato, L., and Colombo, A. L. (2018). *Candida auris*: What have we learned about its mechanisms of pathogenicity? *Frontiers in Microbiology*, *9*, 3081.
44. Sauna, Z. E., Richards, S. M., Maillere, B., Jury, E. C., and Rosenberg, A. S. (2020). Immunogenicity of proteins used as therapeutics. *Frontiers in Immunology*, *11*, 614856.
45. Schoch, C. L., Ciufo, S., Domrachev, M., Hotton, C. L., Kannan, S., Khovanskaya, R., Robbertse, B. (2020). NCBI Taxonomy: A comprehensive update on curation, resources, and tools. *Database*.
46. Segrelles-Calvo, G., de S Araújo, G. R., Llopis-Pastor, E., Carrillo, J., Hernández-Hernández, M., Rey, L., Zamarro, C. (2021). *Candida* spp. co-infection in COVID-19 patients with severe pneumonia: Prevalence study and associated risk factors. *Respiratory Medicine*, *188*, 106619.
47. Sen, T. Z., Jernigan, R. L., Garnier, J., and Kloczkowski, A. (2005). GOR V server for protein secondary structure

prediction. *Bioinformatics, 21*(11), 2787-2788.

48. Serçinoğlu, O., and Ozbek, P. (2020). Sequence-structure-function relationships in class I MHC: A local frustration perspective. *PLoS One, 15*(5), e0232849.
49. Shamsinejad, F. S., Zafari, Z., and Zafari, Z. (2022). Prediction of potential drug targets and vaccine candidates against antibiotic-resistant *Pseudomonas aeruginosa*. *International Journal of Pharmaceutical Research and Therapeutics*, *28*(6), 1-11.
50. Steyerberg, E. W., Vickers, A. J., Cook, N. R., Gerds, T., Gonen, M., Obuchowski, N., Kattan, M. W. (2010). Assessing the performance of prediction models: A framework for some traditional and novel measures. *Epidemiology*, *21*(1), 128.
51. Thomas-Rüddel, D. O., Schlattmann, P., Pletz, M., Kurzai, O., and Bloos, F. (2022). Risk factors for invasive *Candida* infection in critically ill patients: A systematic review and meta-analysis. *Clinical Microbiology*, *161*(2), 345-355.
52. Torres, M., Yang, H., Romero, A. E., and Paccanaro, A. (2021). Protein function prediction for newly sequenced organisms. *Nature Microbiology Insights*, *3*(12), 1050-1060.
53. Vila, T., Sultan, A. S., Montelongo-Jauregui, D., and Jabra-Rizk, M. A. (2020). *Candida auris*: A fungus with an identity crisis. *Pathogens and Disease, 78*(4), ftaa034.
54. Wang, R., and Chen, L. (2022). Identification of

human protein subcellular location with multiple networks. *Cellular Physiology*, *19*(4), 344-356.

55. Wu, B., Zhang, H., Lin, L., Wang, H., Gao, Y., Zhao, L., Gu, L. (2019). A similarity searching system for biological phenotype images using deep convolutional encoder-decoder architecture. *Computational Biology*, *14*(7), 628-639.

56. Yang, J., Yan, R., Roy, A., Xu, D., Poisson, J., and Zhang, Y. (2015). The I-TASSER Suite: Protein structure and function prediction. *Nature Methods*, *12*(1), 7-8.

57. Yu, C.-S., Cheng, C.-W., Su, W.-C., Chang, K.-C., Huang, S.-W., Hwang, J.-K., and Lu, C.-H. (2014). CELLO2GO: A web server for protein subCELlular LOcalization prediction with functional gene ontology annotation. *PLOS One*, *9*(6), e99368.

58. Zaharieva, N., Dimitrov, I., Flower, D. R., and Doytchinova, I. (2019). VaxiJen dataset of bacterial immunogens: An update. *Current Computer-Aided Drug Design*, *15*(5), 398-400. Zhang, Y. (2008). I-TASSER server for protein 3D structure prediction. *BMC Bioinformatics*, *9*(1), 1-8.

59. Zhang, Y. (2009). Protein structure prediction: When is it useful? *Current Opinion in Structural Biology*, *19*(2), 145-155.